Diss. ETH No. 16408

CARBON DIOXIDE CATALYZED OXIDATION OF PHENOLS BY PEROXYNITRITE

A dissertation submitted to the

SWISS FEREDAL INSTITUTE OF TECHNOLOGY ZURICH

for the degree of

Doctor of Natural Sciences

presented by

Alina Alexandrovna Papina

Dipl. Chem. Novosibirsk State University

born 09.01.1977

citizen of the Russian Federation

accepted on the recommendation of

Prof. Dr. Willem H. Koppenol, examiner

Prof. Dr. Joseph S. Beckman, co-examiner

2005

ACKNOWLEDGEMENTS

This work would not have been possible without many people. In particular, I would like to express my deepest gratitude to:

Prof. Dr. Willem H. Koppenol for providing me the opportunity to conduct research in his group and giving me freedom in defining and carrying out my Ph.D. project, for his patience in correcting and reviewing my muddled drafts and helping me to improve my writing skills.

Dr. J. Beckman, whose brilliant hypothesis revolutionized toxicology 15 years ago and inspired many Ph.D. students, including myself, to conduct research in this field. I greatly appreciate his interest in my work and co-examining the thesis.

Dr. Reinhard Kissner for helping me in the experimental work and for being forthcoming and inspiring during scientific discussions.

Dr. Susanna Herold for her help, enthusiasm, and interest in the work.

Peter Latal for maintaining the HPLC facility.

All former and present members of the group for creating a warm and friendly atmosphere. A special thanks to Dr. Benedikt Galliker for translating the summary into German.

All my friends in and outside the ETH for making my leisure time interesting and joyful.

And last, but not least, my family. My parents for their unconditional love and support throughout my life, my daughter Sonja, who might not appreciate it yet (if ever), for revealing the meaning of life to me, and my husband Kirill for his love, care, and support over the years.

ABBREVIATIONS AND SYSTEMATIC NAMES

Abbreviations: ESR, electron spin resonance; MS, mass spectrometry; HPLC, high performance liquid chromatography; UV-Vis, ultraviolet and visible; OD, optical density; DEMPO, 5,5-dimethyl-1-pyrroline-*N*-oxide; HEPES, *N*-2-hydroxyehtylpiperazine-*N*'-2- ethanesulfonic acid; DMSO, dimethyl sulfoxide; SOD – superoxide dismutase; ABTS, 2,2′-azino-bis-(3-ethyl-1,2-dihydrobenzothiazoline 6-sulfonate); cyclam, 1,4,8,11-tetraazacyclotetradecane; bpy, 2,2′-bipyridyl; KTBA, 2-keto-4-thiomethylbutanolic acid; 4-HPA, 4-hydroxyphenylacetic acid; BQ, benzoquinone; HQ, hydroquinone; NP, nitrophenol; BP, biphenol.

Systematic names: peroxynitrite, oxoperoxonitrate (1–); peroxonitrous acid, hydrogen oxoperoxonitrate; peroxynitrite/carbon dioxide adduct ($ONOOCO_2^-$), 1-carboxylato-2-nitrosodioxidane; nitrogen monoxide, oxonitrogen (•); nitrogen dioxide, dioxonitrogen (•); superoxide, dioxide (•1–); dithionite, bis(dioxosulfate)(*S*-*S*)(2–); $SO_2^{\bullet-}$, dioxosulfate(•1–); *para*-benzoquinone, cyclohexa-2,5-dien-1,4-dione; hydroquinone, benzene-1,4-diol.

Table of Contents

OBJECTIVES

Peroxynitrite is an inorganic toxin implicated in many diseases as a nitrating and oxidizing agent. Finding a suitable scavenger for peroxynitrite *in vivo* is an important task of modern toxicology. In order to achieve this, a fundamental understanding of peroxynitrite reactivity is essential. Calculations based on rate constants and concentrations indicate that physiologically relevant reactions of peroxynitrite are those that are catalyzed by carbon dioxide. However, the mechanisms of these reactions are not yet well understood. Among them, the oxidation of the aromatic amino acid tyrosine is of particular interest. We therefore undertook a kinetics and mechanistic study of carbon dioxide catalyzed reaction of peroxynitrite with phenols as model compounds of tyrosine. The main objectives were: (i) to clarify the identities of the reactive species formed, (ii) to elucidate the reaction mechanisms with phenols and, (iii) to contribute to the understanding of action of phenolic antioxidants.

Objectives

SUMMARY

The mechanism of carbon dioxide catalyzed oxidations by peroxynitrite are commonly rationalized in terms of formation of trioxocarbonate(•1–) / nitrogen dioxide radical pair in *ca.* 30% yield. Peroxynitrite and carbon dioxide first form an adduct, which itself is considered too short-lived to be a relevant oxidant, and which homolyses to a radical pair. With phenols, only biphenols and nitrophenols have been reported as oxidation products. Formation of these products would be in accordance with a radical mechanism, whereby phenoxyl radicals are produced by the reaction of trioxocarbonate(•1–) with phenol and phenolate, and nitrogen dioxide with phenolate. Coupling of phenoxyl radicals with each other and with nitrogen dioxide yields nitro- and biphenols. Formation of biphenols at higher pH was considered as an additional proof of a radical mechanism.

We reinvestigated this reaction and discovered important aspects that were overlooked.

Products. With phenol in excess, product yields are not higher than *ca.* 20% relative to peroxynitrite. The detected products are: 2-nitrophenol, 4-nitrophenol, 2,2′-biphenol, 4,4′-biphenol, and *para*-benzoquinone, previously unreported. The dependence of product yields on peroxynitrite, carbon dioxide and phenol concentrations, and on pH was studied. The isomer ratio of 2,2′- to 4,4′-biphenols changes with pH and phenol concentration, while the ratio of 2- to 4-nitrophenols is constant, *ca.* 1.4 to 1. The yields of 2-nitrophenol, 4-nitrophenol and 4,4′-biphenol decrease with pH and phenol concentration, while the yield of 2,2′-biphenol increases. The dependence of the *para*-benzoquinone yield is more complex and requires optimal phenolate concentrations. At pH 7 and 10, this yield is maximal at a phenol-to-peroxynitrite ratio of *ca.* 3 : 1, and *ca.* 1 : 10, respectively. Increasing the carbon dioxide concentration suppresses formation of 2,2′-biphenol, but favors

formation of all four isomeric biphenols and nitrophenols as well as the formation of *para*-benzoquinone.

Biphenols. The yield of 4,4′-biphenol decreases with pH and phenol concentration, while the yield of 2,2′-biphenol increases. Thus, the carbon dioxide catalyzed oxidative coupling of phenol by peroxynitrite occurs by two pathways distinguished by the isomer ratio of 2,2′- to 4,4′-biphenols. At neutral pH and moderate phenol concentrations, both biphenols are formed in comparable yields, most probably, by coupling of two phenoxyl radicals. Nitrophenols are likely to be formed *via* this pathway, too, and thus the reactive intermediate is a trioxocarbonate(•1–) and nitrogen dioxide radical pair. At high pH and phenol concentration, 2,2′-biphenol is the only identified coupled product, and its formation does not involve phenoxyl radicals. Instead, under conditions favoring the formation of 2,2′-biphenol, a previously unreported long-lived ($t_{1/2}$ ~ 10 s at pH 10 and 1 mM phenol) diamagnetic intermediate with an absorption maximum at 400 nm is observed. This intermediate is formed from phenolate concomitantly with the decay of peroxynitrite and, when sufficient excess of phenol is present, disappears *via* reaction with phenol, to form 2,2′-biphenol.

***Para*-benzoquinone.** *Para*-benzoquinone is formed in up to 5% yield relative to the initial peroxynitrite concentration. Given a maximum 20% product yield, it is one of the major reaction products, previously overlooked, no doubt, due to its instability in alkaline aqueous solutions. We confirmed the formation of *para*-benzoquinone by three methods – HPLC, MS, and the kinetics of its disappearance in alkaline solutions as followed by UV-Vis spectrophotometry. *Para*-benzoquinone is a product of four-electron oxidation of phenol and, given that peroxynitrite is at best a two-electron oxidant, must be formed by oxidation of a precursor. The appearance of an absorption band above 500 nm, which might be due to quinhydrone, a 1:1 charge-transfer complex between hydroquinone and

benzoquinone, indicates that hydroquinone is a likely *para*-benzoquinone precursor. The dependence of *para*-benzoquinone yields on pH and phenol concentration suggests that its formation is related to the non-radical pathway of 2,2′-biphenol formation. Indeed, the maximum yields of *para*-benzoquinone require an optimal phenolate concentration. It is likely therefore, that *para*-benzoquinone and 2,2′-biphenol stem from a common intermediate, which itself requires phenolate and may isomerize to hydroquinone or react with another phenolate molecule to form 2,2′-biphenol.

Intermediate. The identity of the intermediate, that is both a 2,2′-biphenol and hydroquinone precursor, is of interest. Because of its low yields (*ca.* 20 μM) and relatively short lifetime (~100 s), we were unable to characterize the intermediate by conventional structural methods. We thus studied the kinetics of its formation and decay in a wide concentration and pH range, its reactivity by a sequential-mix stopped-flow kinetics experiments, and characterized it by ESR spectrometry and UV-Vis spectrophotometry. Given the absence of the ESR signal, this intermediate is diamagnetic; it has an absorption maximum at 400 nm with $\varepsilon_{400} = (61 \pm 1) \times 10^3$ $M^{-1}cm^{-1}$, and its UV-Vis spectrum remains unchanged over, at least, the pH range 5 to 11. The intermediate is formed at alkaline pH concomitantly with the decay of peroxynitrite and disappears *via* reaction with phenol and/or phenolate ($k = (40 \pm 9)$ $M^{-1}s^{-1}$ at pH 7.2 and $k = (30 \pm 1) \times 10$ $M^{-1}s^{-1}$ at pH 10.6), concomitantly with the formation of 2-2′-biphenol. The yield of this intermediate is proportional to peroxynitrite and phenolate concentrations, and it decreases somewhat with increasing carbon dioxide concentration from 2 to 20 mM. The study of pH and phenol concentration dependencies indicates that this intermediate is only formed from phenolate. The maximal yield of 2-2′-biphenol relative to the concentration of the intermediate is ca. 65%. At alkaline pH, when phenolate is the limiting reagent, p*ara*-benzoquinone is a major reaction product.

Under these conditions, the decay of the intermediate becomes zero-order and independent of the phenol concentration. The zero-order decay is probably due to a fast ($k = (7.7 \pm 0.5) \times 10^7$ $M^{-1}s^{-1}$ at pH 10.5) reaction between the intermediate and hydroquinone, which, in turn, is formed during the alkaline hydrolysis of a *para*-benzoquinone. At pH > 12 the intermediate decays *via* the reaction with hydroxide ($k \sim 100$ $M^{-1}s^{-1}$). The intermediate reacts rapidly with biologically important reductants. The second-order rate constant at pH 7 are $(4.2 \pm 0.1) \times 10^5$ $M^{-1}s^{-1}$ with ascorbate, $(6.2 \pm 0.1) \times 10^4$ $M^{-1}s^{-1}$ with dithionite, $(1.15 \pm 0.05) \times 10^5$ $M^{-1}s^{-1}$ with L-glutathione, $(1.24 \pm 0.07) \times 10^5$ $M^{-1}s^{-1}$ with L-cysteine, $(3.3 \pm 0.3) \times 10^4$ $M^{-1}s^{-1}$ with *N*-acetyl-L-cysteine, and $(3.9 \pm 0.5) \times 10^5$ $M^{-1}s^{-1}$ with hydroquinone. The intermediate is likely to be a two-electron oxidant. As an example, it reacts with dithionite ($S_2O_4^{2-}$), rather than with $SO_2^{\bullet-}$. Hydroquinone is oxidized to *para*-benzoquinone quantitatively.

Substituted phenols. Phenols bearing electron-withdrawing groups, *e.g* cyano and nitro, do not form the intermediate. *Para*-substituted phenols do not form intermediates with appreciable absorption above 350 nm. *Diortho*-substituted phenols form two consecutive intermediates with maxima at *ca.* 420 nm and *ca.* 360, these intermediates are likely to give rise to corresponding *para*-quinones at alkaline pH. We suggest that the key intermediate in biphenol and quinone formation might be a *para*-nitrito-substituted cyclohexadienone.

Two pathway of biphenol formation and the reactive intermediates in carbon dioxide catalyzed decay of peroxynitrite. We conclude that two reactive pathways operate during the carbon dioxide catalyzed oxidative coupling of phenol by peroxynitrite; one that predominates at neutral pH and another at higher pH. We suggest that the first pathway is the commonly accepted one, through the formation of trioxocarbonate(•1–) / nitrogen dioxide radical pair that leads to the formation of phenoxyl radicals and their subsequent recombination with each other and nitrogen

dioxide at *ortho* and *para* positions. The second pathway is novel and leads to 2-2′-biphenol. This pathway operates though the formation of a diamagnetic intermediate and its consecutive coupling with phenol. This process does not involve any phenoxyl radicals, as no 4,4′-biphenol or nitrophenols are formed. The partition between the pathways depends on pH, phenol and carbon dioxide concentrations. Phenolate is the reacting species in the second pathway, therefore, high pH and phenol concentration facilitate the formation of 2,2′-biphenol. Carbon dioxide increases the rate of radical generation and therefore favors the radical pathway and formation of all four isomeric bi- and nitrophenols. The existence of the two different pathways of biphenol formation implies that, apart from the trioxocarbonate(•1–)/nitrogen dioxide radical pair, another reactive intermediate is formed during the carbon dioxide catalyzed decay of peroxynitrite. This intermediate is likely to be the peroxynitrite/carbon dioxide adduct, which was previously considered too short-lived to react. Our estimates suggest that its lifetime could be in the millisecond range, which implies that it is a biologically relevant oxidant and subject to scavenging *in vivo*. Our finding of a new non-radical pathway of 2,2′-biphenol formation might be relevant to the mechanism of peroxynitrite reactions with phenolic anti-oxidants. For instance, sinapinic acid, which is, in essence, a 2,4,6-substituted phenol, is known to be a particularly efficient inhibitor of a peroxynitrite-mediated nitration. In the absence of any substrates, it reacts with peroxynitrite to exclusively give mono-lactone – a product of oxidative coupling. We have observed that sinapinic acid gives rise to colored intermediates and thus its oxidative coupling might proceed *via* coupling of initially formed diamagnetic intermediate with another molecule of sinapinic acid, rather than *via* coupling of the two aryloxyl radicals, as considered previously.

ZUSAMMENFASSUNG

Die Mechanismen der durch Kohlendioxid-katalysierten Oxidationen mit Peroxynitrit werden allgemein durch die Bildung des Trioxocarbonat(•1–) / Stickstoffdioxid Radikalpaars in einer Ausbeute von *ca.* 30% erklärt. Peroxynitrit und Kohlendioxid bilden zuerst ein Addukt, welches aber selbst zu kurzlebig ist, um ein relevantes Oxidans zu sein und sogleich teilweise zum Radikalpaar homolysiert. Bei den durch Kohlendioxid katalysierten Oxidationen von Phenolen mit Peroxynitrit wurden Biphenole und Nitrophenole als einzige Produkte gefunden. Die Bildung dieser Produkte wäre im Einklang mit einem Radikalmechanismus, bei welchem Phenoxylradikale einerseits durch die Reaktion von Trioxocarbonat(•1–) mit Phenol und Phenolat und andererseits durch die Reaktion von Stickstoffdioxid mit Phenolat gebildet werden.

Die Reaktion von Phenoxylradikalen miteinander führt zu Biphenolen, während die Reaktion von Phenoxylradikalen mit Stickstoffdioxid Nitrophenole liefert. Die Bildung von Biphenolen bei höheren pH-Werten wurde als zusätzlicher Nachweis eines Radikalmechanismus betrachtet.

Wir haben diese Reaktion nochmals untersucht und dabei wichtige Merkmale, welche zuvor übersehen wurden, gefunden.

Produkte. Mit Phenol im Überschuss sind die Ausbeuten an Produkt nicht höher als *ca.* 25% relativ zu Peroxynitrit. Die Produkte, die gefunden werden konnten, sind 2-Nitrophenol, 4-Nitrophenol, 2,2′-Biphenol, 4,4′-Biphenol und das zuvor nicht identifizierte *para*-Benzochinon. Die Abhängigkeiten der Produktausbeuten von der Peroxynitrit-, Kohlendioxid- und Phenolkonzentration sowie vom pH-Wert wurde genauer untersucht. Dabei wurde herausgefunden, dass das Verhältnis der Biphenolenausbeuten vom pH-Wert und der Phenolkonzentration abhängt, das Verhältnis zwischen 2- zu 4-Nitrophenol aber

einen konstanten Wert von *ca.* 1.4 besitzt. Mit grösser werdendem pH-Wert und steigender Phenolkonzentration nehmen die Ausbeuten an 2-Nitrophenol, 4-Nitrophenol und 4,4′-Biphenol ab und jene an 2,2′-Biphenol zu. Die Abhängigkeit der Ausbeute an *para*-Benzochinon ist komplexer und erfordert optimale Phenolatkonzentrationen. Die Ausbeuten sind maximal bei pH 7 und einem Phenol zu Peroxynitrit Verhältnis von ca. 3:1 sowie pH 10 und einem Verhältnis von ca. 1:10. Eine steigende Kohlendioxidkonzentration unterdrückt die Bildung von 2,2′-Biphenol und favorisiert die Bildung von 2- und 4-Nitrophenol, 4,4′-Biphenol und *para*-Benzochinon.

Biphenole. Mit grösser werdendem pH-Wert und steigender Phenolkonzentration nimmt die Ausbeute an 4,4′-Biphenol ab und jene an 2,2′-Biphenol zu. Also erfolgt die durch Kohlendioxid katalysierte oxidative Kupplung von Phenol durch Peroxynitrit auf zwei verschiedenen Wegen, welche durch das Verhältnis der isomeren 2,2′- zu 4,4′-Biphenole unterschieden werden können. Bei neutralem pH und moderaten Phenolkonzentrationen werden beide Biphenole, wahrscheinlich durch Kopplung zweier Phenoxylradikale, mit beachtlicher Ausbeute gebildet. Nitrophenole werden wahrscheinlich auch auf diese Weise mit einem Trioxocarbonat(•1–)/Stickstoffdioxid Radikalpaar als Zwischenprodukt gebildet. Bei hohem pH und hohen Phenolkonzentrationen kann als einziges gekoppeltes Produkt nur 2,2′-Biphenol identifiziert werden, welches nicht über ein Phenoxylradikal gebildet wird. Unter Bedingungen, welche die Bildung des 2,2′-Biphenols fördern, kann man sogar ein bisher nicht beschriebenes langlebiges ($t_{1/2}$ ~ 10 s bei pH 10 und 1 mM Phenol) diamagnetisches Zwischenprodukt mit einem Absorptionsmaximum bei 400 nm erkennen. Zeitgleich mit dem Zerfall von Peroxynitrit wird dieses Intermediat aus Phenolat gebildet und verschwindet durch Reaktion mit Phenol, wodurch das 2,2′-Biphenol entsteht.

***Para*-Benzochinon.** *Para*-Benzochinon wird in Mengen von bis zu 5% der ursprünglichen Peroxinitritkonzentration gebildet. Unter der Annahme einer maximal 25%igen Ausbeute an Produkten handelt es sich dabei um ein Hauptprodukt der untersuchten Reaktion, welches bisher auf Grund seiner Instabilität in alkalischen wässrigen Lösungen zweifelsohne übersehen wurde. Uns ist es gelungen, die Bildung von *para*-Benzochinon mittels dreier unterschiedlicher Methoden nachzuweisen: HPLC, MS und durch Kinetische Messung, wobei in alkalischen Lösungen das Verschwinden UV-Vis spektroskopisch verfolgt wurde. *Para*-Benzochinon ist das Produkt einer Vierelektronen-Oxidation von Phenol und muss – unter der Voraussetzung, dass Peroxynitrit höchstens ein Zweielektronen Oxidans ist – durch Oxidation eines oder mehrerer ursprünglich gebildeter Vorgänger entstanden sein. Das Auftauchen einer Absorptionsbande oberhalb von 500 nm ist ein Indiz für eine Zwischenstufe, bei welcher es sich um einen 1:1 Charge-Transfer-Komplex zwischen Hydrochinon und Benzochinon handeln könnte. Das bedeutet, dass Hydrochinon sehr wahrscheinlich eine Vorstufe des *para*-Benzochinons ist. Die Abhängigkeit der Ausbeute an *para*-Benzochinon vom pH-Wert und der Phenolkonzentration deutet darauf hin, dass seine Bildung mit jener des 2,2′-Biphenols, welche über einen nicht radikalischen Weg erfolgt, verwandt ist.

Zwischenprodukt. Die Identität des Zwischenprodukts (ein 2,2′-Biphenol und Hydrochinon Vorläufer) ist von grossem Interesse. Auf Grund seiner sehr geringen Ausbeute (*ca.* 20–30 μM) und relativ kurzen Lebenszeit (*ca.* 100 s) war es uns nicht möglich, dieses Zwischenprodukt mit konventionellen Strukturaufklärungsmethoden zu charakterisieren. Wir untersuchten stattdessen die Kinetik seiner Bildung und seines Zerfalls über einen grossen Konzentrations- und pH-Bereich hinweg. Seine Reaktivität studierten wir in sequentiellen Stopped-flow Kinetik Experimenten. Zudem charakterisierten wir das Zwischenprodukt mittels

ESR-Spektrometrie und UV-Vis-Spektrophotometrie. Auf Grund der Absenz eines ESR-Signals muss das Zwischenprodukt diamagnetisch sein. Das UV-Vis-Spektrum des Zwischenprodukts zeigt ein Absorptionsmaximum bei 400 nm mit $\varepsilon_{400} = (61 \pm 1) \times 10^3\ M^{-1}cm^{-1}$ und bleibt unverändert über einen pH-Bereich von mindestens 5 bis 11. Das Zwischenprodukt wird bei alkalischem pH zeitgleich mit dem Zerfall des Peroxynitrits gebildet. Es wird durch Reaktion mit Phenol und/oder Phenolat ($k = (40 \pm 5)\ M^{-1}s^{-1}$ bei pH 7.2 und $k = (30 \pm 1) \times 10\ M^{-1}s^{-1}$ bei pH 10.6) unter zeitgleicher Bildung des 2,2′-Biphenols abgebaut. Die Ausbeute an Zwischenprodukt ist proportional zur Peroxynitrit- und Phenolat-Konzentration und nimmt mit steigender Kohlendioxidkonzentration von 2 bis 20 mM etwas ab. Die Untersuchungen der Abhängigkeiten der Ausbeute vom pH-Wert und der Phenolkonzentration deuten darauf hin, dass das Zwischenprodukt nur ausgehend von Phenolat gebildet werden kann. Die maximale Ausbeute an 2,2′-Biphenol beträgt über 60% relativ zur Konzentration des Zwischenprodukts. Bei alkalischem pH, mit Phenolat als limitierendem Reagens, ist *para*-Benzochinon das Hauptreaktionsprodukt. Unter diese Bedingungen ist der Zerfall des Zwischenproduktes nullter Ordnung und unabhängig von der Phenolkonzentration. Ein Zerfall nullter Ordnung kommt vermutlich durch eine schnelle Reaktion ($k = (7.7 \pm 0.5) \times 10^7\ M^{-1}s^{-1}$ bei pH 10.5) zwischen dem Zwischenprodukt und Hydrochinon zustande. Letzteres wird durch alkalische Hydrolyse des *para*-Benzochinons gebildet. Bei pH > 12 zerfällt das Zwischenprodukt, indem es mit Hydroxid reagiert ($k \sim 100\ M^{-1}s^{-1}$). Das Zwischenprodukt reagiert sehr schnell mit biologisch relevanten Reduktionsmitteln. Die Geschwindigkeitskonstanten zweiter Ordnung sind bei pH 7 $(4.2 \pm 0.1) \times 10^5\ M^{-1}s^{-1}$ mit Ascorbat, $(6.2 \pm 0.1) \times 10^4\ M^{-1}s^{-1}$ mit Dithionit, $(1.15 \pm 0.05) \times 10^5\ M^{-1}s^{-1}$ mit L-Glutathion, $(1.24 \pm 0.07) \times 10^5\ M^{-1}s^{-1}$ mit L-Cystein, $(3.3 \pm 0.3) \times 10^4\ M^{-1}s^{-1}$ mit *N*-Acetyl-L-Cystein und $(3.9 \pm 0.5) \times 10^5\ M^{-1}s^{-1}$ mit Hydrochinon. Sehr wahrscheinlich handelt es sich beim

Zwischenprodukt um ein Zweielektronen-Oxidans. Es reagiert z.B. eher mit Dithionit ($S_2O_4^{2-}$) als mit $SO_2^{\bullet-}$. Hydrochinon wird quantitativ zu *para*-Benzochinon oxidiert.

Substituierte Phenole. Phenole mit elektronenziehenden Substituenten, z.B. Cyano- oder Nitro-Gruppen, bilden das eben beschriebene Zwischenprodukt nicht aus. Die Kinetik der Bildung von Biphenolen oder Chinonen wird durch Substituenten in *ortho*- oder *para*-Position beeinflusst. *Para*-substituierte Phenole bilden Zwischenprodukte mit einem Absorptionsmaximum bei *ca.* 300 nm und Extinktionskoeffizienten, welche *ca.* hundertmal tiefer sind als bei Phenolen mit einer unbesetzten *para*-Position. *Diortho*-substituierte Phenole bilden zuerst Zwischenprodukte mit einem Absorptionsmaximum bei *ca.* 400 nm. Ausgehend von diesen werden weitere Zwischenprodukte mit einem Absorptionsmaximum bei *ca.* 350 nm erhalten, welche ihrerseits zu den entsprechenden *para*-Chinonen zerfallen. Wir vermuten, dass das alles entscheidende Zwischenprodukt der Bildung von Biphenolen und Chinonen ein *para*-Nitrito-substituiertes Cyclohexadienon sein könnte.

Zwei Reaktionswege der Bildung von Biphenol und die dabei auftretenden reaktiven Zwischenprodukte beim Kohlendioxid katalysierten Zerfall von Peroxynitrit. Auf Grund unserer Beobachtungen folgern wir, dass bei der Kohlendioxid-katalysierten oxidativen Kupplung von Phenolen durch Peroxinitrit zwei verschiedene Reaktionswege existieren. Der eine davon dominiert bei neutralen und der andere bei höheren pH-Werten. Der erste Reaktionsweg ist der bereits bekannte und allgemein anerkannte, bei welchem ein Trioxocarbonat(•1) / Stickstoffdioxid Radikalpaar als Zwischenprodukt auftritt. Ausgehend von diesem werden Phenoxylradikale gebildet, deren Rekombination miteinander und mit Stickstoffdioxid an *ortho* und *para* Positionen erfolgt. Der zweite Reaktionsweg ist neu und führt zu 2,2′-Biphenol. Dieses entsteht über die

Bildung eines diamagnetischen Zwischenprodukts und dessen anschliessender Kopplung mit Phenol. Da weder 4,4′-Biphenol noch Nitrophenole gebildet werden, treten bei diesem Reaktionsweg keine Phenoxylradikale auf.

Die Produktverteilung und die damit verknüpften Reaktionswege werden durch den pH-Wert sowie durch die Phenol- und Kohlendioxidkonzentrationen gesteuert. Beim zweiten Reaktionsweg ist Phenolat die reagierende Spezies, wodurch ein hoher pH-Wert sowie eine hohe Phenolkonzentration die Bildung von 2,2′-Biphenol erleichtern. Kohlendioxid erhöht die Radikalbildung, woraus ein radikalischer Reaktionsweg resultiert und alle vier isomeren Bi- und Nitrophenole gebildet werden. Die Existenz zweier unterschiedlicher Reaktionswege impliziert, dass neben dem Trioxocarbonat(•1)/Stickstoffdioxid Radikalpaar noch eine weiteres reaktives Zwischenprodukt während des Kohlendioxid-katalysierten Zerfalls von Peroxynitrit gebildet werden muss. Dieses Zwischenprodukt ist wahrscheinlich das Peroxinitrit/Kohlendioxid Addukt, welches bis anhin als zu kurzlebig betrachtet wurde, um weiterreagieren zu können. Wir schätzen, dass die Lebenszeit im Bereich von Millisekunden liegen könnte, was bedeutet, dass es ein biologisch relevantes Oxidationsmittel ist und *in vivo* als Radikalfänger dient. Unsere Entdeckung eines nicht radikalischen Reaktionswegs der Bildung von 2,2′-Biphenol könnte auch relevant für Reaktionsmechanismen von Peroxynitrit mit phenolischen Antioxidantien sein. So z.B. auch Sinapinsäure, im Wesentlichen ein 2,4,6-substituiertes Phenol, welche als sehr effizienter Hemmer der Nitrierung durch Peroxynitrit bekannt ist. In Abwesenheit eines Substrats reagiert es mit Peroxynitrit ausschliesslich zu mono-Lacton, einem Produkt der oxidativen Kopplung. Wir haben beobachtet, dass Sinapinsäure zu farbigen Zwischenprodukten führt und seine oxidative Kopplung somit über die Kopplung eines ursprünglich gebildeten diamagnetischen Zwischenprodukts mit einem

anderen Sinapinsäure-Molekül verläuft, und nicht wie ursprünglich angenommen wurde, über die Kopplung zweier Aryloxylradikale.

1 INTRODUCTION

1.1 Brief history of peroxynitrite

Peroxynitrous acid is a strong inorganic oxidant, discovered in 1901 by Baeyer and Villiger, who reported that a mixture of hydrogen peroxide and nitrous acid has unusual oxidizing properties [1]. In 1929 Gleu and Roell published the correct formula of peroxynitrous acid, ONOOH [2]. In 1952 Halfpenny and Robinson showed that peroxynitrous acid hydroxylates and nitrates aromatic compounds and rationalized their observation in terms of homolysis of peroxynitrous acid to hydroxyl and nitrogen dioxide radicals [3]. Generally, there was a lack of interest in the chemistry of peroxynitrous acid and its conjugated anion, peroxynitrite, until the nineties. At that time, attention was drawn to peroxynitrite again, but this time to its role in biochemistry. The physiological role of nitrogen monoxide had been discovered [4,5], and it was suggested that peroxynitrite could be formed *in vivo* from nitrogen monoxide and superoxide [6], and that this specie plays an important role in nitrogen monoxide induced toxicity [7].

1.2 Nitrogen monoxide in biology

The discovery of the biological functions of nitrogen monoxide[1] in the eighties came as a complete surprise. Nitrogen monoxide acts as a short-lived signaling molecule in the body. Signal transmission by a small molecule, produced in one cell, but which penetrates membranes and regulates the function of other cells constitutes an entirely new principle for signaling in the human organism. The Nobel Prize in Medicine in 1998 was awarded to Robert F. Furchgott, Louis J.

[1] A commonly used trivial name for nitrogen monoxide is nitric oxide

Ignarro, and Ferid Murad for their discovery, and this has stimulated the intense interest in biochemistry of nitrogen monoxide and related species. Nitrogen monoxide was named "Molecule of the Year" in 1992 by the journal Science, a "Nitric Oxide Society" was founded, and a scientific journal devoted entirely to nitrogen monoxide was created. It is estimated that yearly about 3,000 scientific articles about the biological roles of nitrogen monoxide are published.

1.3 Peroxynitrite and its relevance in biology

Superoxide is a radical, generated in oxygen-metabolizing cells by a one-electron reduction of dioxygen. *In vivo*, it is efficiently eliminated by the enzyme superoxide dismutase (SOD). This enzyme was known to reduce injury in many diseases, which implicated superoxide as a toxic species *in vivo* [8]. Because superoxide itself is a mild reductant and not very reactive, the protection by SOD was explained by scavenging of superoxide and therefore preventing the reduction of unidentified iron(III) complexes, which in turn prevented the Fenton reaction and the formation of hydroxyl radicals. According to this scenario, a redox-active metal ion is required, and since their concentration is extremely low *in vivo* and Fenton-type reactions are not fast, that was not a satisfactory explanation [6].

In 1990, Beckman and co-workers suggested that nitrogen monoxide reacts with superoxide to form peroxynitrite *in vivo* [6]. Peroxynitrite decomposition generates a strong oxidant with reactivity similar to hydroxyl radical and thus its formation *in vivo* would lead to injury. SOD would reduce superoxide levels and thus partly or completely inhibit formation of peroxynitrite and reduce the injury. The remarkable feature of this hypothesis is that a strong oxidant is generated from precursors that are at best weakly oxidizing in a reaction that does not involve metal ions.

Calculations show that formation of peroxynitrite *in vivo* is plausible [9]. The rate constant of the reaction between superoxide and nitrogen monoxide, measured by pulse radiolysis, ranges from 3 to 6 × 10^9 $M^{-1}s^{-1}$ [10-12]. A value, determined by three different flash photolysis experiments, is even higher – (1.6 ± 0.3) × 10^{10} $M^{-1}s^{-1}$ [13]. The rate constant of reaction of superoxide with SOD, determined in the seventies, is 2.3 × 10^9 $M^{-1}s^{-1}$ at pH 7 [14]. Recently, Michel et al. [15] revised this value downwards. They determined the second-order rate constant of (0.7 ± 0.1) × 10^9 $M^{-1}s^{-1}$ at pH 7 and physiologically relevant ionic strength of 150 mM, and assumed that previous experiments were contaminated with trace amount of free copper. Still, under normal conditions in the cell, where the levels of SOD and nitrogen monoxide are *ca.* 10 μM and 10 nM, respectively, all superoxide is scavenged by SOD and peroxynitrite is not formed [16]. However, if the concentration of nitrogen monoxide increases, for instance, in the event of an immune response, the formation of peroxynitrite becomes more feasible. Furthermore, peroxynitrite can be formed outside a cell, for instance, near activated macrophages, where the concentration of nitrogen monoxide is *ca.* 10 μM [17] and that of SOD is likely to be lower than 10 μM, and diffuse inside a cell after protonation. The *in vivo* formation of peroxynitrite is indirectly supported by experimental observation that SOD increases the biological activity of nitrogen monoxide [18].

The hypothesis that peroxynitrite is formed *in vivo* has revolutionized toxicology, and an intense investigation by biochemists, radical and inorganic chemists begun. This process is reflected in the number of publications found in "Scifinder" with a research topic "peroxynitrite" (Figure 1). Starting from 1990 the number of publication increased and has now reached a level of *ca.* 900 per year (Figure 1).

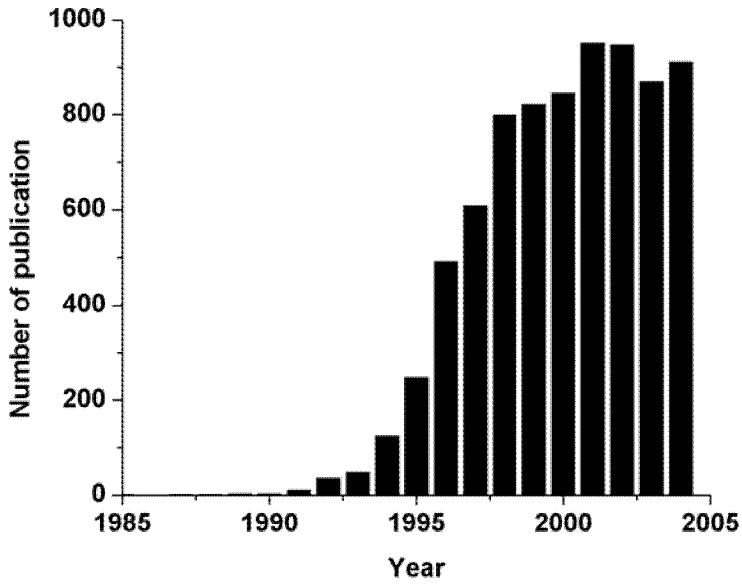

Figure 1. Number of publications per year found in SciFinder with the research topic "peroxynitrite".

1.4 Physiologically relevant reactions of peroxynitrite

At a physiological pH of 7.2–7.4, peroxynitrite is mostly deprotonated. The peroxynitrite anion is reasonably stable and non-oxidizing. However, it becomes a strong oxidant when protonated or combined with a Lewis acid. Given the rate constant of 5.8×10^4 $M^{-1}s^{-1}$ at 37°C [19], and an *in vivo* concentration of carbon dioxide of *ca.* 1.3 mM[2], the latter should efficiently scavenge any peroxynitrite anion generated in biological fluids [20]. Carbon dioxide modulates the reactivity of peroxynitrite, changes the rates of oxidations, the yields and distribution of the oxidized products. In particular, the yields of aromatic nitration increase several fold in the presence of carbon dioxide [19,20].

Under *in vivo* conditions of low pH, peroxynitrous acid (pK_a = 6.8) can be relevant, too. Peroxynitrous acid reacts rapidly (*ca.* 10^3 $M^{-1}s^{-1}$) with thiols [21] and,

[2] Most physiological fluids contain 20 – 25 mM carbonate, which, under physiological conditions, is in equilibrium with *ca.* 1.3 mM carbon dioxide.

given the *in vivo* concentration of glutathione of several mM, would predominantly react with this molecule [22]. Peroxynitrous acid also reacts with heme proteins, which catalyze its decay [23].

1.5 Properties of peroxynitrite and peroxynitrous acid

Peroxynitrite is a relatively stable anion while peroxynitrous acid isomerizes rapidly to nitrate [24-26].

The peroxynitrite anion has a UV absorption maximum at 302 nm with ε = 1700 $M^{-1}cm^{-1}$ [27]; the values for peroxynitrous acid are *ca.* 250 nm with ε = 600 $M^{-1}cm^{-1}$ and there is no appreciable absorption above 300 nm [24].

The values for the pK_a of peroxynitrous acid listed in the literature vary from *ca.* 5 to 8 [9]. The discrepancy is no doubt due to the instability and reactivity of peroxynitrous acid. The decay of peroxynitrite is accelerated in the presence of almost all buffers: borate, HEPES, formate, ammonia, and phosphate, which results in overestimated pK_a values [24]. Phosphate buffers are found to be the most inert and the pK_a extrapolated to zero phosphate buffer concentrations is 6.5 [24]. The correct value in 100 mM phosphate buffer and the one most commonly used is 6.8.

The one-electron electrode potential of a peroxynitrous acid was calculated to be 1.6 ± 0.1 [9] and 1.70 V [28] at pH 7 and the two-electron electrode potential 1.3 ± 0.1 [9] and 1.37 [28] at pH 7. The former estimates refer to the potential of the ONOOH, H^+ / $NO_2^{\bullet}$, H_2O couple. However, as follows from electrochemical measurements, the one-electron reduction of peroxynitrous acid is pH-independent at pH range 3.2 to 5.6 and therefore the ONOOH, H^+ / $NO_2^{\bullet}$, H_2O couple cannot account for the oxidative chemistry of peroxynitrous acid [29]. It is possible that oxidations by peroxynitrous acid proceed *via* a short-lived intermediate $[ONOOH]^{\bullet-}$. A similar radical anion has been identified after the reduction of nitrite by hydrated electrons [30].

The peroxynitrite anion is not oxidizing. Koppenol et al. [25] estimated the electrode potential of the couple $ONOO^{\bullet}$ / $ONOO^{-}$ to be 0.43 ± 0.13 V. Goldstein et al. obtained a value of 0.8 V from the kinetics of its oxidation by inorganic radicals and supported it by a theoretical estimate of 0.9 V [31]. From electrochemical measurements, the electrode potential of the couple $ONOO^{\bullet}$ / $ONOO^{-}$ is 0.51 ± 0.02 V [32].

1.5.1 Decay of peroxynitrite

The disappearance of peroxynitrite proceeds *via* 2 pathways. Peroxynitrous acid isomerizes to nitrite (reaction 1).

$$ONOOH \rightarrow H^{+} + NO_3^{-} \quad (1)$$

Under neutral and alkaline pH peroxynitrite decays slowly to dioxygen and nitrite (reaction 2) [33].

$$ONOOH + ONOO^{-} \rightarrow O_2 + 2NO_2^{-} + H^{+} \quad (2)$$

1.5.1.1 Isomerization of peroxynitrous acid

The rate constant of the isomerization of peroxynitrous acid to nitrate is 1.25 ± 0.05 s^{-1} at 25°C. Some reactions of peroxynitrous acid are zero-order in the substrate that is being oxidized and afford only maximum yields of 30–40%. It was suggested, therefore, that a highly oxidizing intermediate is formed in a rate-limiting step (reaction 4) on a minor pathway of peroxynitrous acid isomerization to nitrate (reactions 4–6).

$$ONOO^{-} + H^{+} \rightleftarrows ONOOH \quad (3)$$

$$ONOOH \xrightarrow{\text{rate limiting}} ONOOH^{*} \quad (4)$$

$$ONOOH \longrightarrow NO_3^- + H^+ \quad (5)$$

$$ONOOH^* \longrightarrow NO_3^- + H^+ \quad (6)$$

The identity of this intermediate is hotly debated. Presently, the two major views on peroxynitrite reactivity are (i) homolysis of peroxobond, and (ii) formation of activated forms (for instance, a rotationally activated trans-isomer).

1.5.1.2 Decay to nitrite and dioxygen

Above the pK_a of peroxynitrous acid, the decay of peroxynitrite to nitrite and dioxygen in 2:1 stochiometry (reaction 2) becomes increasingly important. Radical and non-radical mechanisms were suggested to rationalize the kinetics of the decay and product distribution.

Pfeiffer et al. [33] reported that the nitrite-to-nitrate ratio increased with pH and temperature and was independent of the total peroxynitrite concentration. They suggested that nitrite might be formed *via* reactions 7–9. This sequence leads to the net reaction 2.

$$ONOOH \rightleftarrows OH^\bullet + NO_2^\bullet \quad (7)$$

$$OH^\bullet + ONOO^- \rightarrow OH^- + NO^\bullet + O_2 \quad (8)$$

$$NO^\bullet + NO_2^\bullet \rightarrow N_2O_3 \xrightarrow{H_2O} 2NO_2^- + 2H^+ \quad (9)$$

Kissner et al. [24] observed that at slightly alkaline pH, the decay of more concentrated peroxynitrite solutions becomes slower and deviates from the first-order behavior, the deviation being proportional to the square of the total peroxynitrite concentration. To rationalize these kinetics, they proposed the formation of a 1:1 adduct between peroxynitrite and peroxynitrous acid (reaction 10). Later Kissner et al. found that the contribution of the decay pathway (reaction

2) is higher at higher peroxynitrite concentration, *i.e.* under conditions that favor the formation of the adduct, and proposed that the adduct X^- between peroxynitrite and peroxynitrous acid decays to nitrite and dioxygen (reaction 11) [34].

$$ONOOH + ONOO^- \leftrightarrow X^- \quad (10)$$

$$X^- \rightarrow 2NO_2^- + O_2 + H^+ \quad (11)$$

Lymar et al. [35] criticized the results of Kissner et al., pointing out that (i), in their hands, the yields of nitrite are independent of the total peroxynitrite concentration and (ii) at sufficiently high concentration of peroxynitrite, the decay half-time becomes concentration-independent. The second observation, according to Lymar et al., supports the mechanism in which reaction 7 initiates the decay, but contradicts the bimolecular mechanism (reactions 10–11), in which the rate of decay should be always proportional to peroxynitrite concentration. Lymar et al. supplemented reactions 7–9 with other possible radical pathways of peroxynitrite decay. The calculated yields of nitrite and nitrate, and the rate of peroxynitrite decay, were in good agreement with their experimental results. Because the individual rate constants of all reactions, used for modeling, were independently measured, Lymar et al. [35] considered this as an additional support of a radical mechanism.

In a rebuttal paper [16] Kissner et al. pointed out the following: (i) Their nitrite and nitrate determinations were more reliable, because they determined both nitrite and nitrate, and always obtained mass balance. Lymar et al. only determined nitrite, and the nitrite yields may have been inflated by extra nitrite generated in concentrated peroxynitrite solutions at room temperatures. In addition, the analytical results of another group [36] are very similar to those of Kissner et al. (ii) Lymar et al. had argued [35] that, because at sufficiently high concentration the decay rate becomes concentration-independent, the bimolecular mechanism is

inadequate. Kissner et al. [16] pointed out that this is only true if one assumes that an adduct is present in steady state concentrations. They list rate constants for reactions 10 and 11 from which it is evident that the steady state approximation may not be applied. In fact, the bimolecular model provides an even better fit for a concentration dependence of reaction 2 than the radical model. Moreover, the bimolecular model of Kissner et al. [34] explains why the decay of more concentrated peroxynitrite solutions deviates from first-order behavior and becomes slower. In the radical model of Lymar et al. this observation is ignored.

The bimolecular mechanism of peroxynitrite decomposition, proposed by Kissner et al., is analogous to that of other peracids [37]. For peroxynitrite, however, one can postulate an alternative bimolecular pathway, namely the transfer of oxygen from ground-state peroxynitrous acid to the anion, reaction 12, to give peroxynitrate, which is unstable at alkaline pH [38,39] and decomposes to nitrite and dioxygen (reaction 13) [40].

$$ONOOH + ONOO^- \rightarrow O_2NOO^- + NO_2^- + H^+ \quad (12)$$

$$O_2NOO^- \longrightarrow NO_2^- + O_2 \quad (13)$$

Indeed, the oxygen transfer reactions of ground-state peroxynitrous acid are known [41,42], and the decay of peroxynitrate to nitrite and dioxygen is well documented [40]. This model, thus, explains all experimental observations: (i) Peroxynitrate has an absorption maximum at 290 nm [43], close to that of peroxynitrite, and the decay, observed at 300 nm, could actually be the decay of peroxynitrate (reaction 13), and should therefore be concentration-independent. (ii) This pathway of peroxynitrite decomposition results in reaction 2, *i.e.* the products are nitrite and oxygen in 2:1 stochiometry. (iii) Finally, the biphasic kinetics of decay is explained as in the model of Kissner et al.

Within this scenario, the decay of peroxynitrite at neutral to slightly alkaline pH and high peroxynitrite concentration does not involve an activated form of peroxynitrous acid, and would be in accord with the well established oxygen atom transfer reaction by ground-state peroxynitrous acid (*cf.* below, reaction 16).

1.5.2 Oxidations by peroxynitrous acid

1.5.2.1 First- and second-order reactions

Peroxynitrous acid reacts with substrates *via* two pathways: direct and indirect one [44,45]. The direct oxidation reaction is first-order in peroxynitrite and first-order in substrate, and the oxidation yields approach 100%. The indirect oxidation reaction is first-order in peroxynitrite and zero-order in substrate, and a stochiometric oxidation can never be achieved. Some substrates react with peroxynitrous acid by a mixed mechanism. Whether a substrate would react with peroxynitrous acid directly or indirectly, could be rationalized in a simple model (reactions 4, 14, and 15). If a direct reaction between a substrate and ground-state peroxynitrous acid is faster than its unimolecular isomerization, $k_{14}[\boldsymbol{S}] >> k_4 = 1.2$ s^{-1}, then a substrate reacts directly *via* reaction 14. If $k_{14}[\boldsymbol{S}] << k_4$, then a substrate reacts indirectly *via* reaction 4 and 15. Because ONOOH* is highly reactive, *i.e.* $k_{14}[\boldsymbol{S}] >> k_4$, indirect reactions are zero-order in substrate. If $k_{14}[\boldsymbol{S}] \sim k_4$ then all three reactions 4, 14, and 15 take place and a substrate reacts *via* a mixed mechanism – indirectly at low concentration and directly at high concentrations.

$$\mathrm{ONOOH} + \boldsymbol{S} \longrightarrow \qquad (14)$$

$$\mathrm{ONOOH}^* + \boldsymbol{S} \longrightarrow \qquad (15)$$

Some substrates are listed in Table 1 in order of decreasing of k_{14}. For the last 8 entries, the direct reaction was not observed, we thus calculated the upper limit of k_{14}, using the maximum concentrations of substrates used in these studies.

Table 1. Second-order rate constants of reaction with ground-state peroxynitrous acid

Substrate	k_{14}, $M^{-1}s^{-1}$, 25 °C	Reference
Ascorbate	1×10^6, $k_{-16} = 500\ s^{-1}$[a]	[46]
Ni^{II}(cyclam)	3.25×10^4	[44]
Iodide	2.3×10^4	[44]
Cysteine	5.9×10^3	[21]
KTBA	1.4×10^3	[41]
Methionine	9.0×10^2	[42]
Tryptophan	1.8×10^2	[47], [48]
DEMPO	8.7	[49]
Dihydrorodamine	$<< 10^4$	[50]
Trolox	$<< 10^4$	[51]
Tyrosine	$<< 10^3$	[52]
4-HPA	$<< 10^3$	[53]
$Fe^{II}(CN)_6$	<< 30	[44]
ABTS	<< 40	[54], [55]
DMSO	<< 30	[54], [6]
H_2O_2	<< 2	[56], [57]

[a] The rate constant for the formation of an intermediate between peroxynitrous acid and ascorbate, determined at pH 5.8

1.5.2.2 Oxidation products

Direct oxidation by peroxynitrous acid: Direct oxidations of substrates by ground state peroxynitrous acid can amount to a net oxygen atom transfer (reaction

16) or an electron transfer (reaction 17). An example of a net oxygen atom transfer is the oxidation of methionine to methionine sulfoxide [41,42]. Thiols are oxidized to disulfides, but intermediates such as RSOH, RSONO, or $RSNO_2$ may be involved [21,58,59]. Examples of one-electron direct oxidations are reactions with halogens and metal complexes [44]. A mechanism was proposed [44] in which peroxynitrous acid oxidizes these substrates by one electron with the concomitant formation of nitrogen dioxide radical, and the latter, depending on the electrode potential of the substrate may oxidize another substrate molecule by one electron (reaction 18).

$$ONOOH + \boldsymbol{S} \longrightarrow "\boldsymbol{S}O" + NO_2^- + H^+ \quad (16)$$

$$ONOOH + \boldsymbol{S} \longrightarrow "\boldsymbol{S}^{+\bullet}" + NO_2^{\bullet} + OH^- \quad (17)$$

$$NO_2^{\bullet} + \boldsymbol{S} \longrightarrow "\boldsymbol{S}^{+\bullet}" + NO_2^- + OH^- \quad (18)$$

Indirect oxidation by peroxynitrous acid: Indirect oxidations yield reaction products characteristic of one-electron oxidations like those found in reactions of hydroxyl radical. For example, thiomethyl ethers react with ONOOH* ultimately to produce ethylene [60], a typical one-electron oxidation product for these type of compounds and also observed with hydroxyl radicals. Aromatic compounds are hydroxylated and nitrated [61]. Therefore, it is not surprising that peroxynitrite oxidations were ascribed to the hydroxyl radical.

1.5.3 Homolysis of peroxynitrous acid: Pro and Contra

The highly oxidizing activated form of peroxynitrous acid is formed on a minor pathway (30–40%) of peroxynitrite isomerization to nitrate. The identity of this activated form is still a controversy. The $OH^{\bullet}/NO_2^{\bullet}$ radical pair, trans-peroxynitrous acid were suggested as possible candidates for ONOOH*.

A number of experimental and theoretical considerations, aiming to identify the reactive intermediates have been published. They include the decay of peroxynitrite to nitrite and dioxygen, discussed above (*cf.* pp. 25–28), thermodynamic calculations, estimates of reduction potentials, determinations of activation volumes, analysis of reaction products, spin and radical traps studies, and other approaches. We will briefly review these and show that there is no consensus.

1.5.3.1 Thermodynamic calculations

Initially, the species ONOOH* was believed to be the hydroxyl radical, co-produced with nitrogen dioxide during homolysis of ONOOH in water [6,62] (reaction 7). In 1992, this view was abandoned when thermodynamic estimates of Koppenol et al. suggested that the peroxobond was too strong to account for the indirect oxidations of peroxynitrous acid [25]. An alternative mechanism was proposed which assigned the activation step to a transition from the ground state *cis* to an intermediate close to the *perp* conformation of peroxynitrous acid. Later, the thermodynamic analysis of Koppenol et al. was questioned by Merényi and Lind [28]. They used a different set of premises and calculated rate of homolysis of 2.5 s^{-1}, close to the value of formation of activated intermediate [28]. Koppenol et al. [63] measured the temperature dependence of the decay of peroxynitrous acid and calculated the standard Gibb´s energy of homolysis of $(7 \pm 1) \times 10$ kJ/mole, which resulted in a rate of homolysis of 1×10^{-2} s^{-1} and concluded that homolysis was unlikely. In a subsequent paper, Merényi et al. [64] calculated the Gibb´s energy of homolysis to be 57 ± 2 kJ/mole, based on the experimentally determined equilibrium constant of reaction 19 [65] and the known ionization constant of peroxonitrous acid. From that value they calculated a rate constant of homolysis of 0.38 ± 0.19 s^{-1}, assuming that the rate of the reverse reaction is the experimentally

determined rate of hydroxyl and nitrogen dioxide radical recombination[3]. Recently, these researchers have shown that calculation of the Gibb's energy of formation of peroxynitrous acid based upon a kinetically determined equilibrium constant for reaction 20 yields the same value [67].

$$ONOO^- \rightleftarrows O_2^{\bullet -} + NO^{\bullet} \quad (19)$$

$$ONOOH + H_2O \rightleftarrows HNO_2 + H_2O_2 \quad (20)$$

Experimental discrepancies between the laboratories in determining activation parameters of reaction 7, as well as assumptions, made during calculations, lead to opposing conclusions about the plausibility of homolysis. Thus, the thermodynamics argument is the most controversial and as yet unresolved.

1.5.3.2 Activation volumes

There is also disagreement on the activation volume of the reaction 1. From a pressure dependence of the rate of peroxynitrous acid isomerization one calculates the activation volume. If homolysis were a rate determining step in peroxynitrous acid isomerization, it would require a substantial volume increase in attaining the transition state, and thus reaction would be characterized by a rather high positive activation volume. As a rule, reactions initiated by single O–O bond fission of peroxocompounds in apolar environments have activation volumes of *ca.* 10 cm^3/mole [68]. Kissner et al. [24] first reported an activation volume of 1.7 cm^3/mole for the isomerization of peroxynitrous acid and thus concluded that this low value is consistent with an activation step involving intramolecular

[3] Strictly speaking, the rate of hydroxyl and nitrogen dioxide radical recombination to form peroxynitrous acid is unknown. Nitrogen dioxide can recombine with hydroxyl radical *via* nitrogen or oxygen atom to form peroxynitrous acid and nitrate, respectively, and an effective second-order rate constant of radical disappearance is 5×10^9 $M^{-1}s^{-1}$ [66].

rearrangement, *e.g.*, *cis–perp* isomerization, followed by nitrate formation, but not with a mechanism involving O–O bond homolysis. However, other researchers [69,70], reported activation volumes around 10 cm^3/mole, in agreement with the homolysis. Later, Kissner et al. published a series of experiments and revised their value upwards to 6.9 ± 0.9 cm^3/mole [71]. The earlier value of 1.7 cm^3/mole was in error because the experiments were performed at pH values too close to the pK_a of peroxynitrous acid [71]. They also critically analyzed the experimental data of other researchers and noted that higher activation volumes were obtained by a pulse radiolysis technique, whether somewhat lower values were derived from the stopped-flow experiments. Coddington et al. [72] reported high pressure stopped-flow experiments, in which the activation volume increased from +6 to +14 cm^3/mole when the nitrite content was increased from ~50 μM to 5 mM. High (mM) nitrite concentrations, as used in pulse radiolysis experiments, can therefore account for the higher activation volumes in these experiments, as compared to the stopped-flow ones. Although Coddington et al. [72] suggested that their results support a homolysis model, Kissner et al. [71] noted that moderately positive activation volumes of *ca.* 6 cm^3/mole, calculated from the stopped-flow experiments, do not support a definite conclusion regarding the mechanism of peroxynitrous acid isomerization. Interestingly, at 3°C Kissner et al. measured a value of 4.8 cm^3/mole, which could indicate that the mechanism is temperature-dependent.

1.5.3.3 Bond dissociation energies

The bond dissociation energy for ONOOH was calculated to be 92 kJ/mole [73] by *ab inito* calculations. For comparison, the O–O bond dissociation energy of HOOH is 214 kJ/mole. Therefore, it was concluded that an exceptionally weak

peroxobond is a distinctive feature of peroxynitrite and that its cleavage is likely to be involved in the unimolecular isomerization to nitrate [74].

1.5.3.4 Reactivity

The reactivity of ONOOH* is very similar to that of the hydroxyl radical [60], whose electrode potential is 2.3 V at pH 7 [75]. Lymar et al. [74] argued that, given the estimates for the electrode potential of a ground state peroxynitrous acid of 1.6 V [25] to 1.7 V [28] at pH 7, such a difference in the electrode potentials of ONOOH and ONOOH* would not be compatible with a *cis – trans* rotamers, because *ab inito* calculations [73,76,77] show that they are nearly isoenergetic.

1.5.3.5 Product yields

In a radical model, yields, limited to *ca.* 35 %, can be explained with a concept of a caged pair. Radicals, formed in solution can either recombine within a solvent cage (reactions 5a) or diffuse out of it. Because only radicals escaping the solvent cage can react with the solutes, the limiting oxidation yield of *ca.* 35% represents the yield of escape from the cage [74]. Thus, within a radical model, there is no need to postulate an additional pathway of isomerization to nitrate (reactions 5).

$$\left\{NO_2^{\bullet} + OH^{\bullet}\right\}_{cage} \longrightarrow NO_3^- + H^+ \qquad (5a)$$

1.5.3.6 Spin traps

The results of spin-trap studies are highly controversial. While results from several studies strongly implicate hydroxyl radical [78-80], other provide no evidence for its formation [49,81,82]. There might be several pitfalls in interpreting the results of spin trap studies. For instance, Lemercier at al. [49] and later Grossi et al. [83] found a spin-trapped hydroxyl radical with DEMPO as a spin trap. They

observed, however, a delay in the formation of the spin-trapped product, which was inversely proportional to the concentration of DEMPO. Clearly, these results can be interpreted by postulating an intermediate formation between peroxynitrous acid and DEMPO. If this intermediate decays to an adduct, formed from the hydroxyl radical and DEMPO, then its appearance does not prove the formation of hydroxyl radicals.

1.5.3.7 Radical scavengers and oxidation yields

The results of competitive inhibition studies are also highly controversial. In some cases hydroxyl radical scavengers have no [50,84] or little [44,52,54,55] effect on the oxidation yield. However, in some cases, the extent of inhibition correlates well with the known rate constants of reaction of these scavengers with hydroxyl radicals [6,54,56,57].

Coddington et al. [85] suggested that the discrepancy in experimental result might arise from nitrite contamination. Indeed, nitrite, a major contaminant in almost all peroxynitrite syntheses, reacts with hydroxyl radical with a diffusion-controlled rate constant of $k_{32} = 10^{10}$ $M^{-1}s^{-1}$ (reaction 21) and might thus compete with the organic radical scavengers used to test the formation of hydroxyl radicals. This reaction produces nitrogen dioxide radical – a more selective oxidant that might still oxidize substrates, but not the hydroxyl radical scavengers.

$$OH^{\bullet} + NO_2^- \longrightarrow OH^- + NO_2^{\bullet} \qquad (21)$$

Merényi et al. commented that the very reactive ground state peroxynitrous acid molecule is likely to participate in reactions with secondary species produced in reaction of hydroxyl radicals with a scavenger, which can influence the reaction yields [64]. One may add that the same could apply to peroxynitrous anion in the presence of Lewis acids. In particular, one possible complication could be

carbonate contamination of the buffers in experiments at neutral pH. Because many of these studies were carried out before the reaction of peroxynitrite anion with carbon dioxide was recognized (*cf.* pp. 40–44), no precautions to avoid contamination were taken. The presence of carbon dioxide would modify the reactivity of peroxynitrite at neutral pH and reduce the yield of hydroxyl radical, produced in reaction 7.

As an example, one might consider the oxidation of DMSO, a classical scavenger of hydroxyl radicals. Different researchers have found different yields and oxidation products. In an early paper, Beckman et al. [6] reported up to *ca.* 30% formaldehyde production from DMSO in aerated solutions at pH 6. They also showed the yield to decrease with pH. Uppu et al. [86] found only 8% formaldehyde yield in the same system at pH 7. Richeson et al. [87] detected no formaldehyde in an oxygen free solutions, instead, they found Me_2SO_2, $MeSO_2H$, $MeSO_3H$ and MeOH. Two techniques used to quantify the yield of hydroxyl radical gave different results 8% and 13%. Richeson et al. [87] thus concluded that the homolysis of peroxynitrous acid is only *ca.* 10%. Lobachev et al. [88] reported a total yield of 25 % and yet different products for the same reaction – MeONO, $MeONO_2$, and CH_4. The nature and multiplicity of the products clearly implicate secondary oxidations. The reaction conditions employed, namely large peroxynitrite concentrations and neutral pH, are most favorable for involvement of peroxynitrite anion in the oxidations. If, indeed, formaldehyde is formed as a primary oxidation product, one can see why researchers who conducted their experiments at higher pH found lower yields and a variety of oxidation products. Carbonyl compounds, aldehydes and ketones, are known to react with peroxynitrite and were used to mimic the carbon dioxide reaction with peroxynitrite [89,90]. One would expect formaldehyde to react with peroxynitrite anion and modulate its reactivity, which would lead to different oxidation products. Furthermore, one

could expect formaldehyde to be further oxidized to carbonate, which was not analyzed for. Thus, the experimentally determined product yields would be underestimated. This example shows how many pitfalls exist in the interpretation of experimental results and therefore an unambiguous interpretation might only be possible if all reactions are taken into account. Experiments at physiological pH, where both peroxynitrous acid and peroxynitrite coexist, make this complex situation even worse.

1.5.3.8 Viscosity

Pryor et al. [91] suggested that, if the decay of peroxynitrous acid involved homolysis and subsequent recombination of hydroxyl and nitrogen dioxide radicals, then peroxynitrite should disappear more slowly in solvents of higher viscosity. This should happen because for peroxynitrous acid, as for all free radicals initiators undergoing single-bond homolysis, cage return is substantial and more of the radicals in the cages would return to re-form peroxynitrous acid as the viscosity of medium increases. Pryor et al. found that a viscosity change that would results in a *ca.* 10–20 fold decrease of the diffusion constant of the radicals caused no change in the rate of peroxynitrite disappearance. They concluded therefore, that the viscosity experiment does not support a homolysis model of peroxynitrous acid decomposition.

The results of Pryor et al. were criticized by several researchers [64,85]. They noted that polyethers, added to change viscosity, react with hydroxyl radicals to produce reductive carbon-centered radicals. These radicals are expected to reduce peroxynitrous acid and, therefore, a possible decrease of the decay rate because of increased viscosity would not be observed [64].

1.6 Peroxynitrite and carbon dioxide

In 1929, Gleu and Roell [2], and later, in 1969, Keith and Powell [92] demonstrated that peroxynitrite was unstable in carbonate-containing media.

When the chemistry of peroxynitrite was re-examined during the beginning of the nineties, considerable disagreement existed between the laboratories especially regarding experiments at neutral pH. Catalysis by transition metals was proposed to take place [93], but, most likely, the discrepancies were caused by carbonate contamination of the buffers.

1.6.1 Carbon dioxide catalyzed decay of peroxynitrite

In 1995 a systematic study of Lymar and Hurst appeared [20]. They demonstrated by means of pH-jump technique that the peroxynitrite anion reacted with carbon dioxide – not hydrogen carbonate – with a second-order rate constant of 3×10^4 $M^{-1}s^{-1}$ at 25°C. The physiological relevance of this reaction was noted. Pryor et al. [94] showed that the products of the reaction are nitrate and carbon dioxide and thus carbon dioxide acts as a true catalyst for peroxynitrite isomerization (reaction 22).

$$ONOO^- + CO_2 \rightarrow NO_3^- + CO_2 \qquad (22)$$

Carbon dioxide was found to modulate the reactivity of peroxynitrite, altering reaction rates, product yields and distribution. As in indirect oxidations by peroxynitrous acid, carbon dioxide catalyzed oxidations (i) are zero-order in substrate (ii) afford maximum yields of only *ca.* 35%. It was suggested, therefore, that two intermediates with profoundly different chemical properties are formed during the carbon dioxide catalyzed isomerization of peroxynitrite. One, which is formed during a minor pathway (*ca.* 35%), is highly oxidizing, and another, which is formed during the major decay pathway does not react with substrates.

1.6.2 Formation of trioxocarbonate(•1–) and nitrogen dioxide radicals

Unlike with peroxynitrous acid, formation of radicals in the reaction of carbon dioxide and peroxynitrite is more or less agreed upon.

The thermodynamic driving force for the direct reaction 23 was calculated to be close to zero (*cf.* Table 2). *Ab initio* calculations even yielded a value of –71 kJ/mole [73].

$$ONOO^- + CO_2 \rightleftharpoons NO_2^{\bullet} + CO_3^{\bullet -} \qquad (23)$$

Table 2. Calculated Gibbs energy for reaction 23

ΔG°, kJ/mole	Reference
–5.9	[95]
11.3	[96]
7.1	[28]
–71	[73]

Carbon dioxide catalyzed one-electron oxidations of $Os(bpy)_3^{2+}$ and $Ru(bpy)^{2+}$ were observed, establishing that is capable of oxidizing compounds whose electrode potentials are as large as 1.3 V [95]. Thus, the electrode potential of an intermediate, formed during the carbon dioxide catalyzed isomerization of peroxynitrite to nitrate, is consistent with that of the trioxocarbonate(•1–) radical, $E^0\left(CO_3^{\bullet -}/CO_3^{2-}\right) = 1.59$ V [97].

The trioxocarbonate(•1–) radical is longer-lived than the hydroxyl radical and could be observed directly. In 1999, Bonini et al. [98] and Meli et al. [99] independently studied the carbon dioxide catalyzed decay of peroxynitrite by ESR and reported a signal with a g-value of 2.0115 ± 0.0002, typical for the

trioxocarbonate(•1–) radical. The latter researchers, however, concluded that the yield of homolysis was not higher than 3%, based on the yields of nitrite and nitrate, formed in the carbon dioxide catalyzed isomerization of peroxynitrite in the presence of nitrogen monoxide [100].

1.6.3 The lifetime of peroxynitrite/carbon dioxide adduct

Lymar et al. first suggested that peroxynitrite forms an adduct with carbon dioxide provisionally identified as $ONOOCO_2^-$ [20]. Later, formation of the adduct was confirmed experimentally [101] and shown to be theoretically feasible [73].

The following reaction sequence (reactions 24–27) has been suggested to take place during the carbon dioxide catalyzed isomerization of peroxynitrite [96,101].

$$ONOO^- + CO_2 \rightleftarrows ONOOCO_2^- \quad (24)$$

$$ONOOCO_2^- \rightleftarrows NO_2^\bullet + CO_3^{\bullet-} \quad (25)$$

$$NO_2^\bullet + CO_3^{\bullet-} \longrightarrow O_2NOCO_2^- \quad (26)$$

$$O_2NOCO_2^- \longrightarrow NO_3^- + CO_2 \quad (27)$$

Nitrocarbonate ($O_2NOCO_2^-$) is likely to be very short-lived. Calculations show that it decomposes to nitrate and carbon dioxide within a few vibrations and, thus, its participation in bimolecular reactions is precluded [96]. Lymar et al. first suggested, by analogy with peroxynitrous acid, that the homolysis of the adduct ($ONOOCO_2^-$), reaction 25, is the rate-limiting step [102], [103], but later revised his view and anticipated that the rate-limiting step is the formation of the adduct, reaction 24, and the latter is too short-lived to react with substrates [74]. This view was shared by other researchers [28,104] and was based on the following experimental observations and thermodynamic estimates: (i) All oxidations reactions in the presence of carbon dioxide afford maximum oxidation yields of *ca.*

35% and the rates of such reactions are identical to the rate of carbon dioxide catalyzed isomerization of peroxynitrite. In other words, no direct oxidations by the adduct are observed. (ii) The isomerization of peroxynitrite follows a first-order decay, which would not be expected for long-lived absorbing intermediates. (iii) Several theoretical estimates of the lifetime of $ONOOCO_2^-$ were published [28,96]. Merenyi et al. estimated k_{25} to be 10^6 s^{-1} and argued that the lifetime of the adduct would be in the micro- to submicrosecond range [28]. Squadrito et al. estimated k_{25} at 10^9 s^{-1} [96]. Both values are based on thermodynamic estimates of the equilibrium constant of reaction 25 (10^2 M^{-1} [28] and $2*10^{-2}$ M^{-1} [96]) and the assumption that the rate constant of the reverse reaction is the experimentally determined rate constant of recombination of nitrogen dioxide and trioxocarbonate(•1–) radicals, *i.e*, $k_{-25} = 5 \times 10^8$ $M^{-1}s^{-1}$ [105,106]. However, in a recent pulse radiolysis study [106], peroxynitrite was not observed as an intermediate in the reaction of nitrogen dioxide and trioxocarbonate(•1–) radicals. It was suggested, therefore, that these radicals recombine primarily through the N–O bond and not the O–O bond, *i.e.*, $k_{-25} < k_{26}$. If, indeed, $k_{-25} < k_{26} = 5 \times 10^8$ $M^{-1}s^{-1}$, then the values of k_{25}, calculated in [28] and [96] are overestimated and the lifetime of the adduct is underestimated.

In an *ab initio* study, Houk et al. [73] predicted that reaction 24 is exothermic (ΔG = –108 kJ/mole), that there is no barrier to the formation of the adduct, and that homolysis (reaction 25) requires 37 kJ/mole. According to this scenario, the homolysis (reaction 25), rather than the formation of $ONOOCO_2^-$ (reaction 24), is the rate-limiting step, and $ONOOCO_2^-$ should be quite long-lived.

Thus, although formation of trioxocarbonate(•1–) and nitrogen dioxide radical pair is more or less agreed upon, there is no agreement on the detailed mechanism and the energetics of the individual steps.

1.6.4 Carbon dioxide catalyzed oxidations

All reported carbon dioxide catalyzed oxidations are indirect with the limiting yield of 30–40% and with rates independent of substrate concentrations. Carbon dioxide protects thiols from oxidation [58] and increases the extent of aromatic nitration [19,20]. It was suggested, that carbon dioxide diverts the reactivity of peroxynitrite towards one-electron oxidations [107]. Therefore substrates, e.g. thiols, which react directly with peroxynitrous acid [21] are "protected" by carbon dioxide. Some indirect reactions, for instance, nitration of aromatic molecules, are facilitated by carbon dioxide. Low (μM) carbon dioxide concentrations were shown to catalyze nitrosation reactions at neutral to alkaline pH [108]. Because no hydrogen peroxide was detected, nitrosations are not likely to proceed *via* a "NO^{+}" group transfer, rather, secondary nitrosating species N_2O_3, N_2O_4, [109], and $CO_3^{\bullet-}/NO^{\bullet}$ [110] were proposed as reactive intermediates.

1.7 Reaction of peroxynitrite with phenols

Nitration of the amino acid tyrosine is associated with neurodegenerative diseases, such as amyotrophic lateral sclerosis, Parkinson's disease, and Alzheimer's disease [111]. Peroxynitrite is considered to be a plausible nitrating agent *in vivo*, many researchers consider nitrated tyrosine residues a footprint of peroxynitrite [7,112]. Therefore, reactions of peroxynitrite with tyrosine and phenols, as model compounds of tyrosine, were studied. Depending on pH and the presence of carbon dioxide, hydroxylation, nitration, nitrosation, and oxidative coupling of phenols were observed.

We discuss 3 cases: (i) the reaction of peroxynitrous acid, (ii) the carbon dioxide catalyzed reaction of peroxynitrite, and (iii) the reaction of peroxynitrite at alkaline pH. Reaction rates, yields and distribution of products, and oxidizing

intermediates in all three cases differ. In common is, however, that rates of reaction are zero-order in phenol and yields are never higher than *ca.* 30%.

1.7.1 Phenols and peroxynitrous acid

Hydroxylated and nitrated phenols were found as products of the reaction of peroxynitrous acid with phenols [61,113,114]. The major products are hydroxylated phenols, with maximum yields at pH 4–5. Quinones, present in small yields are, probably, the result of further oxidation. Nitrophenols are formed in lower yields, maximally at pH 6–7. Lemercier et al. [114] proposed that nitration, observed at neutral pH, could be due to contaminating carbonate. They measured the *ortho:para* isomer ratio with and without added carbon dioxide and found it to be 1.2 in both cases and thus concluded that the same nitrating species are reacting. Lymar et al. [103] noted, however, that if nitrophenols would be formed by the recombination of phenoxyl and nitrogen dioxide radicals both in the absence and in the presence of carbon dioxide, then the same isomer ratio should be expected. However, the pH dependence of the nitrophenol yields in the absence of carbon dioxide is not well explained within this scenario.

1.7.2 The carbon dioxide catalyzed reaction of peroxynitrite with phenols

Phenol undergoes nitration and oxidative coupling in the presence of millimolar concentrations of carbon dioxide. Although quite a few studies were devoted to the carbon dioxide catalyzed nitration of phenols, they were all carried out to mimic physiological conditions *i.e.* at pH 7–7.5 in *ca.* 100 mM phosphate buffer and 25 mM total carbonate. At these pH values several reactive species coexist, which results in multiple pathways of phenol oxidation. Only one systematic study was published for the oxidation of tyrosine in which a wide pH and concentration range was covered [103]. It shows that at neutral to alkaline pH, with carbon dioxide present in excess, the two major products are 3-nitrotyrosine

and 3,3′-dityrosine. The total product yield is independent of the reaction conditions, about 20% relative to the initial peroxynitrite concentration, but the ratio of products is pH- and concentration-dependent. The yields of nitration decrease and the yields of oxidative coupling increase with pH and tyrosine concentration. These observations are in agreement with a mechanism consisting of reactions 25, 28–31. Because the rate of reaction 31 increases *ca.* 100-fold upon deprotonation of tyrosine (pK_a = 10.1) [115], at high pH and tyrosine concentrations, nitrogen dioxide would be consumed in reaction 31, rather than in reaction 30 and thus 3,3′-dityrosine would be formed at the expense of 3-nitrotyrosine.

$$CO_3^{\bullet-} + TyrH \longrightarrow Tyr^{\bullet} + HCO_3^- \quad (28)$$

$$Tyr^{\bullet} + Tyr^{\bullet} \longrightarrow 3,3'-\text{dityrosine} \quad (29)$$

$$Tyr^{\bullet} + NO_2^{\bullet} \longrightarrow 3-\text{nitrotyrosine} \quad (30)$$

$$NO_2^{\bullet} + TyrH \longrightarrow Tyr^{\bullet} + NO_2^- + H^+ \quad (31)$$

1.7.3 Nitrosation of phenols at alkaline pH

At alkaline pH and without deliberately added carbon dioxide, para-nitrosophenol is a major oxidation product of phenol [109,113]. Since no hydrogen peroxide was found [109], nitrosation does not involve the transfer of the nitrosyl group, in agreement with theoretical predictions [116]. Uppu et al. suggested that the nitrosation pathway proceeds parallel to the decay to nitrite and dioxygen (reaction 2) [110]. However, in a study of reaction with amines, significant nitrosation yields were reported already at neutral pH and the yields of nitrosation correlated with the basicity of substrates [117]. Low (μM) concentrations of carbon dioxide accelerated nitrosophenol formation, but higher (mM) inhibited formation of nitrosophenol at the expense of nitrophenol. Uppu et al. [109] first suggested that

nitrosation might be caused by N_2O_3, formed *via* reaction 9, or other NO^+-carriers ($ONONO_2$, ONO_2NO_2, $ONOCO_2^-$), but later [110] found that azide does not inhibit the peroxynitrite-mediated nitrosation, and thus NO^+-donors are unlikely nitrosating species. They suggested that trioxocarbonate(•1–), formed *via* reaction 25, reacts with phenol to generate the phenoxyl radical, which subsequently couples with nitrogen monoxide, produced in reaction 19. Since the ratio of spin densities at the *ortho*- and *para*-positions of the phenoxyl radical is 0.67 [118], 1.34 *ortho/para* ratio is expected, close to that observed for the formation of nitrophenols [61,114]. However, no [109] or little [113] *ortho*-nitrosophenol has been found. Thus, the mechanism of nitrosation by peroxynitrite remains poorly understood.

1.8 Oxidative coupling of phenols

Carbon dioxide catalyzed oxidative coupling of phenols by peroxynitrite was ultimately regarded as a proof of phenoxyl radical involvement and, by many researchers, as additional proof of homolysis of the peroxybond in the peroxynitrite/carbon dioxide adduct. We want to show here that the recombination of two phenoxyl radicals has been too universally accepted as a general mechanism of oxidative coupling.

According to McDonald and Hamilton [119], plausible mechanisms of oxidative coupling can be grouped into two broad classes: radical and non-radical. The radical mechanisms would include the formation of phenoxyl radicals and their coupling with each other or a homolytic aromatic substitution pathway. Non-radical mechanisms would proceed *via* heterolytic coupling either preceded by (reactions 32–34) or concomitant with (reactions 32 and 35) a two-electron transfer. According to the first mechanism, phenoxy cation is formed as an intermediate,

while in the second mechanism formation of a phenoxyl cation is obviated by a concerted electron transfer and coupling.

$$ArOH + Ox^{n+} \longrightarrow Ar - Ox^{(n-1)+} \quad (32)$$

$$Ar - Ox^{(n-1)+} \longrightarrow ArO^{+} + Ox^{(n-2)+} \quad (33)$$

$$ArO^{+} + ArOH \longrightarrow HOAr - ArOH + H^{+} \quad (34)$$

$$ArOH + Ar - Ox^{(n-1)+} \longrightarrow HOAr - ArOH + Ox^{(n-2)+} + H^{+} \quad (35)$$

A number of metal complexes and metal oxides react with phenols *via* concerted electron transfer and coupling (reactions 32 and 35). As an example, oxidations of phenols by lead tetra-acetate are now proved to proceed *via* a non-radical mechanism (Scheme 1). This reaction was studied extensively by Wessely and co-workers [120] and is known in the literature as Wessely acetoxylation. It provides a path to quinols, but, depending on the number and nature of substituents, biphenols and quinones might be formed as minor or major products (*cf.* Scheme 1). Although initially thought to be a radical reaction, the Wessely acetoxylation is now proved to be radical free. Indeed, given the lifetime of the acetoxyl radical of 10^{-9}–10^{-10} s, formation of quinols by coupling of phenoxyl radicals with acetoxyl radical is precluded. The effects of ring substituents on the rate of acetoxylation of phenols suggest a transition state which resembles an aryloxy cation.

Scheme 1. Wessely acetoxylation

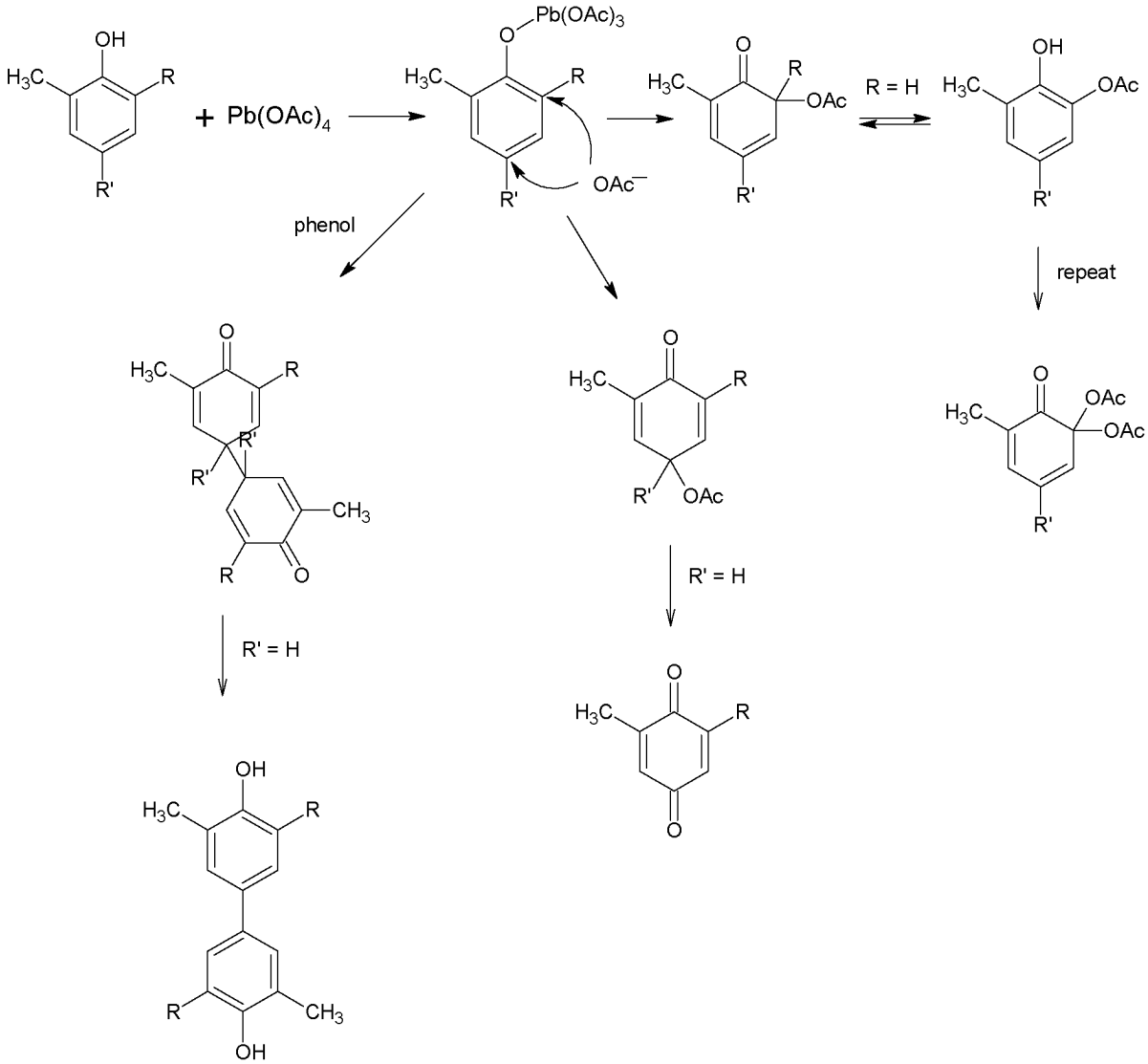

Several quinones are known to dehydrogenate phenols to phenoxyl cations. Some cations (e. g. tropylium ion) so formed have been isolated as stable salts. In these cases, oxidative coupling proceeds *via* reactions 32–34.

Recently, a coupling of cyclohexydienone with phenols was reported [121]. Cyclohexadienone was prepared by bromination of phenol and, in the presence of silver(I) ions, it coupled to another phenol. The intermediate formation of a phenoxyl cation was assumed (Scheme 2).

Scheme 2. Coupling of cyclohexadienone with phenol

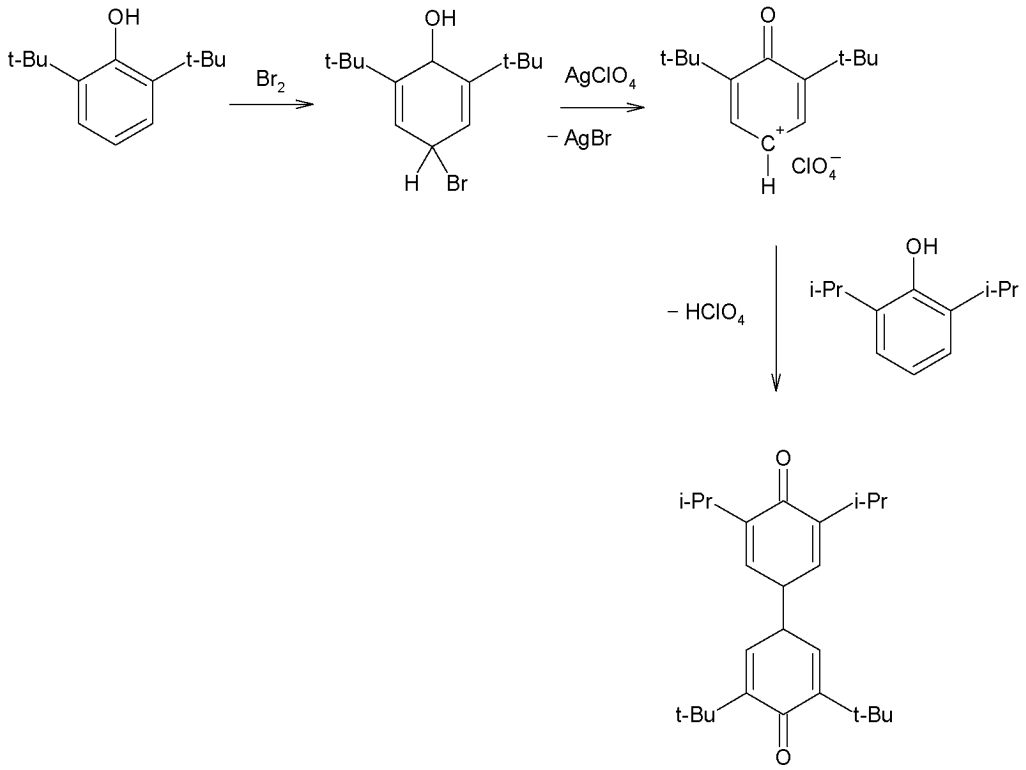

References

[1] Baeyer, A.; Villiger, V. Ueber die salpetrige Säure. *Ber. deutschen chem. Ges.* **34**:755-762; 1901.

[2] Gleu, K.; Roell, E. Die Einwirkung von Ozon auf Alkaliazid. Persalpetrige Säure I. *Zeitschr. anorg. allgem. Chemie* **179**:233-266; 1929.

[3] Halfpenny, E.; Robinson, P. L. The nitration and hydroxylation of aromatic compounds by pernitrous acid. *J. Chem. Soc.* 939-946; 1952.

[4] Moncada, S.; Palmer, R. M. J.; Higgs, E. A. Nitric oxide: Physiology, pathophysiology, and pharmacology. *Pharmacol. Rev.* **43**:109-142; 1991.

[5] Ignarro, L. J. Nitric oxide: A unique endogenous signaling molecule in vascular biology (Nobel lecture). *Angew. Chem. Int. Edit.* **38**:1882-1892; 1999.

[6] Beckman, J. S.; Beckman, T. W.; Chen, J.; Marshall, P. A.; Freeman, B. A. Apparent hydroxyl radical production by peroxynitrite: Implications for endothelial injury from nitric oxide and superoxide. *Proc. Natl. Acad. Sci. USA* **87**:1620-1624; 1990.

[7] Beckman, J. S.; Ye, Y. Z.; Anderson, P. G.; Chen, J.; Accavitti, M. A.; Tarpey, M. M.; White, C. R. Extensive nitration of protein tyrosines in human atherosclerosis detected by immunohistochemistry. *Biol. Chem. Hoppe-Seyler* **375**:81-88; 1994.

[8] Tamura, Y.; Chi, L.; Driscoll, E. M., Jr.; Hoff, P. T.; Freeman, B. A.; Gallagher, K. P.; Lucchesi, B. R. Superoxide dismutase conjugated to polyethylene glycol provides sustained protection against myocardial ischemia/reperfusion injury in canine heart. *Circ. Res.* **63**:944-959; 1988.

[9] Koppenol, W. H. Chemistry of peroxynitrite and its relevance to biological systems. In Sigel, A.; Sigel, H. eds. *Interrelations Between Free Radicals and Metal Ions in Life Processes.* New York: Marcel Dekker, Inc.; 1999:597-619.

[10] Huie, R. E.; Padmaja, S. Reaction of NO• with $O_2^{\bullet -}$. *Free Radical Res. Commun.* **18**:195-199; 1993.

[11] Goldstein, S.; Czapski, G. The reaction of $NO^{\cdot}$ with $O_2^{\cdot -}$ and $HO_2^{\cdot}$: A pulse radiolysis study. *Free Radical Biol. Med.* **19**:505-510; 1995.

[12] Kobayashi, K.; Miki, M.; Tagawa, S. Pulse-radiolysis study of the reaction of nitric oxide with superoxide. *J. Chem. Soc. Dalton Trans.* 2885-2889; 1995.

[13] Nauser, T.; Koppenol, W. H. The rate constant of the reaction of superoxide with nitrogen monoxide: Approaching the diffusion limit. *J. Phys. Chem. A* **106**:4084-4086; 2002.

[14] Klug, D.; Rabani, J.; Fridovich, I. A direct demonstration of the catalytic action of superoxide dismutase through the use of pulse radiolysis. *J. Biol. Chem.* **247**:4839-4842; 1972.

[15] Michel, E.; Nauser, T.; Sutter, B.; Bounds, P. L.; Koppenol, W. H. Kinetics properties of Cu,Zn-superoxide dismutase as a function of metal content. *Arch. Biochem. Biophys.* **439**:234-240; 2005.

[16] Kissner, R.; Nauser, T.; Kurz, C.; Koppenol, W. H. Peroxynitrous acid – Where is the hydroxyl radical? *IUBMB Life* **55**:567-572; 2003.

[17] Marletta, M. A.; Yoon, P. S.; Iyengar, R.; Leaf, C. D.; Wishnok, J. S. Macrophage oxidation of L-arginine to nitrite and nitrate: Nitric oxide is an intermediate. *Biochemistry* **27**:8706-8711; 1988.

[18] Gryglewski, R. J.; Palmer, R. M. J.; Moncada, S. Superoxide anion is involved in the breakdown of endothelium derived vascular relaxing factor. *Nature* **320**:454-456; 1986.

[19] Denicola, A.; Freeman, B. A.; Trujillo, M.; Radi, R. Peroxynitrite reaction with carbon dioxide/bicarbonate: Kinetics and influence on peroxynitrite-mediated oxidations. *Arch. Biochem. Biophys.* **333**:49-58; 1996.

[20] Lymar, S. V.; Hurst, J. K. Rapid reaction between peroxonitrite ion and carbon dioxide: Implications for biological activity. *J. Am. Chem. Soc.* **117**:8867-8868; 1995.

[21] Radi, R.; Beckman, J. S.; Bush, K. M.; Freeman, B. A. Peroxynitrite oxidation of sulfhydryls. *J. Biol. Chem.* **266**:4244-4250; 1991.

[22] Koppenol, W. H. Peroxynitrite uncloaked? *Chem. Res. Toxicol.* **11**:716-717; 1998.

[23] Herold, S.; Shivashankar, K.; Mehl, M. Myoglobin scavenges peroxynitrite without being significantly nitrated. *Biochemistry* **41**:13460-13472; 2002.

[24] Kissner, R.; Nauser, T.; Bugnon, P.; Lye, P. G.; Koppenol, W. H. Formation and properties of peroxynitrite studied by laser flash photolysis, high pressure stopped flow and pulse radiolysis. *Chem. Res. Toxicol.* **10**:1285-1292; 1997.

[25] Koppenol, W. H.; Moreno, J. J.; Pryor, W. A.; Ischiropoulos, H.; Beckman, J. S. Peroxynitrite, a cloaked oxidant formed by nitric oxide and superoxide. *Chem. Res. Toxicol.* **5**:834-842; 1992.

[26] Merényi, G.; Lind, J.; Goldstein, S.; Czapski, G. Mechanism and thermochemistry of peroxynitrite decomposition in water. *J. Phys. Chem. A* **103**:5685-5691; 1999.

[27] Bohle, D. S.; Hansert, B.; Paulson, S. C.; Smith, B. D. Biomimetic synthesis of the putative cytotoxin peroxynitrite, $ONOO^-$, and its characterization as a tetramethylammonium salt. *J. Am. Chem. Soc.* **116**:7423-7424; 1994.

[28] Merényi, G.; Lind, J. Thermodynamics of peroxynitrite and its CO_2-adduct. *Chem. Res. Toxicol.* **10**:1216-1220; 1997.

[29] Kurz, C.; Zeng, X.; Hannemann, S.; Kissner, R.; Koppenol, W. H. On the chemical and electrochemical one-electron reduction of peroxynitrous acid. *J. Phys. Chem. A* **109**:965-969; 2005.

[30] Elliot, A. J.; McCracken, D. R.; Buxton, G. V.; Wood, N. D. Estimation of rate constants for nearly diffusion-controlled reactions in water at high temperature. *J. Chem. Soc. , Faraday Trans.* **86**:1539-1547; 1990.

[31] Goldstein, S.; Saha, A.; Lymar, S. V.; Czapski, G. Oxidation of peroxynitrite by inorganic radicals: A pulse radiolysis study. *J. Am. Chem. Soc.* **120**:5549-5554; 1998.

[32] Amatore, C.; Arbault, S.; Bruce, D.; de Oliveira, P.; Erard, M.; Vuillaume, M. Characterization of the electrochemical oxidation of peroxynitrite: Relevance to oxidative stress bursts measured at the single cell level. *Chem. Eur. J.* **7**:4171-4179; 2001.

[33] Pfeiffer, S.; Gorren, A. C. F.; Schmidt, K.; Werner, E. R.; Hansert, B.; Bohle, D. S.; Mayer, B. Metabolic fate of peroxynitrite in aqueous solution - Reaction with nitric oxide and pH-dependent decomposition to nitrite and oxygen in a 2:1 stoichiometry. *J. Biol. Chem.* **272**:3465-3470; 1997.

[34] Kissner, R.; Koppenol, W. H. Product distribution of peroxynitrite decay as a function of pH, temperature, and concentration. *J. Am. Chem. Soc.* **124**:234-239; 2002.

[35] Lymar, S. V.; Khairutdinov, R. F.; Hurst, J. K. Hydroxyl radical formation by O–O bond homolysis in peroxynitrous acid. *Inorg. Chem.* **42**:5259-5266; 2003.

[36] Kirsch, M.; Korth, H.-G.; Wensing, A.; Sustmann, R.; De Groot, H. Product formation and kinetic simulation in the pH range 1-14 account for a free radical mechanism of peroxynitrite decomposition. *Arch. Biochem. Biophys.* **418**:133-150; 2003.

[37] Goodman, J. F.; Robson, P. Decomposition of inorganic peroxyacids in aqueous alkali. *Trans. Faraday Soc.* **59**:2871-2875; 1963.

[38] Logager, T.; Sehested, K. Formation and decay of peroxynitric acid: a pulse radiolysis study. *J. Phys. Chem.* **97**:10047-10052; 1993.

[39] Goldstein, S.; Czapski, G. Reactivity of peroxynitric acid (O_2NOOH): a pulse radiolysis study. *Inorg. Chem.* **36**:4156-4162; 1997.

[40] Lammel, G.; Perner, D.; Warneck, P. Decomposition of pernitric acid in aqueous solution. *J. Phys. Chem.* **94**:6141-6144; 1990.

[41] Pryor, W. A.; Jin, X.; Squadrito, G. L. One- and two-electron oxidations of methionine by peroxynitrite. *Proc. Natl. Acad. Sci. USA* **91**:11173-11177; 1994.

[42] Perrin, D.; Koppenol, W. H. The quantitative oxidation of methionine to methionine sulfoxide by peroxynitrite. *Arch. Biochem. Biophys.* **377**:266-272; 2000.

[43] Goldstein, S.; Czapski, G. Formation of peroxynitrate from the reaction of peroxynitrite with CO_2: Evidence for carbonate radical production. *J. Am. Chem. Soc.* **120**:3458-3463; 1998.

[44] Goldstein, S.; Czapski, G. Direct and indirect oxidations by peroxynitrite. *Inorg. Chem.* **34**:4041-4048; 1995.

[45] Goldstein, S.; Squadrito, G. L.; Pryor, W. A.; Czapski, G. Direct and indirect oxidations by peroxynitrite, neither involving the hydroxyl radical. *Free Radical Biol. Med.* **21**:965-974; 1996.

[46] Kurz, C.; Kissner, R.; Perrin, D.; Nauser, T.; Koppenol, W. H. Rapid scavenging of peroxynitrous acid by monohydroascorbate. *Free Radical Biol. Med.* **35**:1529-1537; 2003.

[47] Alvarez, B.; Rubbo, H.; Kirk, M.; Barnes, S.; Freeman, B. A.; Radi, R. Peroxynitrite-dependent tryptophan nitration. *Chem. Res. Toxicol.* **9**:390-396; 1996.

[48] Padmaja, S.; Ramezanian, M. S.; Bounds, P. L.; Koppenol, W. H. Reaction of peroxynitrite with L-tryptophan. *Redox. Rep.* **2**:173-177; 1996.

[49] Lemercier, J.-N.; Squadrito, G. L.; Pryor, W. A. Spin trap studies on the decomposition of peroxynitrite. *Arch. Biochem. Biophys.* **321**:31-39; 1995.

[50] Kooy, N. W.; Royall, J. A.; Ischiropoulos, H.; Beckman, J. S. Peroxynitrite-mediated oxidation of dihydrorhodamine 123. *Free Radical Biol. Med.* **16**:149-156; 1994.

[51] Hogg, N.; Joseph, J.; Kalyanaraman, B. The oxidation of a-tocopherol and trolox by peroxynitrite. *Arch. Biochem. Biophys.* **314**:153-158; 1994.

[52] Van der Vliet, A.; Eiserich, J. P.; O'Neill, C. A.; Halliwell, B.; Cross, C. E. Tyrosine modification by reactive nitrogen species: A closer look. *Arch. Biochem. Biophys.* **319**:341-349; 1995.

[53] Beckman, J. S.; Ischiropoulos, H.; Zhu, L.; van der Woerd, M.; Smith, C. D.; Chen, J.; Harrison, J.; Martin, J. C.; Tsai, M. Kinetics of superoxide dismutase- and iron-catalyzed nitration of phenolics by peroxynitrite. *Arch. Biochem. Biophys.* **298**:438-445; 1992.

[54] Crow, J. P.; Spruell, C.; Chen, J.; Gunn, C.; Ischiropoulos, H.; Tsai, M.; Smith, C. D.; Radi, R.; Koppenol, W. H.; Beckman, J. S. On the pH-dependent yield of hydroxyl radical products from peroxynitrite. *Free Radical Biol. Med.* **16**:331-338; 1994.

[55] Yang, G.; Candy, T. E. G.; Boaro, M.; Wilkin, H. E.; Jones, P.; Nazhat, N. B.; Saadalla-Nazhat, R. A.; Blake, D. R. Free radical yields from the homolysis of peroxynitrous acid. *Free Radical Biol. Med.* **12**:327-330; 1992.

[56] Mahoney, L. R. Evidence for the formation of hydroxyl radicals in the isomerization of pernitrous acid to nitric acid in aqueous solution. *J. Am. Chem. Soc.* **92**:5262-5263; 1970.

[57] Alvarez, B.; Denicola, A.; Radi, R. Reaction between peroxynitrite and hydrogen peroxide: Formation of oxygen and slowing of peroxynitrite decomposition. *Chem. Res. Toxicol.* **8**:859-864; 1995.

[58] Zhang, H. W.; Squadrito, G. L.; Uppu, R. M.; Lemercier, J. N.; Cueto, R.; Pryor, W. A. Inhibition of peroxynitrite-mediated oxidation of glutathione by carbon dioxide. *Arch. Biochem. Biophys.* **339**:183-189; 1997.

[59] Quijano, C.; Alvarez, B.; Gatti, R. M.; Augusto, O.; Radi, R. Pathways of peroxynitrite oxidation of thiol groups. *Biochem. J.* **322**:167-173; 1997.

[60] Beauchamp, C.; Fridovich, I. A mechanism for the production of ethylene from methional. *J. Biol. Chem.* **245**:4641-4646; 1970.

[61] Ramezanian, M. S.; Padmaja, S.; Koppenol, W. H. Hydroxylation and nitration of phenolic compounds by peroxynitrite. *Chem. Res. Toxicol.* **9**:232-240; 1996.

[62] Halfpenny, E.; Robinson, P. L. Pernitrous acid. The reaction between hydrogen peroxide and nitrous acid, and the properties of an intermediate product. *J. Chem. Soc.* 928-938; 1952.

[63] Koppenol, W. H.; Kissner, R. Can O=NOOH undergo homolysis? *Chem. Res. Toxicol.* **11**:87-90; 1998.

[64] Merényi, G.; Lind, J.; Goldstein, S.; Czapski, G. Peroxynitrous acid homolyzes into $^{\cdot}OH$ and $^{\cdot}NO_2$ radicals. *Chem. Res. Toxicol.* **11**:712-713; 1998.

[65] Merényi, G.; Lind, J. Free radical formation in the peroxynitrous acid (ONOOH)/peroxynitrite ($ONOO^-$) system. *Chem. Res. Toxicol.* **11**:243-246; 1998.

[66] Logager, T.; Sehested, K. Formation and decay of peroxynitrous acid: a pulse radiolysis study. *J. Phys. Chem.* **97**:6664-6669; 1993.

[67] Merényi, G.; Lind, J.; Czapski, G.; Goldstein, S. Direct determination of the Gibbs' (sic) energy of formation of peroxynitrous acid. *Inorg. Chem.* **42**:3796-3800; 2003.

[68] Isaacs, N. S. Liquid-Phase High-Pressure Chemistry: Wiley: New York; 1981.

[69] Goldstein, S.; Meyerstein, D.; van Eldik, R.; Czapski, G. Peroxynitrous acid decomposes via homolysis: Evidence from high-pressure pulse radiolysis. *J. Phys. Chem. A* **103**:6587-6590; 1999.

[70] Goldstein, S.; Meyerstein, D.; van Eldik, R.; Czapski, G. Spontaneous reactions and reduction by iodide of peroxynitrite and peroxynitrate: Mechanistic insight from activation parameters. *J. Phys. Chem. A* **101**:7114-7118; 1997.

[71] Kissner, R.; Thomas, C.; Hamsa, M. S. A.; van Eldik, R.; Koppenol, W. H. Evaluation of activation volumes for the conversion of peroxynitrous to nitric acid. *J. Phys. Chem. A* **107**:11261-11263; 2003.

[72] Coddington, J. W.; Wherland, S.; Hurst, J. K. Pressure dependence of peroxynitrite reactions. Support for a radical mechanism. *Inorg. Chem.* **40**:528-532; 2001.

[73] Houk, K. N.; Condroski, K. R.; Pryor, W. A. Radical and concerted mechanisms in oxidations of amines, sulfides, and alkenes by peroxynitrite, peroxynitrous acid, and the peroxynitrite-CO_2 adduct: Density functional theory transition structures and energetics. *J. Am. Chem. Soc.* **118**:13002-13006; 1996.

[74] Lymar, S. V.; Hurst, J. K. Radical nature of peroxynitrite reactivity. *Chem. Res. Toxicol.* **11**:714-715; 1998.

[75] Berdnikov, V. M.; Zhuravleva, O. S. Oxidation-reduction potentials of certain inorganic radicals in aqueous solution. *Russ. J. Phys. Chem.* **46**:1521-1523; 1972.

[76] Tsai, J.-H. M.; Harrison, J. G.; Martin, J. C.; Hamilton, T. P.; van der Woerd, M.; Jablonsky, M. J.; Beckman, J. S. Role of conformation of peroxynitrite anion ($ONOO^-$) in its stability and toxicity. *J. Am. Chem. Soc.* **116**:4115-4116; 1994.

[77] Krauss, M. Electronic structure and spectra of the peroxynitrite anion. *Chem. Phys. Lett.* **222**:513-516; 1994.

[78] Augusto, O.; Gatti, R. M.; Radi, R. Spin-trapping studies of peroxynitrite decomposition and of 3-morpholinosydnonimine *N*-ethylcarbamide autooxidation: Direct evidence for metal-independent formation of free radical intermediates. *Arch. Biochem. Biophys.* **310**:118-125; 1994.

[79] Augusto, O.; Radi, R.; Gatti, R. M.; Vásquez-Vivar, J. Detection of secondary radicals from peroxynitrite-mediated oxidations by electron spin resonance. *Methods Enzymol.* **269**:346-354; 1996.

[80] Gatti, R. M.; Alvarez, B.; Vasquez-Vivar, J.; Radi, R.; Augusto, O. Formation of spin trap adducts during the decomposition of peroxynitrite. *Arch. Biochem. Biophys.* **349**:36-46; 1998.

[81] Shi, X.; Lenhart, A.; Mao, Y. ESR spin trapping investigation on peroxynitrite decomposition: No evidence for hydroxyl radical production. *Biochem. Biophys. Res. Commun.* **203**:1515-1521; 1994.

[82] Pou, S.; Nguyen, S. Y.; Gladwell, T.; Rosen, G. M. Does peroxynitrite generate hydroxyl radical. *Biochim. Biophys. Acta* **1244**:62-68; 1995.

[83] Grossi, L. Evidence of an electron-transfer mechanism in the peroxynitrite-mediated oxidation of 4-alkylphenols and tyrosine. *J. Org. Chem.* **68**:6349-6353; 2003.

[84] Radi, R.; Cosgrove, T. P.; Beckman, J. S.; Freeman, B. A. Peroxynitrite-induced luminol chemiluminescence. *Biochem. J.* **290**:51-57; 1993.

[85] Coddington, J. W.; Hurst, J. K.; Lymar, S. V. Hydroxyl radical formation during peroxynitrous acid decomposition. *J. Am. Chem. Soc.* **121**:2438-2443; 1999.

[86] Uppu, R. M.; Squadrito, G. L.; Pryor, W. A. Acceleration of peroxynitrite oxidations by carbon dioxide. *Arch. Biochem. Biophys.* **327**:335-343; 1996.

[87] Richeson, C. E.; Mulder, P.; Bowry, V. W.; Ingold, K. U. The complex chemistry of peroxynitrite decomposition: New insights. *J. Am. Chem. Soc.* **120**:7211-7219; 1998.

[88] Lobachev, V. L.; Rudakov, E. S.; Geletii, Yu. V.; Balavoine, G. G. A.; Zimtseva, G. P. DMSO Oxidation by Peroxynitrite. *Nitric Oxide: Biol. Chem.* **3**:29; 1999.

[89] Uppu, R. M.; Winston, G. W.; Pryor, W. A. Reactions of peroxynitrite with aldehydes as probes for the reactive intermediates responsible for biological nitration. *Chem. Res. Toxicol.* **10**:1331-1337; 1997.

[90] Yang, D.; Tang, Y. C.; Chen, J.; Wang, X. C.; Bartberger, M. D.; Houk, K. N.; Olson, L. Ketone-catalyzed decomposition of peroxynitrite via dioxirane intermediates. *J. Am. Chem. Soc.* **121**:11976-11983; 1999.

[91] Pryor, W. A.; Jin, X.; Squadrito, G. L. Insensitivity of the rate of decomposition of peroxynitrite to changes in viscosity; Evidence against free radical formation. *J. Am. Chem. Soc.* **118**:3125-3128; 1996.

[92] Keith, W. G.; Powell, R. E. Kinetics of decomposition of peroxynitrous acid. *J. Chem. Soc. (A)* 90; 1969.

[93] Edwards, J. O.; Plumb, R. C. The chemistry of peroxonitrites. *Prog. Inorg. Chem.* **41**:599-635; 1993.

[94] Pryor, W. A.; Lemercier, J. N.; Zhang, H. W.; Uppu, R. M.; Squadrito, G. L. The catalytic role of carbon dioxide in the decomposition of peroxynitrite. *Free Radical Biol. Med.* **23**:331-338; 1997.

[95] Lymar, S. V.; Hurst, J. K. CO_2-catalyzed one-electron oxidation by peroxynitrite: Properties of the reactive intermediate. *Inorg. Chem.* **37**:294-301; 1998.

[96] Squadrito, G. L.; Pryor, W. A. Mapping the reaction of peroxynitrite with CO_2: Energetics, reactive species, and biological implications. *Chem. Res. Toxicol.* **15**:885-895; 2002.

[97] Huie, R. E.; Clifton, C. L.; Neta, P. Electron transfer reaction rates and equilibria of the carbonate and sulfate radical anions. *Radiat. Phys. Chem.* **38**:477-81; 1991.

[98] Bonini, M. G.; Radi, R.; Ferrer-Sueta, G.; Ferreira, A. M. D.; Augusto, O. Direct EPR detection of the carbonate radical anion produced from peroxynitrite and carbon dioxide. *J. Biol. Chem.* **274**:10802-10806; 1999.

[99] Meli, R.; Nauser, T.; Koppenol, W. H. Direct observation of intermediates in the reaction of peroxynitrite with carbon dioxide. *Helv. Chim. Acta* **82**:722-725; 1999.

[100] Meli, R.; Nauser, T.; Latal, P.; Koppenol, W. H. Reaction of peroxynitrite with carbon dioxide: Intermediates and determination of the yield of $CO_3^{\bullet-}$ and $NO_2^{\bullet}$. *J. Biol. Inorg. Chem.* **7**:31-36; 2002.

[101] Goldstein, S.; Meyerstein, D.; van Eldik, R.; Czapski, G. Evidence for adduct formation between $ONOO^-$ and CO_2 from high-pressure pulse radiolysis. *J. Phys. Chem. A* **104**:9712-9714; 2000.

[102] Lymar, S. V.; Hurst, J. K. Carbon dioxide: Physiological catalyst for peroxynitrite-mediated cellular damage or cellular protectant. *Chem. Res. Toxicol.* **9**:845-850; 1996.

[103] Lymar, S. V.; Jiang, Q.; Hurst, J. K. Mechanism of carbon dioxide-catalyzed oxidation of tyrosine by peroxynitrite. *Biochemistry* **35**:7855-7861; 1996.

[104] Squadrito, G. L.; Pryor, W. A. Oxidative chemistry of nitric oxide: The roles of superoxide, peroxynitrite, and carbon dioxide. *Free Radical Biol. Med.* **25**:392-403; 1998.

[105] Lilie, J.; Hanrahan, R. J. O^- transfer reactions of the carbonate radical anion. *Radiat. Phys. Chem.* **11**:225-227; 1978.

[106] Alfassi, Z. B.; Dhanasekaran, T.; Huie, R. E.; Neta, P. On the reactions of $CO_3^{\cdot-}$ with NO_x radicals. *Radiat. Phys. Chem.* **56**:475-482; 1999.

[107] Bonini, M. G.; Augusto, O. Carbon dioxide stimulates the production of thiyl, sulfinyl, and disulfide radical anion from thiol oxidation by peroxynitrite. *J. Biol. Chem.* **276**:9749-9754; 2001.

[108] Uppu, R. M.; Squadrito, G. L.; Bolzan, R. M.; Pryor, W. A. Nitration and nitrosation by peroxynitrite: Role of CO_2 and evidence for common intermediates. *J. Am. Chem. Soc.* **122**:6911-6916; 2000.

[109] Uppu, R. M.; Lemercier, J. N.; Squadrito, G. L.; Zhang, H. W.; Bolzan, R. M.; Pryor, W. A. Nitrosation by peroxynitrite: Use of phenol as a probe. *Arch. Biochem. Biophys.* **358**:1-16; 1998.

[110] Uppu, R. M.; Pryor, W. A. Nitrosation of 1,2-phenylenediamine by peroxynitrite/CO_2: Evidence for a free radical mechanism. *J. Am. Chem. Soc.* **121**:9738-9739; 1999.

[111] Beckman, J. S.; Crow, J. P. Pathological implications of nitric oxide, superoxide and peroxynitrite formation. *Biochem. Soc. Trans.* **21**:330-334; 1993.

[112] Ischiropoulos, H.; Zhu, L.; Chen, J.; Tsai, M.; Martin, J. C.; Smith, C. D.; Beckman, J. S. Peroxynitrite-mediated tyrosine nitration catalyzed by superoxide dismutase. *Arch. Biochem. Biophys.* **298**:431-437; 1992.

[113] Daiber, A.; Mehl, M.; Ullrich, V. New aspects in the reaction mechanism of phenol with peroxynitrite: The role of phenoxy radicals. *Nitric Oxide: Biol. Chem.* **2**:259-269; 1998.

[114] Lemercier, J. N.; Padmaja, S.; Cueto, R.; Squadrito, G. L.; Uppu, R. M.; Pryor, W. A. Carbon dioxide modulation of hydroxylation and nitration of phenol by peroxynitrite. *Arch. Biochem. Biophys.* **345**:160-170; 1997.

[115] Prütz, W. A.; Monig, H.; Butler, J.; Land, E. J. Reactions of nitrogen dioxide in aqueous model systems: Oxidation of tyrosine units in peptides and proteins. *Arch. Biochem. Biophys.* **243**:125-134; 1985.

[116] Williams D.L.H. Nitrosating Agents: Is Peroxynitrite a Likely Candidate? *Nitric Oxide: Biol. Chem.* **1**:522-527; 2005.

[117] Masuda, M.; Mower, H. F.; Pignatelli, B.; Celan, I.; Friesen, M. D.; Nishino, H.; Ohshima, H. Formation of N-Nitrosamines and N-Nitramines by the Reaction of Secondary Amines with Peroxynitrite and Other Reactive Nitrogen Species: Comparison with Nitrotyrosine Formation. *Chem. Res. Toxicol.* **13**:301-308; 2000.

[118] Qin, Y.; Wheeler, R. A. Similarities and Differences between Phenoxyl and Tyrosine Phenoxyl Radical Structures, Vibrational Frequencies, and Spin Densities. *J. Am. Chem. Soc.* **117**:6083-6092; 1995.

[119] McDonald, D. M.; Hamilton, G. A. Mechanisms of phenolic oxidative coupling reactions. In Trahanovsky, W. S. eds. *Oxidation in organic chemistry, Part B.* New York: Academic Press; 1973.

[120] Wessely, F.; Sinwel, F. Zur Kenntnis von o-Chinonen. Ueber die Einwirkung von Bleitetraacetat auf Phenole II. *Monatsh.* **81**:1055-1070; 1950.

[121] Omura, K. Silver ion-mediated coupling of 4-bromo-2,6-di-*tert*-butylcyclohexa-2,5-dienone with phenols. *J. Org. Chem.* **63**:10031-10034; 1998.

2 MATERIALS AND METHODS

2.1 Chemicals

Chemicals were purchased from Fluka (Buchs, Switzerland), Sigma-Aldrich Corp. (St. Louis, MO, USA) and ABCR (Karlsruhe, Germany) and were of the highest purity available. Nitrogen monoxide (99.5% purity) was obtained from Linde AG (Unterschleissheim, Germany) and carbon dioxide (>99.8% purity) from PanGas (Luzern, Switzerland). Deionized water was purified further with a Milli-Q unit (Bedford, MA, USA). Nitrogen monoxide was purified by passing it through a saturated potassium hydroxide solution and drying over pellets of potassium hydroxide. Carbon dioxide was used as received.

2.2 Peroxynitrite synthesis

Peroxynitrite was synthesized by addition of gaseous nitrogen monoxide to solid potassium superoxide as described [3]. Briefly, 0.3 g (*ca.* 5.5 mmole) potassium superoxide is stirred with *ca.* 10 g purified quartz sand, placed into an Erlenmeyer flask, and stopped with a rubber septum with inlet and outlet tubes. Synthesis is conducted anaerobically, under intense stirring and cooling. The system is purged with argon for *ca.* 10 minutes and then *ca.* 60 mL nitrogen monoxide at atmospheric pressure (*ca.* 2.7 mmole) is added at a rate of *ca.* 10 mL/min. Once nitrogen monoxide starts to flow, the outlet tubing is removed from a rubber septum and reaction between superoxide and nitrogen monoxide becomes visible by deepening of a pale yellow color of potassium superoxide. After nitrogen monoxide is consumed, manganese dioxide and *ca.* 20–40 ml of ice cold 5 mM potassium hydroxide solution are added. Excess superoxide is hydrolyzed to hydrogen peroxide, which, in turn, is catalytically decomposed by manganese

dioxide. The reaction mixture is filtered through a glass filter under vacuum, and 1 ml aliquots of peroxynitrite solutions are placed in plastic tubes and stored at –80°C for several months without detectable decomposition. The concentration of peroxynitrite is determined by measuring its absorption at 300 nm, ε_{300} = 1700 $M^{-1}cm^{-1}$. The concentration of peroxynitrite stock solutions usually varied from 20 to 50 mM, depending on the amount of 5 mM potassium hydroxide added.

2.3 Instrumentation

Optical spectra were recorded with a double-beam Specord 200 instrument (Jena, Germany). Kinetics experiments were carried out with an Applied Photophysics SX.17MV stopped-flow single-wavelength spectrophotometer (Leatherhead, Surrey, UK) operated in symmetric- or sequential-mixing modes. Time-dependent spectra were obtained with an OLIS RSM 1000 double beam stopped-flow multi wavelength spectrometer (Bogart, GA, USA). Gratings were used with 400 lines per mm blazed at 550 nm. To monitor absorptions at 550 nm, an OG 550 3 mm cut-off filter was used on the Applied Photophysics instrument. Product analysis was performed with a Hewlett Packard (HP) 1050 series HPLC (Wilmington, DE, USA), equipped with a HP 1050 autosampler, a HP 1050 quaternary pump, a HP 1100 diode-array detector, an Agilent 1100 degasser (Palo Alto, CA, USA), and a Prestige HPLC column (250 × 4.6 mM, C18, pore size 100 Å, particle size 5 μM). ESR spectra were recorded with a Bruker EMX 080 instrument (Billerica, MA, USA) equipped with a flow cell. The solutions were injected into the cavity of ESR spectrometer with a KDScientific 220 syringe pump (New Hope, PA, USA) at a flow rate of 1 to 5 mL/min per syringe in a ratio 1:1. MS experiments were carried out with a quadrupole Thermo Finnigan mass spectrometer (San Jose, CA, USA) equipped with a heated electrospray ionization unit.

2.4 pH-jump experiments

Ionization of carbon dioxide is a slow process, because it includes hydration of a carbon dioxide molecule which, in turn, requires the change in geometry (reaction 1). The pH-jump experiments take advantage of this phenomenon. If one rapidly increases pH of a neutral or acidic solution of carbon dioxide, high non-equilibrium concentrations of carbon dioxide at alkaline pH can be generated [4,5].

Ionization of carbon dioxide can occur by two paths [2]. Below pH 8 the predominant mechanism is *via* hydration (reaction 1) and subsequent deprotonation (reaction 3) and above pH 10 – *via* direct reaction with hydroxide (reaction 2) and possible subsequent deprotonation (reaction 4). Between pH 8 and 10 both mechanisms are important.

$$CO_2 + H_2O \rightleftarrows H_2CO_3 \quad k_1 = 0.03\ s^{-1},\ k_{-1} = 20\ s^{-1} \qquad (1)$$

$$CO_2 + OH^- \rightleftarrows HCO_3^- \quad k_2 = 8500\ M^{-1}s^{-1},\ k_{-2} = 2 \times 10^{-4}\ s^{-1} \qquad (2)$$

$$H_2CO_3 \rightleftarrows HCO_3^- + H^+ \quad pK_a^1 = 3.6, \qquad (3)$$

$$HCO_3^- \rightleftarrows CO_3^{2-} + H^+ \quad pK_a^2 = 10.3, \qquad (4)$$

Thus below pH 8, the half-lifetime of carbon dioxide is determined by the rate of its hydration (reaction 1) and $t_{1/2} = \frac{\ln 2}{k_1} = 23\,s$. Above pH 10 the lifetime of carbon dioxide is determined by its reaction with hydroxide. To be able to neglect the change in concentration of carbon dioxide, the pH of reaction mixtures was such that the disappearance of peroxynitrite *via* reaction 5 was at least 10 times faster than the hydrolysis of carbon dioxide.

$$ONOO^- + CO_2 \longrightarrow NO_3^- + CO_2 \qquad k_5 = 3 \times 10^4\ M^{-1}s^{-1} \qquad (5)$$

The limiting pH value was therefore calculated as follows:

$$10 \times \frac{1}{k_5[CO_2]_0} \leq \frac{1}{k_2[OH^-]} \Rightarrow$$

$$pH \leq 14 + \log\left(\frac{k_5}{10k_2} \times [CO_2]\right) = 14 + \log(0.35 \times [CO_2])$$

The carbon dioxide solutions used were either aqueous saturated solutions (78 mM CO_2 at 0°C or 36 mM CO_2 at 20°C [1]) or phosphate buffer solutions at pH 7.2 containing 50 mM total carbonate (*ca.* 4 mM CO_2). Thus, after mixing with peroxynitrite solutions the initial carbon dioxide concentration was not lower than 2 mM, which implies a limiting pH of (14+log(0.007)) = 10.8. The pH after mixing was usually in the range 10–10.5. Despite the low buffer capacity at this pH range, phosphate was the buffer of choice, because it is chemically inert, unlike borate and ammonia buffers.

2.5 Stopped-flow kinetics experiments

All rapid reaction kinetics were studied with stopped-flow instruments, whose typical mixing times are ca. 2 ms. All experiments were performed at 25°C with carbon dioxide in excess over peroxynitrite.

2.6 Sequential mixing stopped-flow experiments

In order to study the reactivity of the reaction intermediates, an Applied Photophysics stopped-flow was operated in a sequential mixing mode. First, two solutions are mixed 1:1 and allowed to incubate in an ageing loop. After some time – to ensure maximal formation of the intermediate – the contents of the ageing loop are mixed 1:1 with a third solution. To do so, another pair of syringes is pushed;

one of which contains a reactant, and the other water or buffer, and serves to displace the pre-mixed solution from the aging loop and ensure the 1:1 mixing. The aging loop has a volume of 115 μL and, unless otherwise stated, the volume of the first pair of syringes was *ca.* 220 μL and that of the second pair *ca.* 180 μL.

2.7 Sample preparation for HPLC and MS analysis

Solutions of peroxynitrite, phenol, and carbon dioxide were mixed in a stopped-flow Applied Photophysics instrument *via* two procedures.

Procedure A. 100 mM phosphate buffer, containing phenol and 40 – 50 mM carbonate at pH 7.2, was mixed with peroxynitrite in 100 mM phosphate buffer at pH ≤ 11.5. The pH after mixing was not higher than 10.5. The initial concentration of carbon dioxide after mixing was *ca.* 2 mM and the half-life more than 0.25 s. The half-life of peroxynitrite was *ca.* 10 ms, thus, the decay of peroxynitrite was much faster than the neutralization of carbon dioxide.

Procedure B. Peroxynitrite in 20 mM potassium hydroxide was mixed with phenol and carbon dioxide (38 mM). The half-life of peroxynitrite under such conditions is about 2 ms and that of carbon dioxide about 15 ms. Thus, peroxynitrite reacted at pH 12 in the presence of an excess and constant amount of carbon dioxide. *Ca.* 100 ms after mixing, the pH dropped to *ca.* 5 due to hydration and of carbon dioxide followed by ionisation of dihydrogen carbonate. This made it possible to conserve and correctly determine the product *para*-benzoquinone, which decays rapidly at alkaline pH.

2.8 Product analysis by HPLC

The reactants were mixed in a stopped-flow apparatus *via* procedures A or B. 20 μL of a product was injected and eluted with acetonitrile – water (25 – 40% v/v) at a flow rate of 1.3 mL/min. The absorption of the eluent was monitored at 230,

250, 280, 300, and 360 nm simultaneously. *Para*-benzoquinone was detected at 230 and 250 nm; phenol at 230, 250, and 280 nm; biphenols at 230, 250, 280, and 300 nm, and nitrophenols at 230, 250, 280, 300, and 360 nm. The retention times with different eluent compositions are given in Table 1.

Table 1. Retention times in minutes for different eluent compositions.

CH_3CN/H_2O, v/v, %	*para*-BQ	phenol	4-NP	4,4′-BP	2-NP	2,2′-BP
25	5	10	16	19	27	51
35	5.6	8.4	11.3	10.2	18.7	23.5
40	3.9	5.3	6.6	5.8	10.8	12.0

The peaks were identified by coelution with authentic samples. The peak areas were quantified with the help of 5 to 6 standard solutions of known concentrations.

2.9 Product analysis by MS

Spectra were acquired in a negative-ion mode over a mass range of 45 – 195 at 2 s using Ar as a collision gas, (collision energy 25 eV), T = 200–350 °C. Reaction mixtures were prepared without buffers as described above in procedure B and diluted with a 1 mM potassium hydroxide solution so that the total concentration of phenols was not higher than 50 μM.

2.10 Statistical analysis

In kinetic stopped-flow experiments 5–8 reproducible runs were performed for each set of concentrations and the average curve was calculated. The kinetic curves were fitted and the standard errors of kinetic experiments were calculated with Origin 6.1. In HPLC experiments mean concentrations and 95% confidence

intervals were calculated from the analysis of at least three reproducible samples. The confidence interval, Δx, was calculated according to the Student's t-test, $x = \bar{x} \pm \Delta x = \bar{x} \pm ts/\sqrt{n}$, where s – standard deviation, n – the number of measurements, t – Student's factor for a 95% probability.

The concentration of a product determined at a particular wavelength was calculated by calibration with standard solutions. For each product determined at several wavelengths, an average concentration was calculated. Because the error in the determination of a product at several wavelengths was usually less then 1%, it was neglected in calculating the resulting standard error. Otherwise an error of a function *f(x,y)* was calculated as follows: $(\Delta f)^2 = \left(\frac{\partial f}{\partial x}\Delta x\right)^2 + \left(\frac{\partial f}{\partial y}\Delta y\right)^2$.

References

[1] Fogg, P. G. T.; Gerrard, W. Solubility of Gases in Liquids: A Critical Evaluation of Gas/Liquid Systems in Theory and Practice: Chichester John Wiley & Sons; 1991.

[2] Kern, D. M. The hydration of carbon dioxide. *J. Chem. Educ.* **37**:14-23; 1960.

[3] Koppenol, W. H.; Kissner, R.; Beckman, J. S. Syntheses of peroxynitrite: To go with the flow or on solid grounds. *Methods Enzymol.* **269**:296-302; 1996.

[4] Lymar, S. V.; Hurst, J. K. Rapid reaction between peroxonitrite ion and carbon dioxide: Implications for biological activity. *J. Am. Chem. Soc.* **117**:8867-8868; 1995.

[5] Pryor, W. A.; Lemercier, J. N.; Zhang, H. W.; Uppu, R. M.; Squadrito, G. L. The catalytic role of carbon dioxide in the decomposition of peroxynitrite. *Free Radical Biol. Med.* **23**:331-338; 1997.

3 TWO PATHWAYS OF CARBON DIOXIDE CATALYZED OXIDATIVE COUPLING OF PHENOL BY PEROXYNITRITE

(submitted to Chemical Research in Toxicology)

*Alina A. Papina and Willem H. Koppenol**

Department of Chemistry and Applied Biosciences, ETH Zurich, Wolfgang-Pauli-Strasse10, CH-8093 Zurich, Switzerland

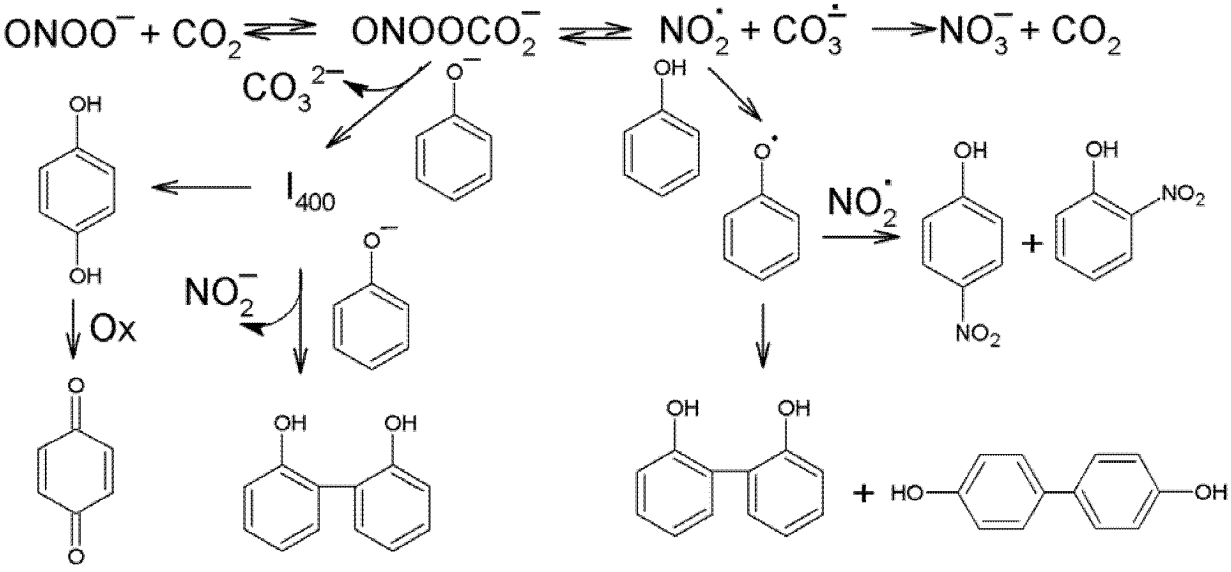

3.1 Abstract

Carbon dioxide catalyzed oxidative coupling of phenol by peroxynitrite occurs by two pathways distinguished by the isomer ratio of 2,2′- to 4,4′-biphenols. As already established, at neutral pH and moderate phenol concentrations, both biphenols are formed in comparable yields by coupling of two phenoxyl radicals. However, at high pH and phenol concentration, 2,2′-biphenol is the only identified coupled product, and its formation does not involve phenoxyl radicals. Instead, under these conditions, a previously unreported long-lived ($t_{1/2}$ ~ 10 s at pH 10 and 1 mM phenol) diamagnetic intermediate with an absorption maximum at 400 nm is observed. This intermediate is formed from phenolate concomitantly with the decay of peroxynitrite and disappears *via* reaction with phenol ($k = (2.4 \pm 0.1) \times 10\ M^{-1}s^{-1}$ at pH 10.5), to form 2,2′-biphenol. We also find that *para*-benzoquinone, previously unreported, is formed in up to 5% yield relative to the initial peroxynitrite concentration. The appearance of an absorption band above 500 nm, which might be due to quinhydrone, indicates that hydroquinone is a likely *para*-benzoquinone precursor. The dependence of *para*-benzoquinone yields on pH and phenol concentration suggests that its formation is related to the non-radical pathway of 2,2′-biphenol formation. This novel non-radical pathway of 2,2′-biphenol formation might be relevant to the mechanisms of reaction of phenolic anti-oxidants with peroxynitrite. The existence of two distinct pathways of biphenol formation implies that, apart from a $CO_3^{\bullet-}$ / $NO_2^{\bullet}$ radical pair, another reactive intermediate is formed during the carbon dioxide catalyzed decay of peroxynitrite.

3.2 Results

3.2.1 Identification of reaction products

The reaction of phenol with peroxynitrite in the presence of excess carbon dioxide at neutral to alkaline pH yields 2- and 4-nitrophenols, 2-2′ and 4-4′-biphenols, and *para*-benzoquinone. Formation of all four isomeric bi- and nitrophenols was previously reported [1]. Because formation of *para*-benzoquinone has not been reported, we wanted to verify this finding. A mass of 108 appears in the negative-ion mass spectra of the reaction mixture (Figure 1).

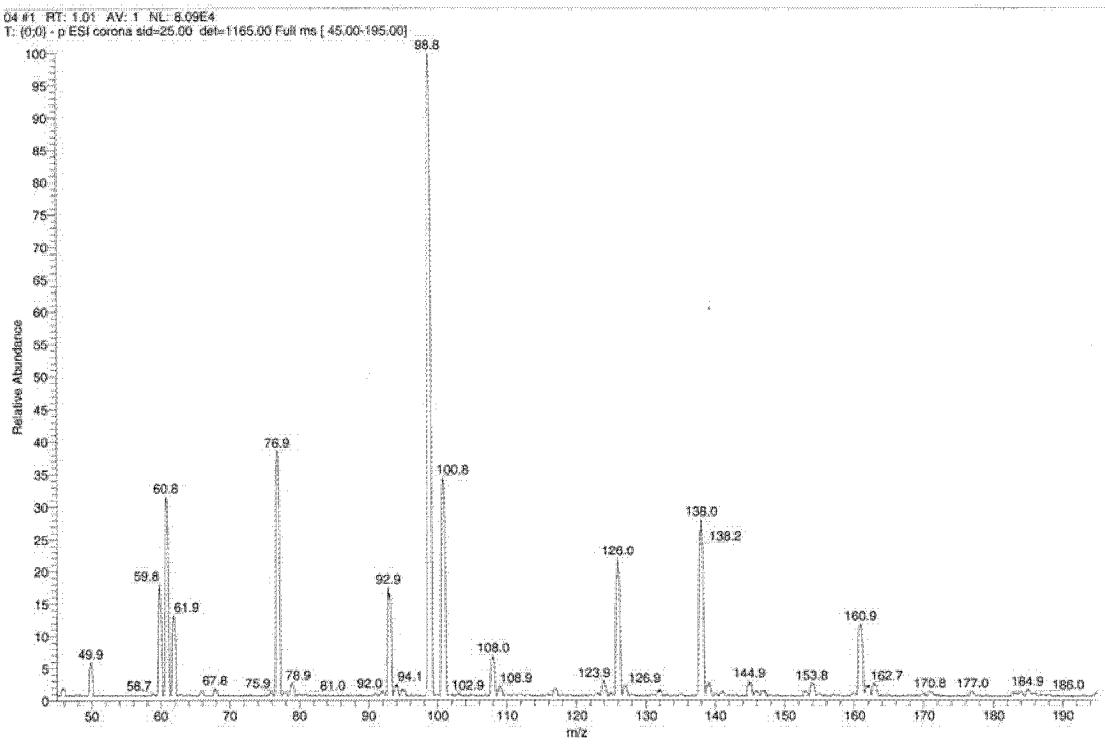

Fiqure 1. Typical mass spectrum of a reaction mixture. Spectrum is acquired in the negative mode over a mass range of 45 – 195 at 2 s using Ar as a collision gas, (collision energy 25 eV), T = 350 °C. Samples were prepared as described in Materials and Methods. The peaks at *m/z* 60, 61, 62, 77, 100 and 101 do not derive from products of phenol oxidation. They persist in blank experiments without addition of phenol and are, most probably, due to the presence of carbonates (HCO_3^-, HCO_3^-:H_2O, KCO_3^-). A peak at *m/z* 93 is due to phenolate, at *m/z* 138 to nitrophenolates; biphenols (*m/z* 185) are not ionized sufficiently. The peak at *m/z* 108 is due to a semiquinone radical produced during ionization of benzoquinone. The intensity of the peak at *m/z* 108 decreases to zero in aged solutions in which *para*-benzoquinone is polymerized.

According to the literature [2], this mass can be ascribed to a semiquinone radical anion formed during ionization of a *para*-benzoquinone. *Para*-benzoquinone has an absorption maximum at 250 nm with an extinction coefficient of *ca.* 20,000 $M^{-1}cm^{-1}$ and is known to be unstable in basic solutions, where it polymerizes to give humic acids [3]. At alkaline pH, we observe slow (hours) changes in the optical spectra after the main reaction (described below) was complete. During this time, the absorption at 250 nm decreases concomitantly with an increase of absorption between 300 and 450 nm (Figure 2A, B). The UV-Vis spectrum of a solution of *para*-benzoquinone under the same conditions undergoes identical changes (Figure 2C).

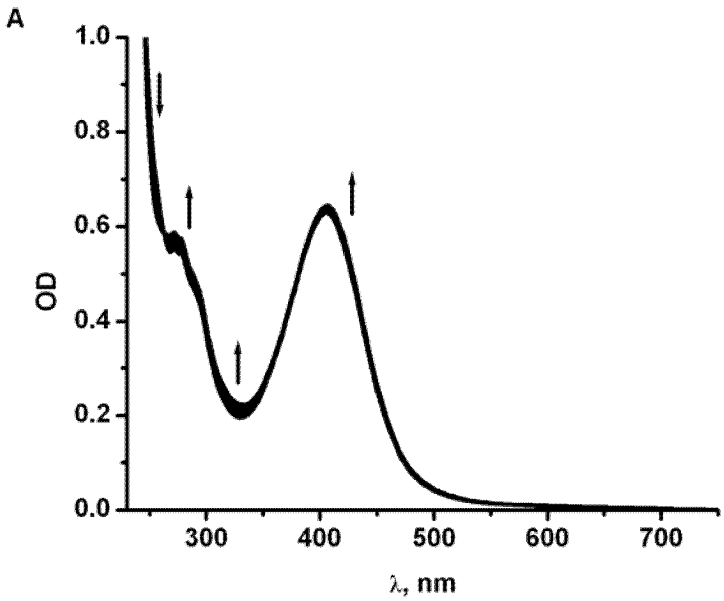

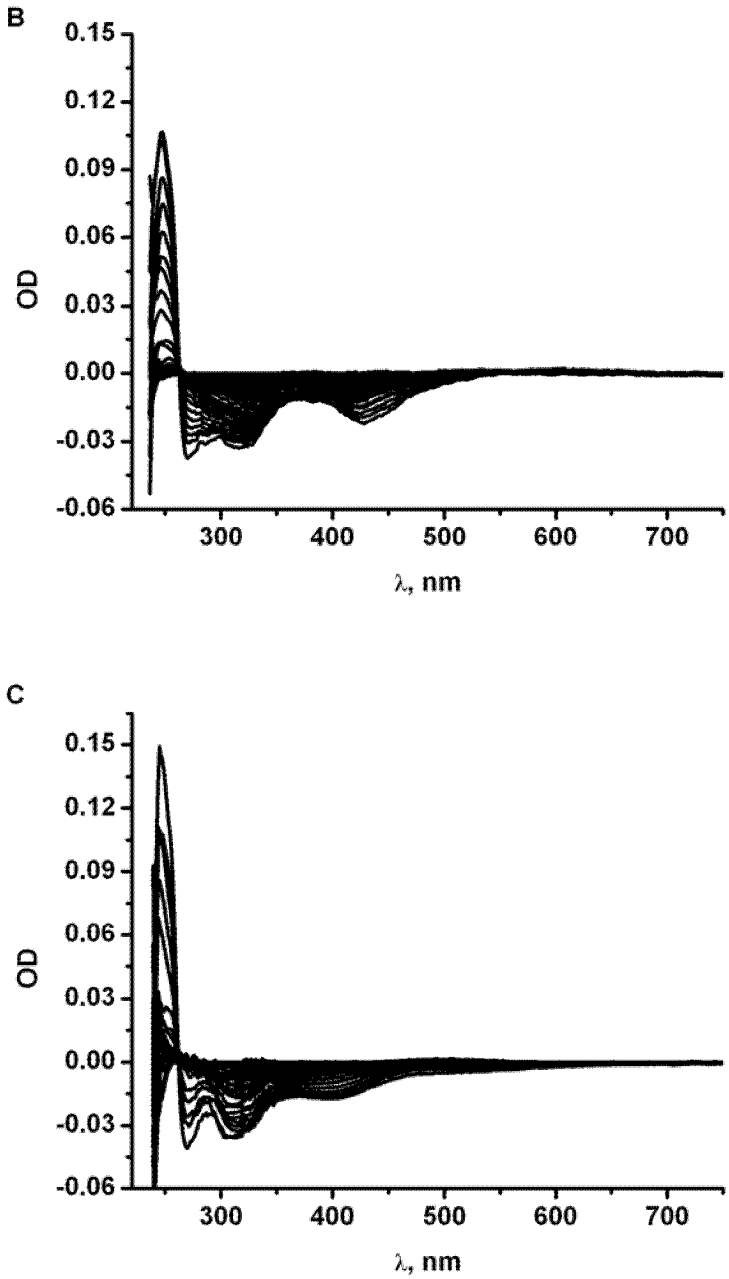

Figure 2. Changes in the absorption spectrum during 5 hours; spectra are taken every 10 minutes in 0.5 cm quartz cuvette. Panel A, 0.6 mM peroxynitrite, 2 mM phenol, 25 mM carbonate, pH jump from 7.2 to 10.2. Panel B, differential spectrum, conditions as in panel A. Reference spectrum is that of reaction mixture after 5 hours. Panel C, changes in the differential spectrum of 5 μM *para*-benzoquinone at pH 10.2 in the presence of 1 mM phenol. The reference spectrum is that of the reaction mixture after 5 hours.

When the reaction was carried out at high pH and high phenol concentration, an unidentified minor product was observed. It appears as a late peak in the HPLC chromatogram (retention time 26 min with 35% v/v acetonitrile/water) and did not absorb above 320 nm. It is possible that this product is 2,4′-biphenol, but, because of the unavailability of an authentic sample, we could not positively identify it by HPLC co-elution. The peak area was *ca.* 3 – 4 times smaller than that of 2,2′-biphenol and the pH and concentration profiles coincided with that of 2,2′-biphenol.

3.2.2 Dependence of product yields on phenol concentration and pH

In agreement with previous studies of carbon dioxide catalyzed oxidations of phenols by peroxynitrite [1,4], we find that the yield of nitrophenols decreases with increasing pH and phenol concentration (Figure 3).

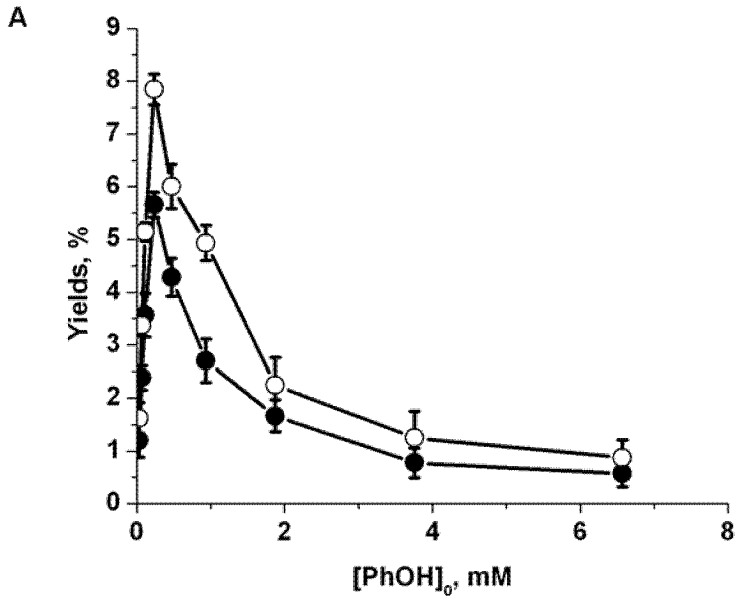

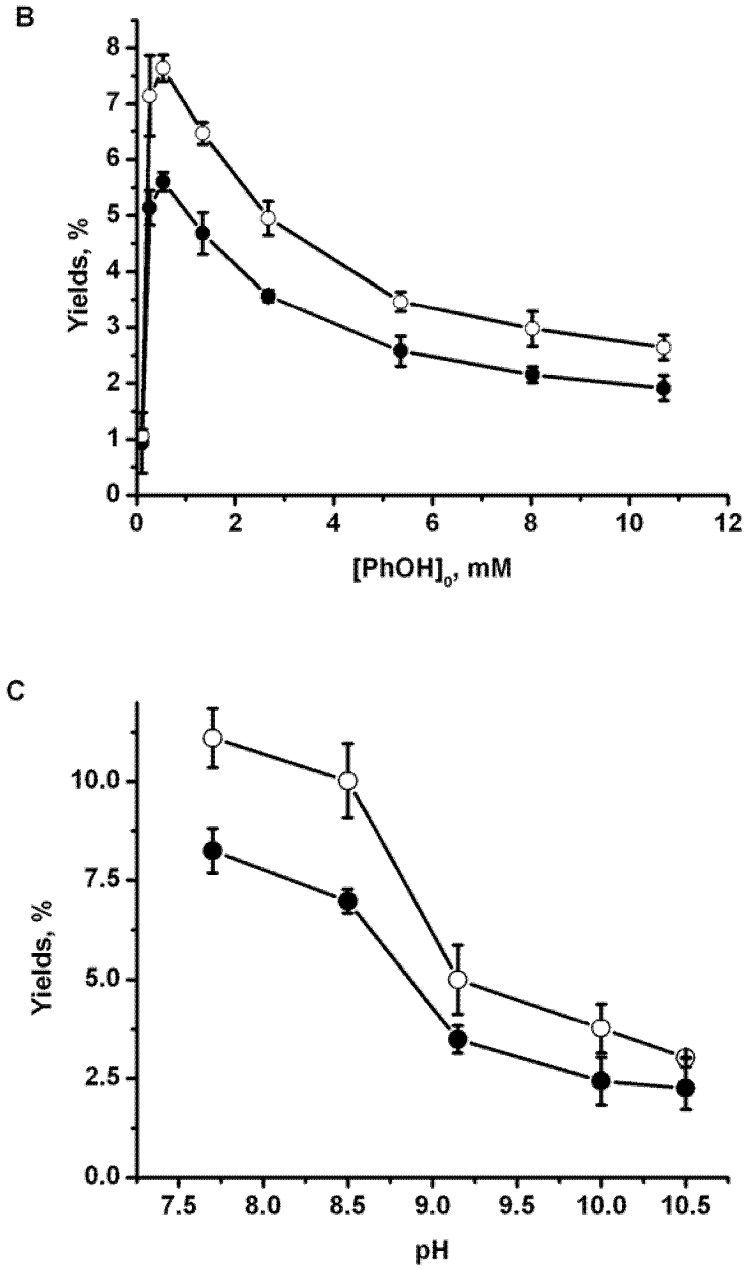

Figure 3. Dependence of yields of 2-(○) and 4-nitrophenols (●) on phenol concentration (panels A and B) and pH (panel C). All concentrations indicated are those after mixing. Panel A, 0.8 mM peroxynitrite, 20 mM carbonate, 100 mM phosphate buffer, pH-jump from pH 7.2 to pH 10.0. Panel B, 0.8 mM peroxynitrite, 20 mM carbon dioxide, 10 mM potassium hydroxide. Panel C, 0.8 mM peroxynitrite, 2 mM phenol, 25 mM carbonate, pH-jump from pH 7.2, 100 mM phosphate buffer.

The ratio of 2- to-4-nitrophenols is 1 to 1.4 under all reaction conditions, in good agreement with the literature [1,5]. However, the ratio of 2,2′-biphenol to 4,4′-biphenol depends on the pH and the phenol concentration: while the yield of 2,2′-biphenol increases with pH and phenol concentration, that of 4,4′-biphenol decreases, similar to the yields of nitrophenols (Figure 4).

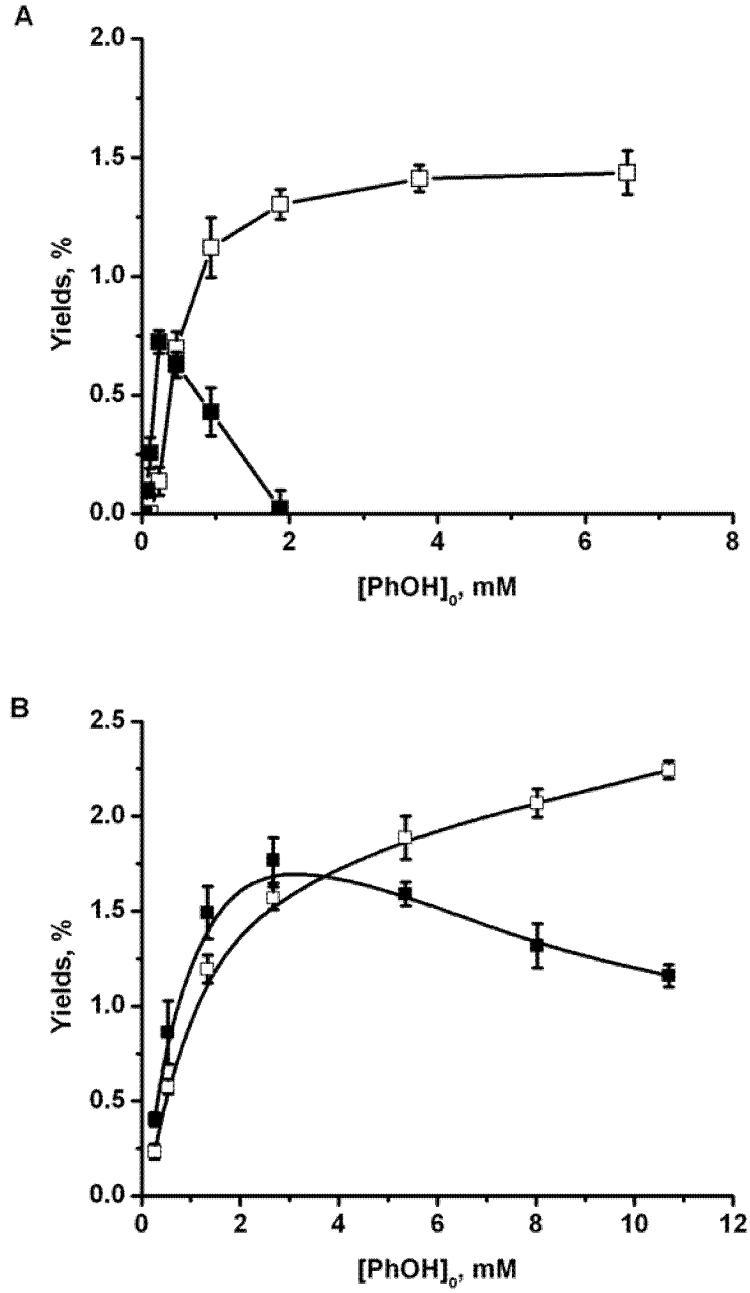

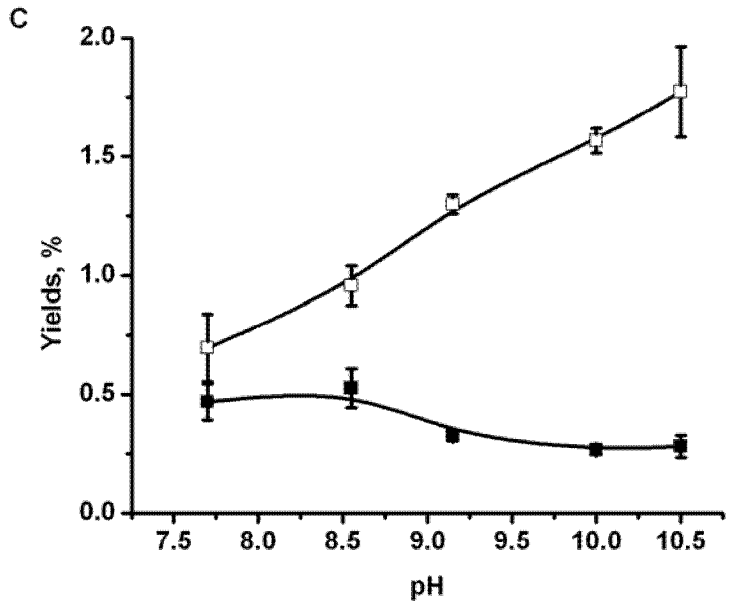

Figure 4. Dependence of yields of 2,2′-biphenol (□) and 4,4′-biphenol (■) on phenol concentration (panels A, B) and pH (panel C). Experimental conditions as described for the individual panels in Figure 3.

Para-benzoquinone is detected in both neutral and alkaline solutions in concentrations up to 20 – 25 μM. Because the hydrolysis of *para*-benzoquinone becomes appreciable at pH > 8, samples at higher pH were brought to pH 7 by addition of a known amount of NaH_2PO_4 and then analyzed. At pH 12, where experiments were conducted without buffers as described under Materials and Methods, carbon dioxide present at a concentration of 20 mM serves to reduce the pH and to preserve *para*-benzoquinone (*cf.* Materials and Methods). Although it is possible that the yields of *para*-benzoquinone are slightly underestimated, they comprise up to 5% of the added peroxynitrite, which, given the overall yield of *ca.* 30%, makes *para*-benzoquinone one of the major products. The dependence of the yield of *para*-benzoquinone on pH and phenol concentration is complex. At pH > 9, the yield of *para*-benzoquinone is maximal when the ratio of phenol to

peroxynitrite is *ca.* 1 to 10 (Figure 5). At pH 7.7, the maximum is reached at *ca.* 3 times excess of phenol over peroxynitrite (Figure 5).

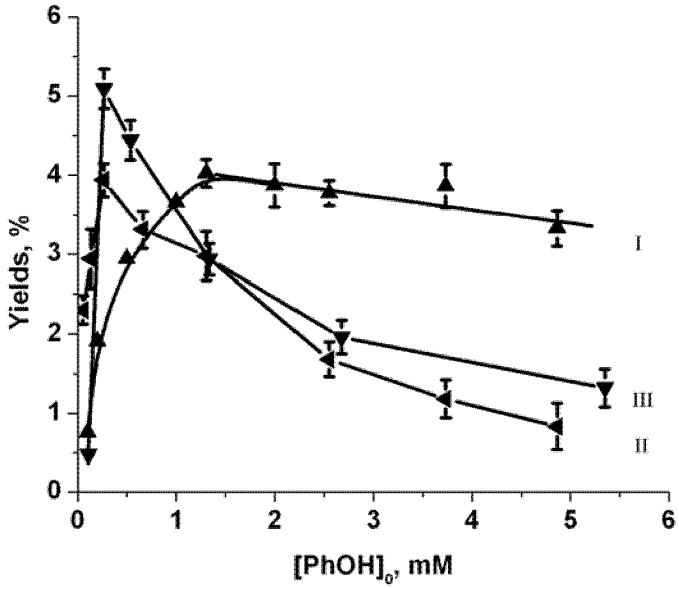

Figure 5. Dependence of the yields of *para*-benzoquinone on phenol concentration at pH 7.7 (curve I), pH 9.2 (curve II), and pH 12 (curve III). 0.8 mM peroxynitrite, curves I and II -25 mM carbonate, pH jump from 7.2, 100 mM phosphate buffer, curve III – 20 mM carbon dioxide, 10mM potassium hydroxide.

3.2.3 UV-Vis detection of reaction intermediates

Under conditions of high pH and high phenol concentration, which favor formation of 2,2′-biphenol, the kinetics of the reaction becomes complex. With the reactants present at *ca.* mM concentrations, the absorption at 400 nm increases considerably, concomitantly with the decay of peroxynitrite, and subsequently decays over a minute (Figure 6C). The absorption decrease at 400 nm is substantial – about one absorption unit – and the residual absorption is due to the presence of nitrophenols. Above 500 nm, one observes that another intermediate with an absorption maximum at *ca.* 550 nm is formed concurrently with the decay of peroxynitrite (Figure 6A and C). The decay of absorption above 500 nm differs from that at 400 nm and is more complex (Figure 6B and D).

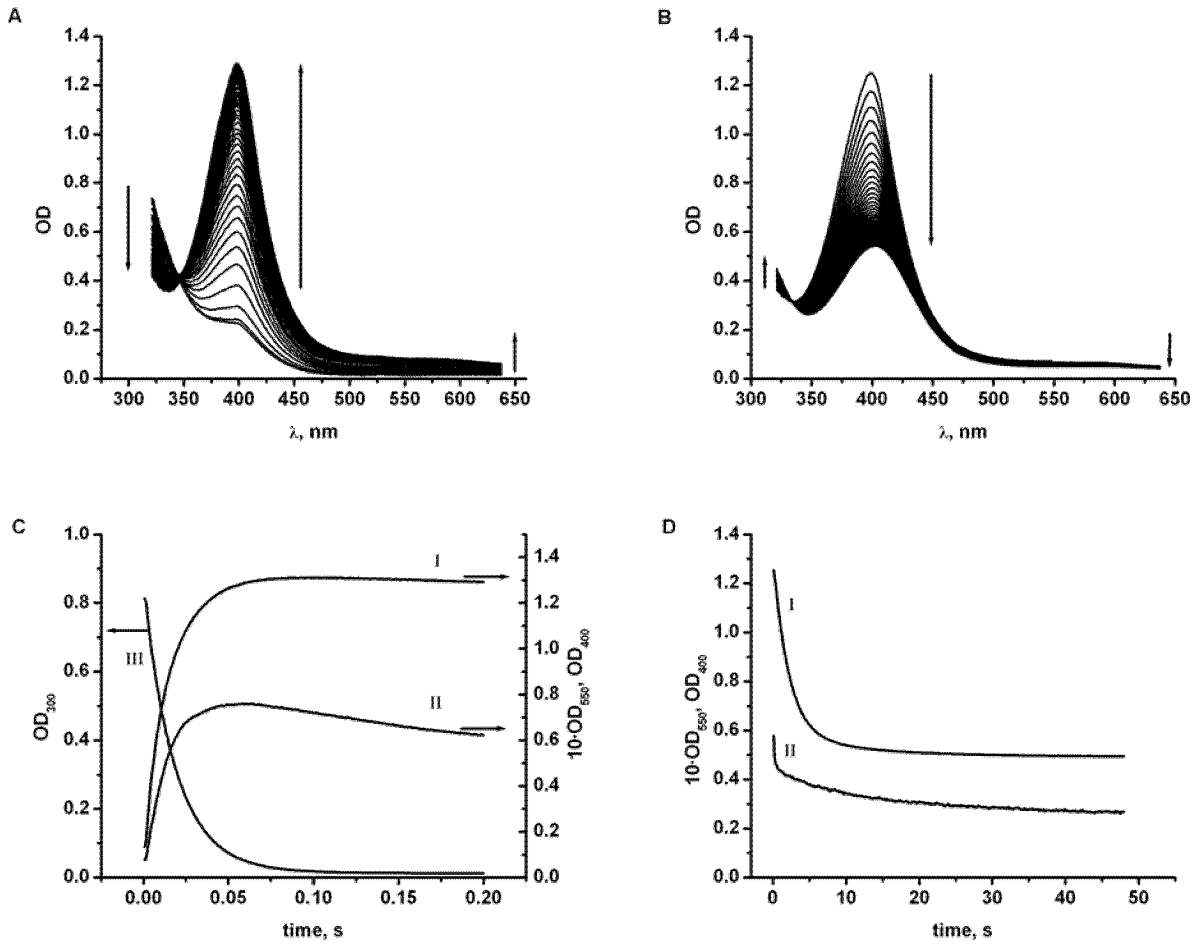

Figure 6. Changes in the absorption spectrum observed after mixing peroxynitrite with phenol and carbon dioxide. 0.5 mM peroxynitrite, 2 mM phenol, 25 mM carbonate, pH-jump from 7.2 to 10.2, 200 mM phosphate buffer. Panel A, spectra taken every ms during the first 50 ms. Panel B, spectra taken every 0.4 s during 30 s. The wavelength span in an OLIS RSM 1000 stopped-flow spectrophotometer is *ca.* 200 nm. To cover a wider wavelength range, two series of spectra were taken under the same conditions, both with a grating blazed at 550, but in one case with the center wavelength at 400 nm and the other at 550 nm. The two series of spectra are shown overlaid in Panels A and B. Panel C and D, kinetics traces at 400 nm (I), 550 nm (II), and, for panel C, a kinetics trace at 300 nm (III) that shows the decay of peroxynitrite in the absence of phenol, but otherwise under identical conditions. The traces were recorded on a single-wavelength instrument with the same solutions.

In the following paragraphs, we show that the intermediate with an absorption maximum at 400 nm (I_{400}) is most likely a precursor of 2,2′-biphenol and that the

absorption above 500 nm is, most probably, associated with the formation of a *para*-benzoquinone *via* the oxidation of initially formed hydroquinone.

3.2.4 Dependence of I_{400} yields on phenol concentration and pH

Because nitrophenols, products of the carbon dioxide catalyzed reaction of peroxynitrite with phenol, absorb near 400 nm, the absorption ascribed to I_{400} must be corrected for that of nitrophenols. Under typical experimental conditions, the increase in absorption at 400 nm is at least 100 times faster than the subsequent decay (*cf.* Figures 6C and 6D), which allows us to treat formation and disappearance separately. We measured, therefore, the initial rate of absorption increase during the first 5–7 ms (W_0^{400}) and the decrease of absorption at 400 nm (ΔOD_{400}) after it reached its maximum. The latter serves to estimate a relative yield of I_{400}.

The dependences of the initial rates on pH and phenol concentration have maxima (Figure 7, squares). Given that the yield of I_{400} increases (Figure 7, circles) and the yield of nitrophenols decreases (Figure 3 and insets in Figure 7) with increasing pH and phenol concentration, the presence of a maximum in a dependence of the initial rate implies that nitrophenols and I_{400} are formed concurrently during the decay of peroxynitrite. Given that the yields of both I_{400} (Figure 7, circles) and 2,2′-biphenol (Figure 4) increases with pH and with the concentration of phenol, it is likely that I_{400} is the precursor of 2,2′-biphenol.

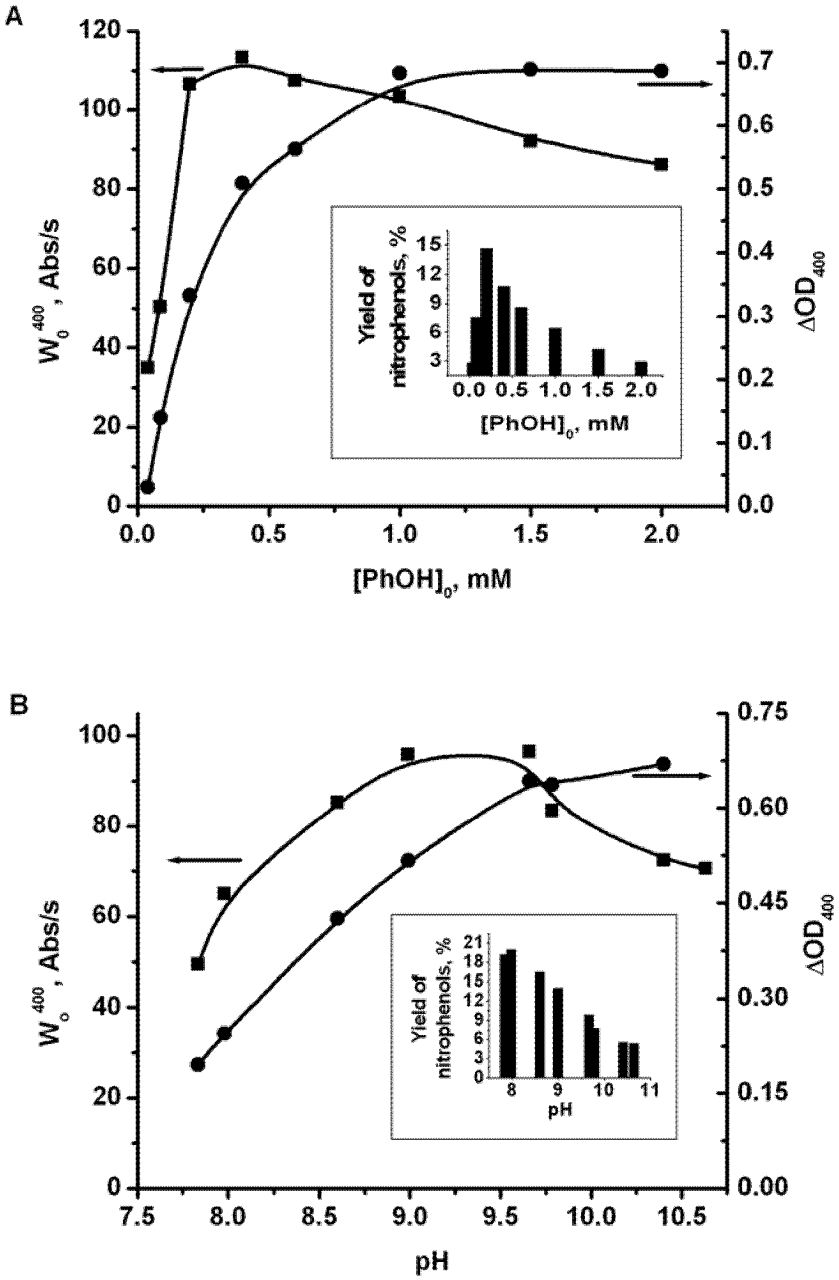

Figure 7. Dependence of the initial rate of absorption increase at 400 nm, (■), the decrease of absorption at 400 nm, (●) and nitrophenol yields (inset) on initial phenol concentration (panel A) and pH (panel B). Panel A, 0.59 mM peroxynitrite; 25 mM carbonate, pH-jump from 7.2 to 10.5, 200 mM phosphate buffer. Panel B, 0.49 mM peroxynitrite; 2 mM phenol; 25 mM carbonate, pH-jump from 7.2; 200 mM phosphate buffer

The pH study indicates that phenolate, rather than phenol, reacts to form I_{400}. If one calculates the concentration of phenolate at a given pH – based on a pK_a of 9.9 for phenol – and plots the yield of I_{400} at different pH values as a function of the phenolate concentration (Figure 8), the resulting saturation curve is identical to that obtained by varying phenol concentration at pH > 10 (Figure 7A, circles).

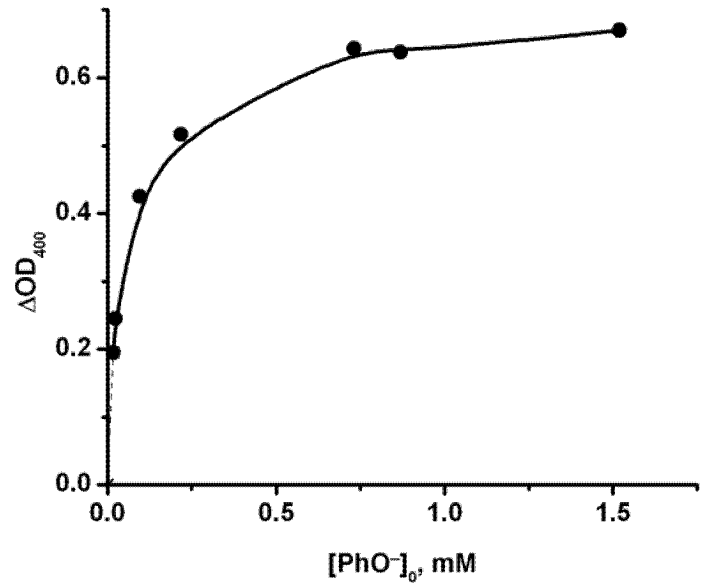

Figure 8. Dependence of the decrease of absorption at 400 nm on calculated phenolate concentrations at different pH values. Conditions as in Figure 4, panel B.

3.2.5 Dependence of I_{400} yields on peroxynitrite and carbon dioxide concentration

With phenol present in excess, the yield of I_{400} is proportional to the peroxynitrite concentration (Figure 9). The yield of I_{400} declines by *ca.* 20% as the carbon dioxide concentration increases from 1 to 10 mM (Figure 10). At the same time, the initial rate of absorption increase at 400 nm rises, most probably due to an increased rate of phenol nitration. This result shows again that I_{400} and nitrophenols are formed by competing pathways during the decay of peroxynitrite.

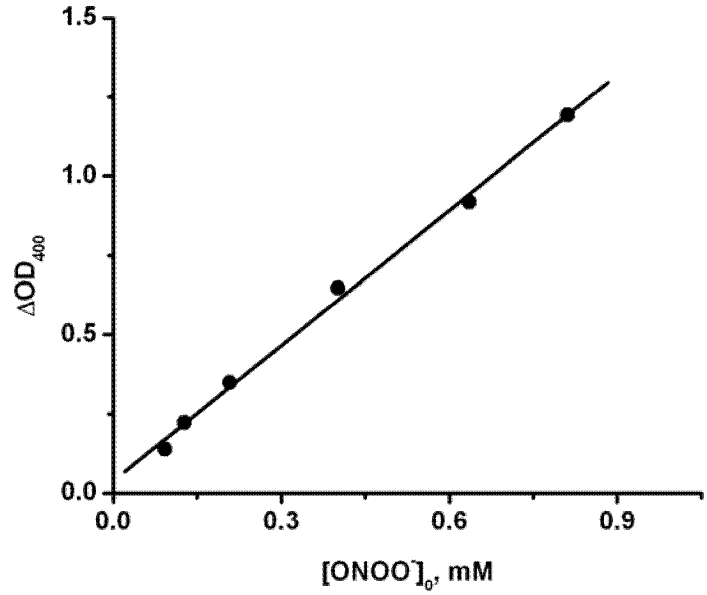

Figure 9. Dependence of the decrease of absorption at 400 nm on peroxynitrite concentration. 2 mM phenol, 25 mM carbonate, 200 mM phosphate buffer, pH jump from 7.2 to 10.3.

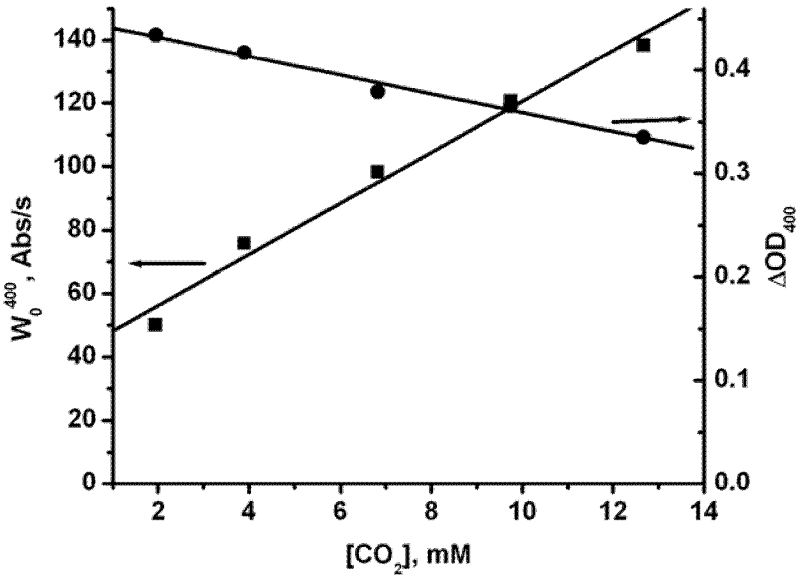

Figure 10. Dependence of the initial rate of absorption build-up at 400 nm, (■), and the decrease of absorption at 400 nm, (●), on the concentration of carbon dioxide. 0.5 mM peroxynitrite, 2 mM phenol, pH 11.2, 100 mM phosphate buffer.

3.2.6 Kinetics of I_{400} decay

Additional proof that I_{400} is a 2,2′-biphenol precursor comes from studying the kinetics of its decay. First, the decay of I_{400} is first order in phenol (Figure 11), the same as observed if, in a sequential flow experiment, I_{400} is pre-formed and phenol is added (not shown). Second, the decay of I_{400} is concomitant with the formation of absorption at *ca.* 300 nm, where 2,2′-biphenol has an absorption maximum (Figures 12 and 6B). The yield of 2,2′-biphenol, estimated from the increase of absorption at 300 nm, is in agreement with the results of the HPLC analysis. For example, given the extinction coefficient of 2,2′-biphenol at 300 nm of *ca.* 8,500 $M^{-1}cm^{-1}$, one calculates from Figure 12 a maximal yield of *ca.* 20 μM. Given that I_{400} probably also absorbs at 300 nm, the yield of 2,2′-biphenol is overestimated and should be less than 20 μM. From Figure 4, one can conclude that, under the conditions of the experiment shown in Figure 12, the yield of 2,2′-biphenol is *ca.* 10 μM. Thus, the two estimates are in agreement.

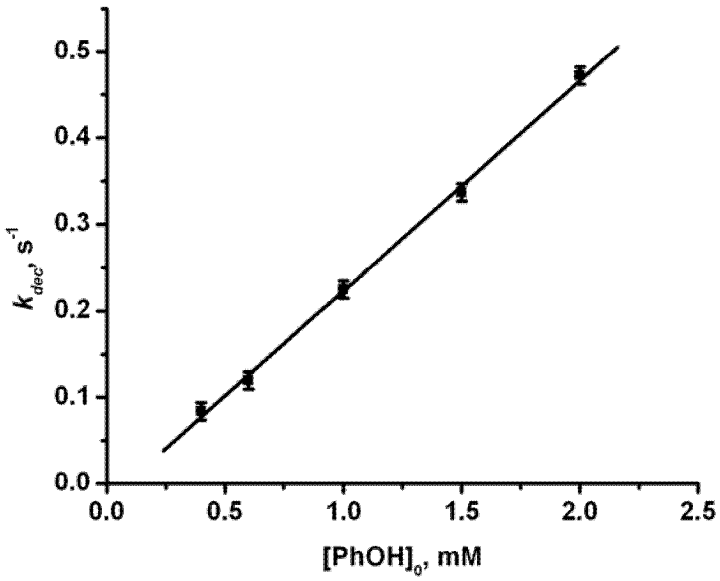

Figure 11. Dependence of the pseudo-first-order rate constant of decay of I_{400} on the initial phenol concentration. 0.59 mM peroxynitrite; 25 mM carbonate, 200 mM phosphate buffer, pH-jump from 7.2 to pH 10.5.

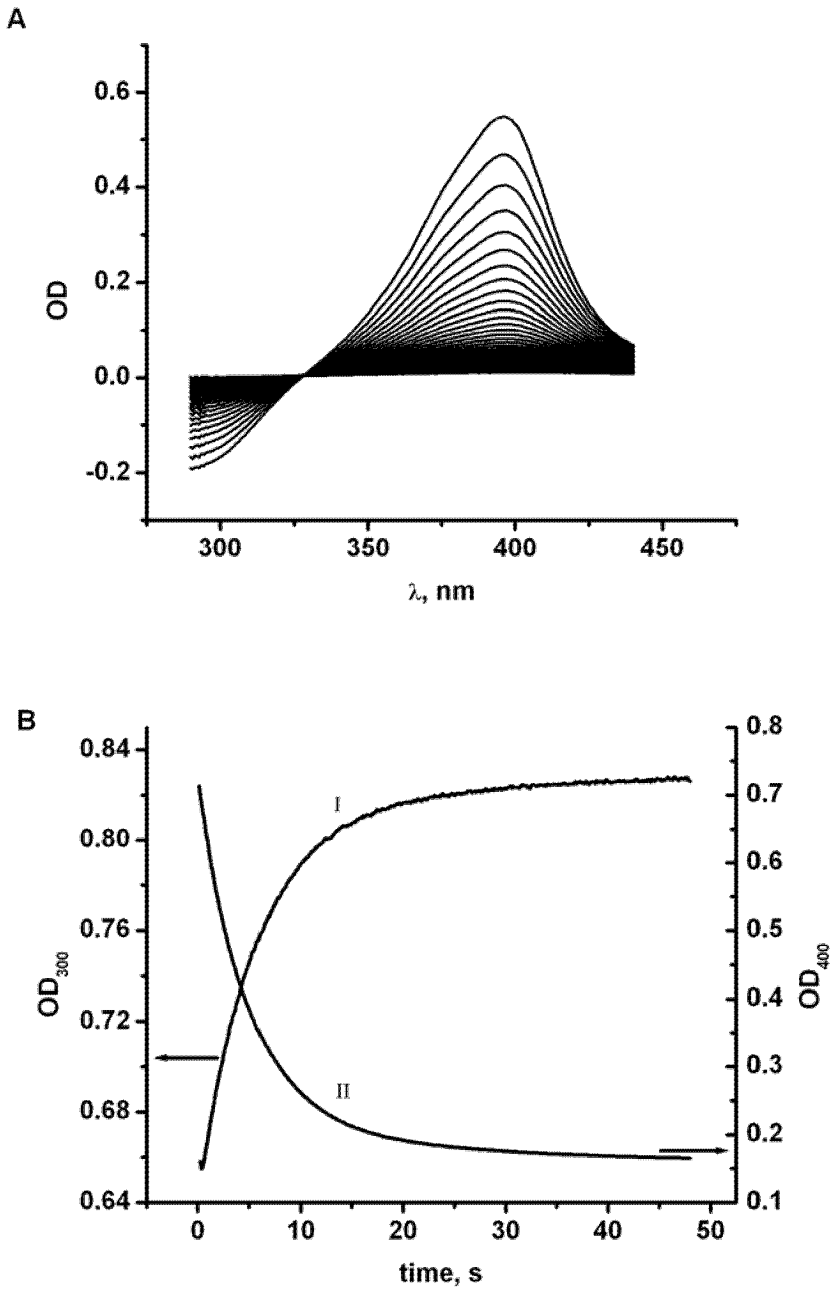

Figure 12. Panel A, Changes in the differential absorption spectrum during the decay of I_{400}. Spectra are taken every second. The reference spectrum is that of the reaction mixture several minutes after mixing. 0.5 mM peroxynitrite, 0.82 mM phenol, 25 mM total carbonate, pH jump from 7.2 to pH 10. Panel B, kinetics traces at 300 (curve I) and 400 nm (curve II), recorded with the same solutions.

Because the increase of absorption at 300 nm has the same rate as the decay of I_{400} (Figure 12B), it is plausible that 2,2′-biphenol is formed *via* a direct bimolecular reaction between I_{400} and phenol. From Figure 11, one derives a second-order rate constant for the reaction of phenol with I_{400} is (2.4 ± 0.1) $\times 10^2$ $M^{-1}s^{-1}$ at pH 10.5. The pH-dependence of the decay of I_{400} suggests that I_{400} reacts with phenolate several times faster than with phenol (Figure 13).

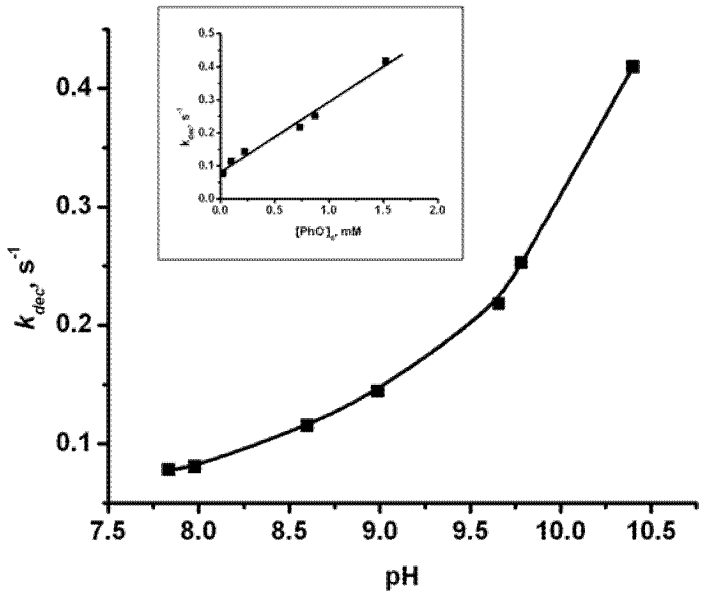

Figure 13. pH-Dependence of the rate constant of the I_{400} decay. 0.49 mM peroxynitrite, 2 mM phenol, 25 mM total carbonate, pH-jump from 7.2. Inset: dependence on a calculated phenolate concentration.

3.2.7 Dioxygen does not influence the kinetics

It has been shown that peroxynitrous acid and a peroxynitrite/carbon dioxide mixture yield peroxynitrate in the presence of dioxygen and a suitable substrate [6,7]. Formation of peroxynitrate leads to a biphasic decay of absorption at 300 nm and one would expect it to complicate the oxidation kinetics. Although, in the presence of phenolates, the formation of peroxynitrate *via* mechanisms proposed in [6] and [7] does not seem possible, we wanted to make sure that dioxygen has no

influence on the observed kinetics. Indeed, when argon-saturated peroxynitrite solutions are mixed with carbon dioxide saturated phenol solutions, the kinetics traces are the same as when no precautions are taken to eliminate oxygen.

3.2.8 I_{400} is diamagnetic

We used an ESR spectrometer equipped with a flow cell that allows recording of spectra within several ms after mixing (*cf.* Materials and Methods). With solutions of the same composition as those used in stopped-flow experiments, we do not detect any signals, which is an indication that I_{400} is diamagnetic.

3.2.9 Absorption at wavelengths above 500 nm

Based on the kinetics trace shown in Figure 6D, another intermediate with a broad absorption maximum above 500 nm is formed concomitantly with the decay of peroxynitrite. Like I_{400}, its formation is first-order in peroxynitrite and carbon dioxide, first- to zero-order in phenol and faster at higher pH values (Figure 14). In contrast to I_{400}, this intermediate can be further oxidized by a mixture of peroxynitrite and carbon dioxide and, possibly, by I_{400} as well (Figures 6C and D, curves II). The decay of the absorption above 500 nm is complex and depends on pH, phenol, and carbon dioxide concentrations. We hypothesized (*cf.* Discussion) that *para*-benzoquinone could be formed by oxidation of an initially formed hydroquinone and, therefore, absorption above 500 nm might be due to quinhydrone – a 1:1 charge-transfer complex between hydroquinone and *para*-benzoquinone. Indeed, under the conditions of our study, the simultaneous presence of *para*-benzoquinone and hydroquinone results in a rapid (seconds) formation of absorption above 500 nm (Figure 15). This absorption reaches a maximum *ca.* 100 s after mixing and decays due to the oxidation of hydroquinone by dioxygen and by alkaline hydrolysis of *para*-benzoquinone.

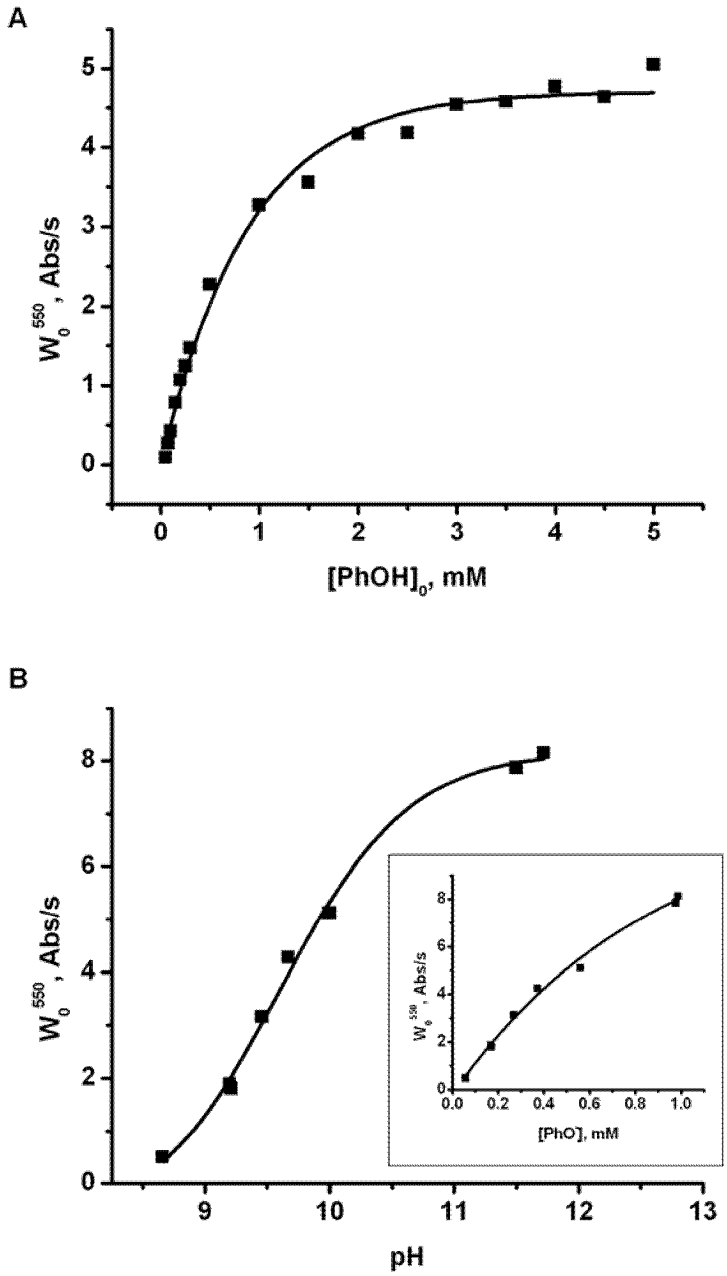

Figure 14. Dependence of the initial rate of the increase of absorption at 550 nm on phenol concentration (panel A), pH (panel B), and the calculated phenolate concentration (inset on panel B). Panel A, 0.6 mM peroxynitrite, 25 mM carbonate, pH jump from 7.2 to 10.2. Panel B, peroxynitrite is pre-mixed with 200 mM phosphate buffer and subsequently mixed with an aqueous solution, containing carbon dioxide and phenol. Concentrations after mixing: 0.45 mM peroxynitrite, 1 mM phenol, 13 mM carbon dioxide.

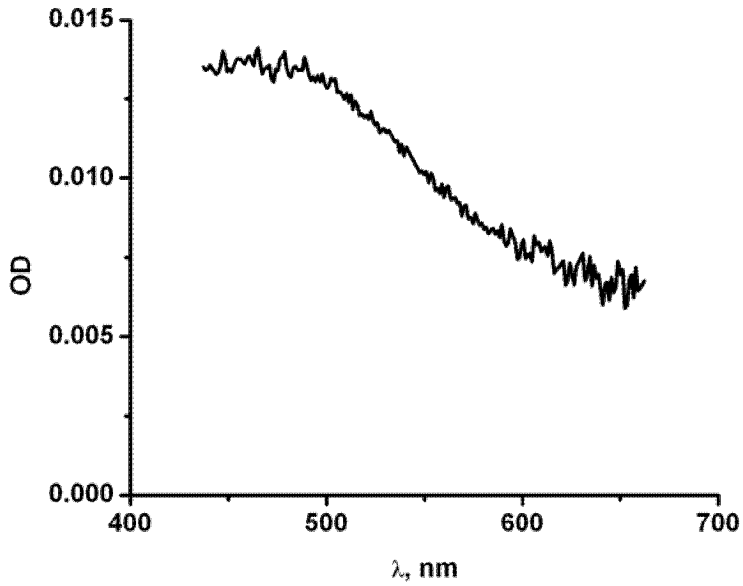

Figure 15. Absorption spectrum of 10 μM hydroquinone and 5 μM para-benzoquinone 100 s after mixing with a phosphate buffer, pH 11.

3.3 Discussion

3.3.1 I_{400}

We have shown that, during the carbon dioxide catalyzed reaction of peroxynitrite with phenolate, a novel intermediate with an absorption maximum at 400 nm ($10^3 \leq \varepsilon_{400} \leq 10^5$)[1] is formed. While work to establish the structure of I_{400} is in progress, we note that, (i) given the absence of an ESR signal, I_{400} is diamagnetic[2] and, (ii) given that one phenolate and one peroxynitrite molecule

[1] The lower estimate is based on the initial peroxynitrite concentration and the higher on the yield of 2,2′-biphenol.

[2] The phenoxyl radical, which, too, has an absorption maximum at 400 nm, can be indisputably excluded on different grounds. Given the extinction coefficient of the phenoxyl radical at 400 nm of *ca.* 5000 $M^{-1}cm^{-1}$ [8,9] and a typical absorption decrease of 0.5 absorption units (Figures 1B, 1D), *ca.* 0.1 mM phenoxyl radical should have been formed. At that concentration, it should have

required, I_{400} is probably a product of a two-electron oxidation of phenolate, and (iii) it couples with phenol(-ate) to form 2,2′-biphenol, most probably *via* a direct bimolecular reaction.

3.3.2 Formation of biphenols

The observation that the ratio of 2,2′- to 4,4′-biphenols depends on pH and phenol concentration indicates that these products are formed by two different mechanisms. A mechanism that operates at high pH and phenol concentrations results in formation of I_{400}, which subsequently couples with phenol. That no 4,4′-biphenol is formed *via* this reaction pathway (Figure 4B) suggests that phenoxyl radicals are not involved.

Via a second mechanism, which largely operates at neutral to slightly alkaline pH and moderate phenol concentrations, both 2,2′- and 4,4′-biphenols as well as 2- and 4-nitrophenols are formed. This pathway is well described in the literature [4] and the reactive intermediates in this pathway are trioxocarbonate(•1–) and nitrogen dioxide radicals [11]. Thus, at neutral pH biphenols are formed *via* coupling of two phenoxyl radicals.

3.3.3 Partition between two pathways

The partition between the two reaction pathways depends, as already mentioned, on the phenol concentration and the pH. Because I_{400} is formed exclusively from phenolate, increasing pH and phenol concentration favors the first pathway (Figure 8). The partition between the two pathways also depends on the carbon dioxide concentration. As shown in Figure 9, the yield of I_{400} decreases somewhat with the concentration of carbon dioxide. Comparing product yields with

---

disappeared *via* a dimerization reaction ($k \sim 10^8$ $M^{-1}s^{-1}$) [8,10] in a matter of microseconds – 10^5 times faster than observed.

2 and 20 mM carbon dioxide (Figures 3A, B and 2A, B),[3] one observes that higher concentrations of carbon dioxide lead to products characteristic of the radical pathway.

3.3.4 Reactive species formed during carbon dioxide catalyzed decay of peroxynitrite

Formation of a nitrogen dioxide / trioxocarbonate(•1–) radical pair is an established pathway of peroxynitrite reactivity in the presence of carbon dioxide [6,11-13]. However, it is not obvious how a mechanism based solely on a radical pair could explain our results, which show that two distinct pathways of biphenol formation exist. In the radical model, the difference in product yields at neutral and alkaline pH is caused by reaction of nitrogen dioxide with phenolate [4,10]. This reaction produces additional phenoxyl radicals and thus biphenols are formed at the expense of nitrophenols. However, the increased concentration of phenoxyl radicals should not lead to a change in the isomer ratio of the biphenols. Moreover, we have shown that, at high pH and phenol concentrations, 2,2′-biphenol is not formed *via* coupling of two phenoxyl radicals, but rather *via* a direct coupling of I_{400}, a diamagnetic intermediate, with phenol. Simultaneous formation of I_{400} and nitrophenols and the pH dependence of their yields are also not compatible with the reactivity of only radicals. Although, theoretically, the coupling of nitrogen dioxide with phenoxyl radicals may lead to multiple products, the ratio of these products should not be pH- and concentration-dependent. Thus, it does not seem possible to rationalize our results based solely on the reactivity of the nitrogen dioxide and trioxocarbonate(•1–) radical pair, and it is likely that another reactive intermediate

[3] In the two experiments, the peroxynitrite concentrations are the same, but the pH and carbon dioxide concentrations differ. Since solutions with higher carbon dioxide concentrations are at higher pH, the argument is even stronger, because increasing pH and carbon dioxide concentration have opposite effects: increasing pH favors the "I_{400} pathway", while increasing carbon dioxide concentration favors the "radical pathway".

is formed. It is possible that this intermediate is less oxidizing than the trioxocarbonate(•1–) radical, as it reacts with electron-rich phenolate, but not with phenol itself.

3.3.5 The lifetime of the peroxynitrite-carbon dioxide adduct and secondary oxidants derived from it

The following reaction sequence (reactions 1 – 4) has been suggested to take place during the carbon dioxide catalyzed isomerization of peroxynitrite [14,15].

$$ONOO^- + CO_2 \rightleftarrows ONOOCO_2^- \quad (1)$$

$$ONOOCO_2^- \rightleftarrows NO_2^\bullet + CO_3^{\bullet-} \quad (2)$$

$$NO_2^\bullet + CO_3^{\bullet-} \longrightarrow O_2NOCO_2^- \quad (3)$$

$$O_2NOCO_2^- \longrightarrow NO_3^- + CO_2 \quad (4)$$

Nitrocarbonate ($O_2NOCO_2^-$) is likely to be very short-lived. Calculations show that it decomposes to nitrate and carbon dioxide within a few vibrations and, thus, its participation in bimolecular reactions is precluded [14]. Formation of the adduct ($ONOOCO_2^-$) was suggested [16], confirmed experimentally [15], and shown to be theoretically feasible [17]. It was concluded, however, that the adduct is also too short-lived to directly react with substrates [14,18,19]. This view is based on the observations that (i) no direct oxidations by the adduct are observed and (ii) the isomerization of peroxynitrite follows a first-order decay, which would not be expected for long-lived absorbing intermediates. From this condition, we can derive that $k_1[CO_2] << k_{-1} + k_2$. Given that k_1 = 3 × 10^4 $M^{-1}s^{-1}$ [16] and a typical experimental concentration of carbon dioxide of *ca.* 1–2 mM, $k_{-1} + k_2 >> 50$ s^{-1}. A k_2 of ~ 10^3 – 10^4 s^{-1} would allow substrates present at mM concentrations to react directly with the adduct before it undergoes homolysis *via* reaction 2, if these

substrates reacted with second-order rate constants of the order of $10^6 - 10^7$ $M^{-1}s^{-1}$. Thus, a rate constant of homolysis of $k_2 \sim 10^3 - 10^4$ s^{-1} would not completely exclude the possibility of direct reactions of the adduct. However, even higher values of k_2 were suggested based on thermodynamic considerations. Merenyi et al. estimated k_2 at 10^6 s^{-1} and argued that the lifetime of the adduct would be in the micro- to submicro-second range [18]. Squadrito et al. estimated k_2 at 10^9 s^{-1} [14]. Both values are based on thermodynamic estimates of the equilibrium constant of reaction 2 and the assumption that the rate constant of a reverse reaction is the experimentally determined rate constant of recombination of nitrogen dioxide and trioxocarbonate(•1–) radicals, *i.e*, $k_{-2} = 5 \times 10^8$ $M^{-1}s^{-1}$ [20,21]. However, in a recent pulse-radiolysis study [21], peroxynitrite was not observed as an intermediate in the reaction of nitrogen dioxide and trioxocarbonate(•1–) radicals. It was suggested, therefore, that these radicals recombine primarily through the N–O bond and not the O–O bond, *i.e.*, $k_{-2} < k_3$. If, indeed, $k_{-2} < k_3 = 5 \times 10^8$ $M^{-1}s^{-1}$, then the values of k_2, calculated in [18] and [14] are overestimated and the lifetime of the adduct is underestimated.[4]

In an *ab initio* study, Houk et al. predicted that reaction 1 is exothermic (ΔE = –25.7 kcal/mole), that there is no barrier to adduct formation, and that homolysis (reaction 2) requires 8.7 kcal/mole. In this scenario, homolysis (reaction 2), rather than formation of $ONOOCO_2^-$ (reaction 1), should be the rate-limiting step. The single-exponential decay of peroxynitrite could be explained if both the forward and reverse reaction of equilibrium 1 are rapid, which implies that the adduct is in

[4] One can argue that peroxynitrite was not observed during coupling of nitrogen dioxide with trioxocarbonate(•1–) because reaction 2 is an equilibrium and reaction 3 is not, and all three reactions are sufficiently fast. If correct, it is possible that $k_{-2} \sim k_3$. But exactly because reaction 2 is an equilibrium, the half-life of the adduct should be longer than $\ln 2/k_2$.

equilibrium with peroxynitrite and carbon dioxide, $\left[\mathrm{ONOOCO_2^-}\right]=\frac{k_1}{k_{-1}}\left[\mathrm{ONOO^-}\right]\left[\mathrm{CO_2}\right]$, and the decay of peroxynitrite is therefore given by $k_{obs}=\frac{k_1k_2}{k_{-1}}=3\times10^4\,\mathrm{M^{-1}s^{-1}}$. The equilibrium constant of reaction 1 was estimated at 10^2 M^{-1} [18]. Given that the typical concentrations of carbon dioxide used in kinetics experiments are in the mM range, only 10% of the peroxynitrite would be in the form of an adduct, and, therefore, the decay of peroxynitrite could be followed at 300 nm, where it absorbs maximally. If, furthermore, the adduct does not absorb significantly at 300 nm, this kinetics scheme would explain the observation made by Meli et al. [22] that, with *ca.* 10 mM carbon dioxide, the initial absorption of peroxynitrite measured at 300 nm is only half of what is expected. According to this model, the value of k_2 could be estimated at $\frac{k_{obs}\times k_{-1}}{k_1}=\frac{3\times10^4}{10^2}$ ~ 10^2 s^{-1} – two orders of magnitude higher than the analogous rate constant of peroxynitrous acid. This may explain why no direct reaction of substrates has been observed with the adduct.

In any event, it is evident that, apart from a radical pair, another oxidant is formed. Given the leeway allowed by theoretical estimates, we assume that the peroxynitrite/carbon dioxide adduct is sufficiently long-lived to directly react with phenolate.

3.3.6 Formation of bi- and nitrophenols

Assuming that the adduct reacts with phenolate, the following reaction scheme may apply: classically, peroxynitrite reacts with carbon dioxide to form the adduct (reaction 1), which subsequently undergoes partial homolysis to trioxocarbonate(•1–) and nitrogen dioxide radicals (reaction 2). These radicals react

with phenol(-ate) to produce phenoxyl radicals (reactions 5 and 6), which couple with each other (reaction 7) or with nitrogen dioxide (reaction 8) [4].

$$CO_3^{\bullet -} + PhOH(PhO^-) \longrightarrow PhO^{\bullet} + HCO_3^-(CO_3^{2-}) \quad (5)$$

$$NO_2^{\bullet} + PhO^- \longrightarrow PhO^{\bullet} + NO_2^- \quad (6)$$

$$PhO^{\bullet} + PhO^{\bullet} \longrightarrow \text{biphenols} \quad (7)$$

$$NO_2^{\bullet} + PhO^{\bullet} \longrightarrow \text{nitrophenols} \quad (8)$$

New is that we propose that at high phenolate concentrations, formation of I_{400}, reaction 9, competes with homolysis, reaction 2.

$$ONOOCO_2^- + PhO^- \longrightarrow I_{400} + CO_3^{2-} \quad (9)$$

The intermediate I_{400} couples with another phenolate to form 2,2′-biphenol (reaction 10)

$$I_{400} + PhO^- \longrightarrow 2,2' - \text{biphenol} + NO_2^- \quad (10)$$

We are not certain that, in reactions 9 and 10, carbonate and nitrite are leaving groups. However, there is no influence of ionic strength (0.1–1M) on the rates of reaction 9 and 10 (not shown), and we therefore surmise that I_{400} is neutral. This mechanism qualitatively explains product distribution as a function of pH and phenol and carbon dioxide concentrations. At high pH and phenol concentration the rate of reaction 9 increases and 2,2′-biphenol is formed by coupling of I_{400} with phenolate, reaction 10. At high carbon dioxide concentrations, the rate of radical

generation (reaction 2) increases,[5] which results in formation of all isomeric bi- and nitrophenols *via* reactions 5 – 8.

One should note that the mechanism based on reactions 1, 2, 4 – 10 explains the dependence of biphenol yields on pH and phenol concentration qualitatively, but not quantitatively. Indeed, if the yields of reactions 9 and 10 were close to 100%, then one should expect the yields of 2,2′-biphenol to reach 100% at high pH and phenol concentrations. However, this is not the case. The yields of 2,2′-biphenol saturate at *ca.* 2% of the initial peroxynitrite concentration (Figure 4). One possible explanation is that I_{400} is formed from a hydrolytically unstable precursor (for instance, phenyl nitrate $O_2NOC_6H_5$), which decays back to phenolate and, by a minor pathway, isomerizes to I_{400}. Also, 2,2′-biphenol might not be the only product formed from I_{400}. For instance, formation of *para*-benzoquinone may be related to the "I_{400}-pathway".

3.3.7 Formation of *para*-benzoquinone

Para-benzoquinone was identified by HPLC, MS, and UV-Vis kinetics experiments. Because *para*-benzoquinone is a product of the four-electron oxidation of phenol, it cannot be formed directly from phenol, but is the product of the oxidation of a precursor. Oxidation of dihydroxybenzols (catechol and hydroquinone) to quinones by peroxynitrous acid [23] and peroxynitrite in the presence of carbon dioxide [24] is well documented. It might be, therefore, that hydroquinone is a *para*-benzoquinone precursor. If *para*-benzoquinone is formed by oxidation of hydroquinone, then the absorption above 500 nm can be explained by the simultaneous presence of both species. Although neither hydroquinone nor

[5] The rate of reaction 2 is proportional to the concentration of carbon dioxide in both kinetics models.

para-benzoquinone has an absorption band above 500 nm, present together, they form a 1:1 charge-transfer complex, quinhydrone, which is intensely colored (Figure 15). The formation and decay of the absorption above 500 (Figure 6C, D) are also well explained if this absorption is due to quinhydrone. The absorption is proportional to the product of the concentrations of hydroquinone and *para*-benzoquinone. It would reach its maximum when the concentrations of *para*-benzoquinone and hydroquinone are equal and decay upon further oxidation of hydroquinone to *para*-benzoquinone. From the kinetics traces one can conclude that hydroquinone is oxidized not only by peroxynitrite in the presence of carbon dioxide, but also by I_{400} (Figure 6D). At alkaline pH, it is readily oxidized even by dioxygen. At pH 7, where hydroquinone is stable towards oxidation by dioxygen and up to 20 μM of *para*-benzoquinone is formed, hydroquinone is not detected. This might be because hydroquinone is much more reactive than phenol towards oxidation by peroxynitrite and I_{400}.

Dihydroxybenzols (catechol and hydroquinone) are well-known products of the reaction of peroxynitrous acid with phenols, which, to our knowledge, have not been reported at alkaline pH in the presence of carbon dioxide. Theoretically, hydroquinone can be formed by hydrolysis of an unstable hydroxyphenyl nitrite ($HO–C_6H_4–ONO$), which, in turn, can be produced by a C–O coupling of phenoxyl radical with nitrogen dioxide [5]. However, in a study of tyrosine oxidation by nitrogen dioxide [10], the only products found were biphenols and nitrophenols. It is, therefore, unlikely that hydroxyphenyl nitrite is formed in substantial amounts during the reaction of phenoxyl radicals with nitrogen dioxide. The observed complex pH and concentration dependence of the yields of *para*-benzoquinone also cannot be accounted for by the formation of a *para*-benzoquinone precursor by the coupling of the two radicals.

The yields of *para*-benzoquinone depend on pH and phenol concentrations (Figure 5). At alkaline pH, the yield of benzoquinone is maximal at a *ca.* 1:10 phenol to peroxynitrite ratio. At pH 7.7, the maximum is reached at *ca.* 3-fold excess of phenol over peroxynitrite. It seems, therefore, that an optimal phenolate concentration is required for the maximal formation of a *para*-benzoquinone. It might be that formation of benzoquinone requires I_{400} (or, possibly, a precursor of I_{400}), which itself requires phenolate (reaction 9). If I_{400} were to decay through isomerization to hydroquinone (reaction 11) and through a second-order reaction with phenolate (reaction 10), then it can be understood why excess phenolate would decrease the yields of *para*-benzoquinone: I_{400} would react to form 2,2′-biphenol. Thus, an optimal concentration of phenolate is required for the formation of *para*-benzoquinone.

$$I_{400} \rightarrow HQ \qquad (11)$$

$$HQ \xrightarrow{ONOO^- + CO_2; I_{400}; O_2} BQ \qquad (12)$$

3.3.8 Relevance

Clearly, formation of dityrosine *via* this novel "I_{400}-pathway" is not likely to be physiologically relevant, given the required participation of phenolate, unless the pK_a of a tyrosine in a protein is much lower than its usual value of 10. However, this finding is relevant to the chemistry of intermediates formed during the carbon dioxide catalyzed isomerization of peroxynitrite. It shows that the reactivity of peroxynitrite cannot be rationalized solely on the basis of the reactivity of the trioxocarbonate(•1–)/nitrogen dioxide radical pair. Formation of I_{400}, a diamagnetic biphenol precursor, might proceed *via* a two-electron oxidation of phenolate and present the first example of a reaction that proceeds *via* the peroxynitrite/carbon dioxide adduct, which was previously considered to be too short-lived to be a

relevant oxidant. This pathway might be more important in reactions with other substrates and opens new perspectives for peroxynitrite scavenging *in vivo*. As an example, the "I_{400}-pathway" might be related to the reaction mechanism of some phenolic antioxidants. Sinapinic acid (3,5-dimethoxy-4-hydroxy-*trans*-cinnamic acid) was shown to efficiently protect tyrosine residues against peroxynitrite-mediated nitration [25,26]. In the absence of tyrosine, sinapinic acid underwent oxidative coupling to form a mono-lactone [25]. In another study, it was shown that a long-lived colored intermediate is produced in the reaction of sinapinic acid with peroxynitrous acid [27].

3.3.9 Conclusions

We have shown that carbon dioxide catalyzed oxidative coupling of phenol by peroxynitrite occurs by two different pathways. These two pathways are distinguished by the isomer ratio of 4,4′- to 2,2′- biphenols. One pathway is based on the coupling of two phenoxyl radicals and affords both 2,2′- and 4,4′-biphenols. The other, probably, overall non-radical pathway, operates *via* the formation of a diamagnetic intermediate I_{400} and its subsequent direct coupling with phenol(ate), to yield 2,2′-biphenol, but no 4,4′-biphenol. The reactive oxidants are trioxocarbonate(•1–) and nitrogen dioxide radicals in the first pathway and, possibly, the peroxynitrite/carbon dioxide adduct in the second pathway. Formation of *para*-benzoquinone is reported for the first time and could be related to the non-radical pathway of biphenol formation.

References

[1] Lemercier, J. N.; Padmaja, S.; Cueto, R.; Squadrito, G. L.; Uppu, R. M.; Pryor, W. A. Carbon dioxide modulation of hydroxylation and nitration of phenol by peroxynitrite. *Arch. Biochem. Biophys.* **345**:160-170; 1997.

[2] Zeller, K.-P.; Müller, R. Mass spectra of quinones. In Patai, S.; Rappoport, Z. eds. *The Chemistry of the Quinonoid Compounds*. Chichester: John Wiley & Sons; 1988:87-109.

[3] Wong, C. F.; LaLonde, R. T. Reversible deuteration of 2,6-dimethoxy-1,4-benzoquinone in alkali. *J. Org. Chem.* **58**:3226-3227; 1975.

[4] Lymar, S. V.; Jiang, Q.; Hurst, J. K. Mechanism of carbon dioxide-catalyzed oxidation of tyrosine by peroxynitrite. *Biochemistry* **35**:7855-7861; 1996.

[5] Ramezanian, M. S.; Padmaja, S.; Koppenol, W. H. Hydroxylation and nitration of phenolic compounds by peroxynitrite. *Chem. Res. Toxicol.* **9**:232-240; 1996.

[6] Goldstein, S.; Czapski, G. Formation of peroxynitrate from the reaction of peroxynitrite with CO_2: Evidence for carbonate radical production. *J. Am. Chem. Soc.* **120**:3458-3463; 1998.

[7] Hodges, G. R.; Ingold, K. U. Cage-escape of geminate radical pairs can produce peroxynitrate from peroxynitrite under a wide variety of experimental conditions. *J. Am. Chem. Soc.* **121**:10695-10701; 1999.

[8] Khudyakov, I. V.; Kuz'min, V. A. Absolute values of rate constants for phenoxyl radical loss reactions in an aqueous medium. *Khim. Vys. En.* **7**:331-334; 1973.

[9] Wojnárovits, L.; Kovács, A.; Földiák, G. Spectral characteristics of monosubstituted phenoxyl radicals. *Radiat. Phys. Chem.* **50**:377-379; 1997.

[10] Prütz, W. A. Tyrosine oxidation by $NO_2^{\bullet}$ in aqueous solution. *Z. Naturforsch.* **39c**:725-727; 1984.

[11] Lymar, S. V.; Hurst, J. K. Radical nature of peroxynitrite reactivity. *Chem. Res. Toxicol.* **11**:714-715; 1998.

[12] Bonini, M. G.; Radi, R.; Ferrer-Sueta, G.; Ferreira, A. M. D.; Augusto, O. Direct EPR detection of the carbonate radical anion produced from peroxynitrite and carbon dioxide. *J. Biol. Chem.* **274**:10802-10806; 1999.

[13] Meli, R.; Nauser, T.; Koppenol, W. H. Direct observation of intermediates in the reaction of peroxynitrite with carbon dioxide. *Helv. Chim. Acta* **82**:722-725; 1999.

[14] Squadrito, G. L.; Pryor, W. A. Mapping the reaction of peroxynitrite with CO_2: Energetics, reactive species, and biological implications. *Chem. Res. Toxicol.* **15**:885-895; 2002.

[15] Goldstein, S.; Meyerstein, D.; van Eldik, R.; Czapski, G. Evidence for adduct formation between $ONOO^-$ and CO_2 from high-pressure pulse radiolysis. *J. Phys. Chem. A* **104**:9712-9714; 2000.

[16] Lymar, S. V.; Hurst, J. K. Rapid reaction between peroxonitrite ion and carbon dioxide: Implications for biological activity. *J. Am. Chem. Soc.* **117**:8867-8868; 1995.

[17] Houk, K. N.; Condroski, K. R.; Pryor, W. A. Radical and concerted mechanisms in oxidations of amines, sulfides, and alkenes by peroxynitrite, peroxynitrous acid, and the peroxynitrite-CO_2 adduct: Density functional theory transition structures and energetics. *J. Am. Chem. Soc.* **118**:13002-13006; 1996.

[18] Merényi, G.; Lind, J. Thermodynamics of peroxynitrite and its CO_2-adduct. *Chem. Res. Toxicol.* **10**:1216-1220; 1997.

[19] Lymar, S. V.; Hurst, J. K. CO_2-catalyzed one-electron oxidation by peroxynitrite: Properties of the reactive intermediate. *Inorg. Chem.* **37**:294-301; 1998.

[20] Lilie, J.; Hanrahan, R. J. O^- transfer reactions of the carbonate radical anion. *Radiat. Phys. Chem.* **11**:225-227; 1978.

[21] Alfassi, Z. B.; Dhanasekaran, T.; Huie, R. E.; Neta, P. On the reactions of $CO_3^{\bullet-}$ with NO_x radicals. *Radiat. Phys. Chem.* **56**:475-482; 1999.

[22] Meli, R.; Nauser, T.; Latal, P.; Koppenol, W. H. Reaction of peroxynitrite with carbon dioxide: Intermediates and determination of the yield of $CO_3^{\bullet-}$ and $NO_2^{\bullet}$. *J. Biol. Inorg. Chem.* **7**:31-36; 2002.

[23] Ramezanian, M. S.; Padmaja, S.; Koppenol, W. H. Nitration and hydroxylation of phenolic compounds by peroxynitrite. *Methods Enzymol.* **269**:195-201; 1996.

[24] Tibi, S.; Koppenol, W. H. Reactions of peroxynitrite with phenolic and carbonyl compounds. *Helv. Chim. Acta* **83**:2412-2424; 2000.

[25] Niwa, T.; Doi, U.; Kato, Y.; Osawa, T. Inhibitory mechanism of sinapinic acid against peroxynitrite-mediated tyrosine nitration of protein in vitro. *FEBS Lett.* **459**:43-46; 1999.

[26] Pannala, A.; Razaq, R.; Halliwell, B.; Singh, S.; Rice-Evans, C. A. Inhibition of peroxynitrite dependent tyrosine nitration by hydroxycinnamates: Nitration or electron donation? *Free Radical Biol. Med.* **24**:594-606; 1998.

[27] Akhter, S.; Green, J. R.; Root, P.; Thatcher, G. J.; Mutus, B. Peroxynitrite and NO^+ donors form colored adducts with sinapinic acid: potential applications. *Nitric Oxide: Biol. Chem.* **8**:214-221; 2005.

4 PROPERTIES OF THE INTERMEDIATE FORMED DURING NON-RADICAL OXIDATIVE COUPLING OF PHENOLATE BY PEROXYNITRITE IN THE PRESENCE OF CARBON DIOXIDE

4.1 Abstract

In the presence of carbon dioxide, at high pH and high phenol concentrations, 2,2′-biphenol is formed *via* a novel non-radical pathway which involves a diamagnetic intermediate and its subsequent direct coupling with phenol. The identity of this intermediate is of interest and here we describe our attempt to characterize it. Because the intermediate is formed in low concentrations and is too short-lived to be analyzed by conventional structural methods, we studied its reactivity by a sequential-mix stopped-flow spectrophotometry and HPLC product analysis. When sufficient excess of phenol is present, this intermediate reacts with phenol to form 2,2′-biphenol, with a yield relative to the concentration of the intermediate of *ca.* 65%. At alkaline pH, and when phenolate is a limiting reagent, *para*-benzoquinone is a major oxidation product. Under these conditions, the decay of the intermediate becomes zero-order and independent of phenol concentration. This decay is due to a fast ($k = (3.9 \pm 0.1) \times 10^5$ $M^{-1}s^{-1}$ at pH 7.2; $k = (7.7 \pm 0.5) \times 10^7$ $M^{-1}s^{-1}$ at pH 10.5) reaction of the intermediate with hydroquinone, which is formed during the alkaline hydrolysis of *para*-benzoquinone. The intermediate reacts rapidly with biologically relevant reductants ($k \sim 10^5$ $M^{-1}s^{-1}$ at pH 7), and quantitatively oxidizes hydroquinone to *para*-benzoquinone. The UV-Vis spectrum of the intermediate shows an absorption maximum at 400 nm, $\varepsilon_{400} = (61 \pm 1) \times 10^3$

$M^{-1}cm^{-1}$, and remains unchanged between pH 5 to 11. *Para*-substituted phenols do not form intermediates with appreciable absorption above 350 nm. *Diortho*-substituted phenols form two consecutive intermediates with maxima at *ca.* 420 nm and *ca.* 360, these intermediates are likely to give rise to corresponding *para*-quinones at alkaline pH.

4.2 Results

4.2.1 Zero-order kinetics of I_{400} decay.

As reported before [1][1], a diamagnetic intermediate with an absorption maximum at 400 nm (I_{400}) is formed during the reaction of peroxynitrite with phenolate in the presence of carbon dioxide. I_{400} was proved to be a 2,2′-biphenol precursor and its decay was shown to be exponential and first-order in phenol, with phenol in excess.

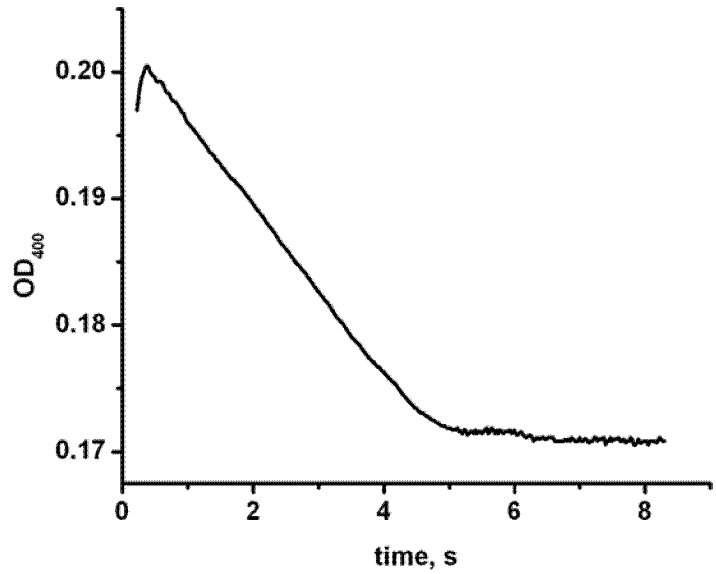

Figure 1. The decay of I_{400}. Conditions: 40 μM phenol, 0.6 mM peroxynitrite, 25 mM carbonate, pH-jump from 7.2 to 10.5.

[1] Chapter 3

Upon examination of the kinetics of I_{400} decay, we found that the decay of I_{400} becomes zero-order when phenol is the limiting reagent (Figure 1).

If the zero-order decay were due to the reaction with phenol, then the mechanism of 2,2′-biphenol formation would be more complex than simply a direct coupling of I_{400} with phenol. To verify this hypothesis, we carried out sequential-mix experiments as described in Materials and Methods, and mixed pre-formed I_{400} with 1 to 5 mM phenol. If there were no change in the mechanism, and I_{400} would still decay through its reaction with phenol, then one could expect that the decay would become exponential and faster at higher phenol concentrations. However, that is not the case. Phenol, up to several mM, does not influence the rapid decay of I_{400} (Figure 2, curves II and III). Therefore, when phenol is the limiting reagent, an oxidation product is formed which reacts with I_{400}.

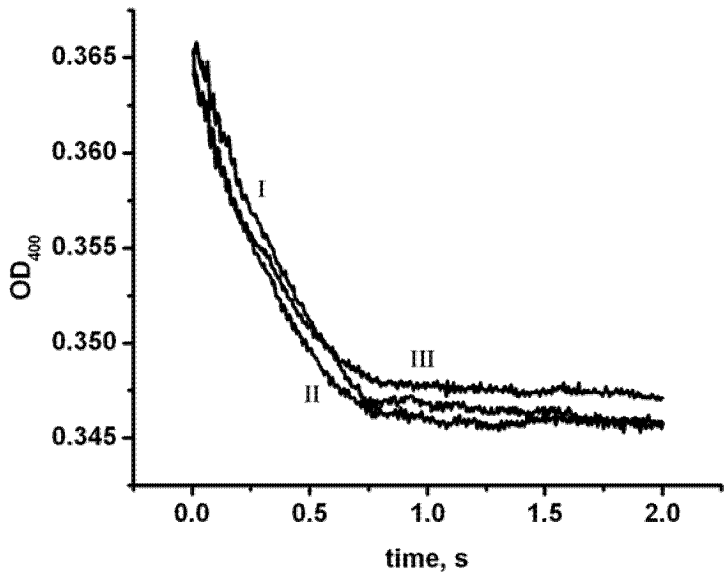

Figure 2. Sequential-mix experiments. The decay of I_{400} in the absence (curve I) and presence of 2 mM (curve II) and 4 mM phenol (curves III). I_{400} is pre-formed at pH 10.2 from 1.3 mM peroxynitrite, 75 μM phenol, and 25 mM carbonate, pH jump from 7.2 to 10.2, and after a delay of 300 ms mixed with water or the aqueous phenol solution.

This is also demonstrated by varying an excess of peroxynitrite over phenol. The decay of I_{400} becomes faster with larger excesses of peroxynitrite over phenol (Figure 3).

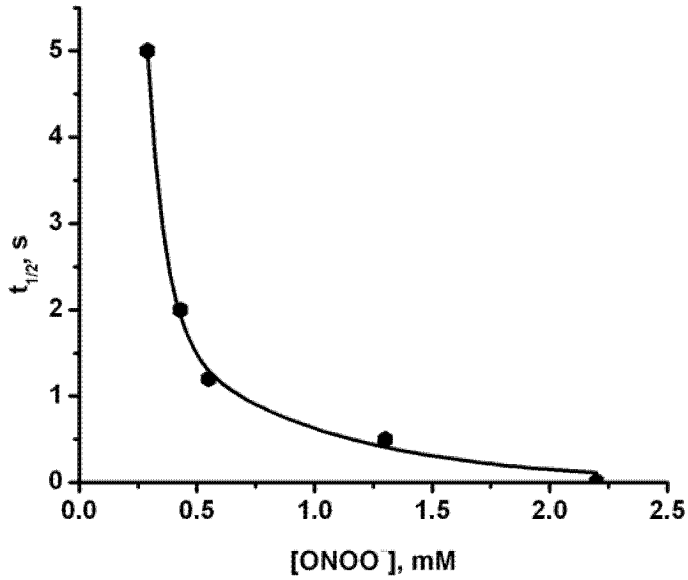

Figure 3. Half-lifes (s) of the zero-order decay of I_{400}, with 10 to 100-fold excess of peroxynitrite over phenol. Conditions: 20μM phenol, pH jump from 7.2 to 10.2, 25 mM carbonate, 200 mM phosphate buffer.

As we have shown in a previous publication, [1][2], at alkaline pH the yield of *para*-benzoquinone increases with excess of peroxynitrite-over-phenol. We assumed, therefore, that the zero-order decay is caused by the presence of *para*-benzoquinone in concentrations up to *ca.* 20 μM. To verify that, we studied the reaction of I_{400} with *para*-benzoquinone by sequential-mix stopped-flow experiments. Since *para*-benzoquinone is unstable in alkaline aqueous solutions, we studied the reaction with freshly prepared and aged solutions and concluded that *para*-benzoquinone itself does not react with I_{400}. Upon standing for several minutes the alkaline solution of *para*-benzoquinone becomes more reactive (Figure

[2] Chapter 3, Figure 5.

4, curves I-III), and the reactivity increases more rapidly at higher pH and *para*-benzoquinone concentrations. It is likely, therefore, that (a) product(s) of the alkaline hydrolysis of *para*-benzoquinone is(are) responsible for the rapid disappearance of I_{400}, but not *para*-benzoquinone itself.

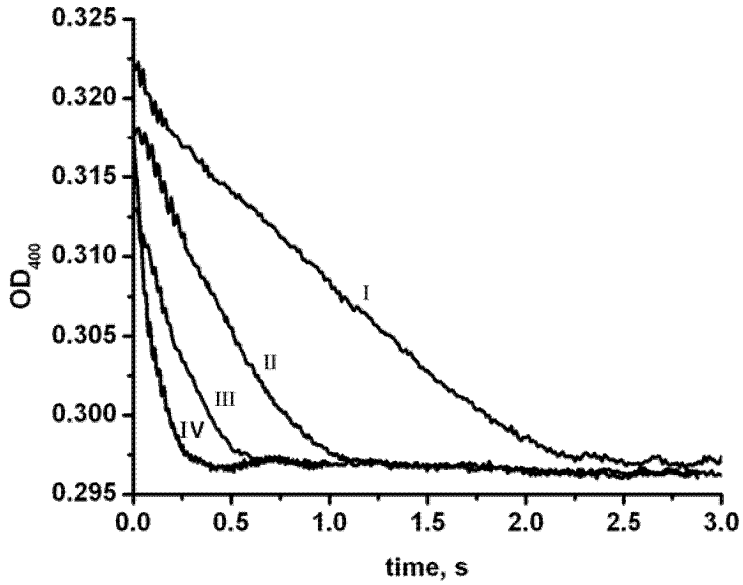

Figure 4. Sequential-mix experiments. I_{400} was pre-formed by mixing 0.47 mM peroxynitrite and 75 μM phenol, a pH jump from 7.2 to 10.2, in the presence of 25 mM carbonate and 200 mM phosphate buffer and then mixed with 200 mM phosphate buffer, pH 11 (curve I), with 70 μM *para*-benzoquinone solution aged for *ca.* 1 minute (curve II), aged for 3 minutes (curve III), and with 1 μM aqueous hydroquinone solution (curve IV).

At alkaline pH, *para*-benzoquinone hydrolyses to amorphous polymers, namely humic acids and hydroquinone. The yield of hydroquinone is higher at higher pH, up to 50% in very alkaline solutions [2]. Hydroquinone reacts indeed rapidly with I_{400} (Figure 4, curve IV). From the sequential-mix experiments performed with excess (100–500 μM) hydroquinone at pH 7.0, the second-order rate constant is found to be $(3.9 \pm 0.1) \times 10^5$ $M^{-1}s^{-1}$. At pH 10.5, the reaction of *ca.* 10 μM I_{400} and hydroquinone is complete within the mixing time of 2 ms. In order to measure the rate constant at alkaline pH, we reduced the concentrations of both

reagents. Thus, I_{400} was pre-formed and allowed to decay for *ca.* 15 s at pH 10.5. After that time *ca.* 0.5 μM I_{400} was left, at which point it was mixed with 1 to 5 μM aqueous solution of hydroquinone. A kinetics trace was fitted to an exponential decay and the second-order rate constant at pH 10.5 was estimated at $(7.7 \pm 0.5) \times 10^7$ $M^{-1}s^{-1}$.

At pH 7, the reaction is clearly biphasic when hydroquinone is the limiting reagent (Figure 5).

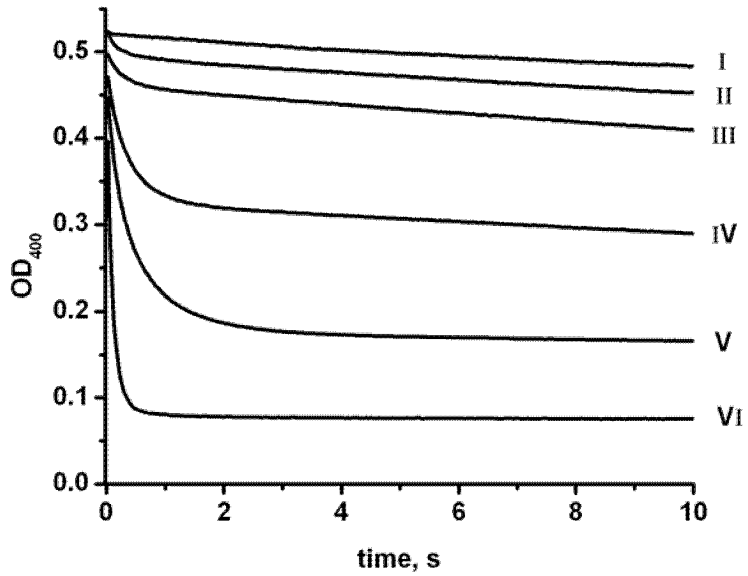

Figure 5. Sequential-mix experiments. I_{400}, pre-formed from 0.5 mM peroxynitrite, 1mM phenol, 25 mM carbonate, pH jump from 7.2 to 10.2, 200 mM phosphate is mixed after 300 ms 1:1 with 200 mM NaH_2PO_4 (curve I), and the following hydroquinone solutions in 200 mM NaH_2PO_4: 0.5 μM (curve II), 1 μM (curve III), 5 μM (curve IV), 10 μM (curve V) or 50 μM (curve VI). The pH after the sequential mixing is 7.2.

Assuming that the stochiometry of this reaction is 1:1 (*cf.* Discussion), we estimate from a rapid decrease of the absorption at 400 nm an extinction coefficient of I_{400} of $(6.1 \pm 0.1) \times 10^4$ $M^{-1}cm^{-1}$.

4.2.2 Hydroquinone is oxidized to *para*-benzoquinone by I_{400}

Hydroquinone is mixed with pre-formed I_{400}, and products of the reaction are analysed by HPLC. As an example, 2.2 mM peroxynitrite at pH 11.3 in 200 mM phosphate buffer is mixed with 5 mM phenol and 50 mM $NaHCO_3$ at pH 7.2 and allowed to incubate in an ageing loop for 300 ms. After that time – to ensure the absence of peroxynitrite and a maximal concentration of I_{400} – the contents of the ageing loop are mixed with hydroquinone in 200 mM H_2PO_4. The pH after the first mixing is 10.2 and after the second 7.0. The aging loop has a volume of 115 µL and the volume of the first pair of syringes was adjusted so that the ageing loop was just filled (58 ± 1 µL each). Then, another two syringes are pushed, 115 ± 1 µL each, of which one contains the hydroquinone solution, and another water that serves to displace the pre-mixed solution from the aging loop and to ensure 1:1 mixing with the hydroquinone solution. The absorption decrease at 400 nm after the second mixing is 0.61 absorption units and the concentration of I_{400} is, therefore, 10.0 ± 0.2 µM. As one can see from the Table 1, hydroquinone is quantitatively oxidised to *para*-benzoquinone by I_{400}.*

Table 1. Products of the reaction of 10 µM I_{400} with 25 µM hydroquinone.

	with 25 µM HQ[a]	without HQ[b]	control[c]	$\|\Delta c\|$ [d]
[HQ] left, µM	11.2 ± 0.1	n. d.	22.3 ± 0.5	11.1 ± 0.5
[BQ] formed, µM	16.1 ± 0.2	2.3 ± 0.4	2.9 ± 0.3	10.9 ± 0.6

[a] – peroxynitrite, pre-mixed with phenol and carbon dioxide, and subsequently mixed with hydroquinone in H_2PO_4; [b] – peroxynitrite, pre-mixed with phenol and carbon dioxide, and subsequently mixed with H_2PO_4; [c] – peroxynitrite, pre-mixed with carbon dioxide, and subsequently mixed with hydroquinone in H_2PO_4; [d] – hydroquinone, consumed and *para*-benzoquinone, formed in reaction of hydroquinone with I_{400}

*Concentrations of hydroquinone and *para*-benzoquinone are corrected for the 2 to 1 dilution with water during the sequential mixing

4.2.3 Reaction with biologically relevant reductants

To gain more information about the reactivity of I_{400}, we measured by sequential-mix stopped-flow experiments rate constants of its reactions with a number of reductants.

Table 2. Second-order rate constants of reactions of I_{400} with reductants at pH 7.2

Compound	k_2, $M^{-1}s^{-1}$
Ascorbate	$(4.2 \pm 0.1) \times 10^5$
Dithionite	$(6.2 \pm 0.1) \times 10^4$
L-Glutathione	$(1.15 \pm 0.05) \times 10^5$
L-Cysteine	$(1.24 \pm 0.07) \times 10^5$
N-acetyl-L-Cysteine	$(3.3 \pm 0.3) \times 10^4$
Hydroquinone	$(3.9 \pm 0.1) \times 10^5$
Phenol	40 ± 5
Nitrite, Iodide, Bromide	≤ 4

Control experiments with buffer and different phenol concentrations provide a rate constant of 40 ± 5 $M^{-1}s^{-1}$ for the reaction of I_{400} with phenol at pH 7.2. Nitrite, iodide, and bromide up to 10 mM do not influence the rate of decay of I_{400}, and, thus, a limit of $k \leq 4$ $M^{-1}s^{-1}$ is estimated. In the presence of 0.2–1.5 mM ascorbate, dithionite, L-cysteine, *N*-acetyl-L-cysteine and L-glutathione, the decay of absorbance at 400 nm is accelerated *ca.* thousand times and the rate of the decay increases linearly with the reductant concentration. No absorption increase at 300 nm and, thus, no formation of 2,2′-biphenol is observed. In each case, rates of decay were measured with 5–6 different concentrations of a reductant. The traces were fitted to a single-exponential decay and second-order rate constants (Table 2) were calculated from the fits.

Except for nitrite, all substances examined could be both one- and two-electron reductants. Dithionite is a classical example. The one-electron reduction of a number of substrates by dithionite has been shown to involve a prior dissociation of dithionite to form $SO_2^{\bullet-}$ as the effective reductant in which case a square root dependence on dithionite concentration is expected. The rate constant of I_{400} reduction by dithionite is linearly proportional to the concentration of $S_2O_4^{2-}$ (Figure 6). That implies that $S_2O_4^{2-}$, and not $SO_2^{\bullet-}$, is the species that reduces I_{400}. At pH 11 the second-order rate constant is $(1.65 \pm 0.05) \times 10^5$ $M^{-1}s^{-1}$.

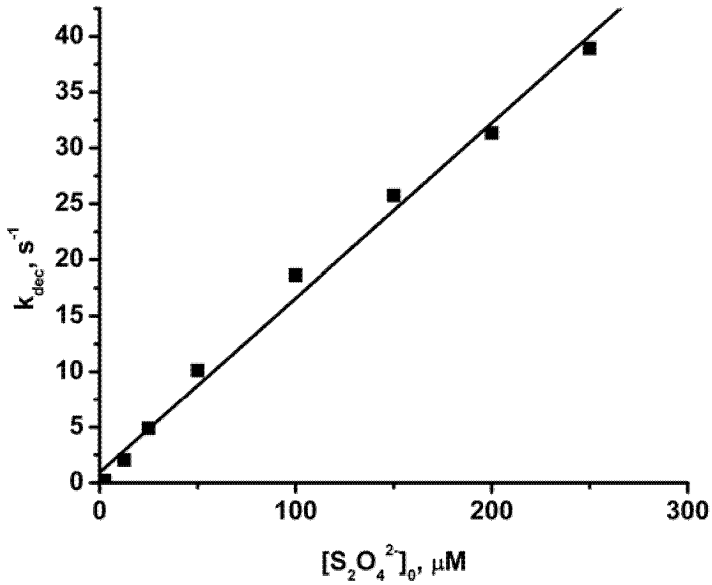

Figure 6. Reaction of dithionite with I_{400}. I_{400}, pre-formed from 400 μM peroxynitrite, 1 mM phenol, and 25 mM carbonate, pH jump from 7.2 to 10.5, after a delay of 150 ms is mixed with dithionite in phosphate buffer, pH 11 after the second mixing.

4.2.4 Yields of 2,2′-biphenol with respect to I_{400}

With the knowledge of the extinction coefficient of I_{400}, we calculate the yields of 2,2′-biphenol relative to the concentration of I_{400}. The results are given in Tables 3 and 4.

Table 3. Yields of 2,2′-biphenol with respect to I_{400} at different phenol concentrations.

Phenol, mM	2,2′-BP, μM	I_{400}, μM	Yield, %
0.23	1.1 ± 0.2	10.5 ± 0.1	10 ± 2
0.47	5.6 ± 0.4	13.2 ± 0.2	42 ± 3
0.94	9.0 ± 0.7	15.7 ± 0.2	57 ± 5
1.88	10.4 ± 0.3	16.5 ± 0.2	63 ± 2
3.75	11.3 ± 0.3	17.3 ± 0.2	65 ± 2
6.57	11.5 ± 0.5	18.1 ± 0.2	63 ± 3

Conditions: 0.8 mM peroxynitrite, pH 10.0, 100 mM phosphate buffer, 20 mM hydrogen carbonate, pH jump from 7.2 to 10.0

Table 4. Yields of 2,2′-biphenol with respect to I_{400} at different pH.

pH	2,2′-BP, μM	I_{400}, μM	Yield, %
7.7	5.6 ± 0.9	3.95 ± 0.06	(14 ± 2) × 10
8.6	7.7 ± 0.5	11.2 ± 0.2	67 ± 4
9.2	10.4 ± 0.2	15.0 ± 0.2	69 ± 2
10.0	12.5 ± 0.3	19.4 ± 0.3	64 ± 2
10.5	14.2 ± 0.9	22.6 ± 0.3	63 ± 4

Conditions: 0.8mM peroxynitrite, 2 mM phenol, 100 mM phosphate buffer, 25 mM hydrogen carbonate, pH jump from pH 7.2 to a specified pH.

4.2.5 Decay of I_{400} at different pH values

The decay of I_{400} is faster at higher pH (Figure 7). A *ca.* 10-fold increase in the decay rate in the pH interval from 7 to 10.5 is observed (Figure 7A). Above pH 13 the increase is more dramatic – *ca.* 700 times upon a pH change from 13 to 14.5 (Figure 7B). The decay at pH 7 and 10 is linear with the phenol concentration and independent of the phenol concentration at pH 14.5 (Figure 7D).

The decrease in the absorption at 400 nm is constant from pH 5 to pH 14.5. It would, therefore, appear that the UV-Vis spectrum of I_{400} remains unchanged in this pH range. At neutral and slightly acidic pH, where the decay of I_{400} is relatively slow, we confirmed this by recording UV-Vis spectra: a maximum at 400 nm is observed at pH 5.

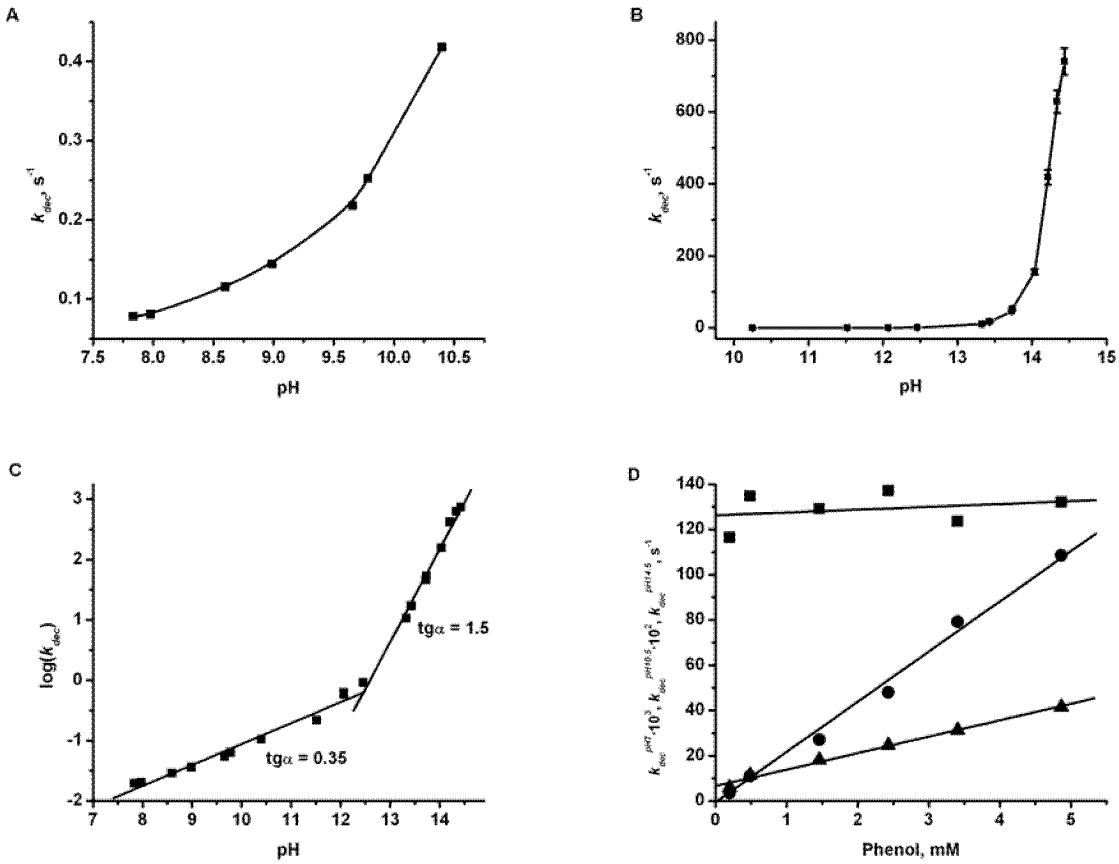

Figure 7. Decay of I_{400} at different pH values. Panel A, dependence of the rate constant of I_{400} decay on pH. Conditions: 2 mM phenol; 490 μM peroxynitrite; 25 mM carbonate; pH jump from 7.2 to 10.5, 200 mM phosphate buffer. Panel B, sequential-mix experiments, I_{400} pre-formed from 1 mM peroxynitrite in 20 mM NaOH, 2 mM phenol, and 36 mM carbon dioxide (saturated solution at 25°C) aged 100 ms is mixed with 200 mM phosphate buffer (first 4 points, pH < 12.5) or NaOH (last 7 points, pH > 13). Panel C, Graphs, shown in Panels A and B, on logarithmic scale. Panel D, Sequential-mix experiments; dependence of the rate constant of I_{400} decay on phenol concentration at pH 7 (triangles), 10.5 (circles), and 14.5 (squares). I_{400} is pre-formed by mixing of 0.5 mM phenol, 0.8 mM peroxynitrite, and 25 mM carbonate, pH jump from 7.2 to 10.5, and subsequently mixed with 1 to 10 mM phenol in 200 mM NaH_2PO_4 (triangles), water (circles), or 2.5 M NaOH (squares). The rate constants at pH 7 are shown 10^3-fold magnified, and those at pH 10.5, 10^2-fold.

4.2.6 Substituted phenols

Phenolates carrying strong electron-withdrawing groups (cyano- and nitro-) at *ortho*- or *para*-positions do not form any absorbing intermediates.

Para-substituted phenolates – 4-chlorophenolate, 4-methylphenolate, 4-methoxyphenolate and L-tyrosinate as well as 2,4,6-trimethylphenolate – do not form intermediates with a significant absorption above 350 nm. With these compounds one observes absorption changes after peroxynitrite has decayed, but these changes are *ca.* 10 times smaller than those observed for phenolate and are at much lower wavelengths (300 ± 20 nm). The lifetime of the observed intermediates is *ca.* 1 s, and is independent of phenol concentration.

Ortho-substituted phenolates such as 2-chlorophenolate, 2-methylphenolate, and 2-methoxyphenolate behave like phenolate, namely, the absorption maxima of these intermediates are found near 400 nm and the absorption decreases are similar to those of phenol shown [1][3].

The kinetics of the reaction with *diortho*-substituted phenolates are more complex. With *ca.* equimolar concentrations of peroxynitrite and 2,6-dimethylphenolate two consecutive intermediates with maxima at *ca.* 420 nm and 360 nm are formed (Figure 8).

[3] Chapter 3, Figure 6

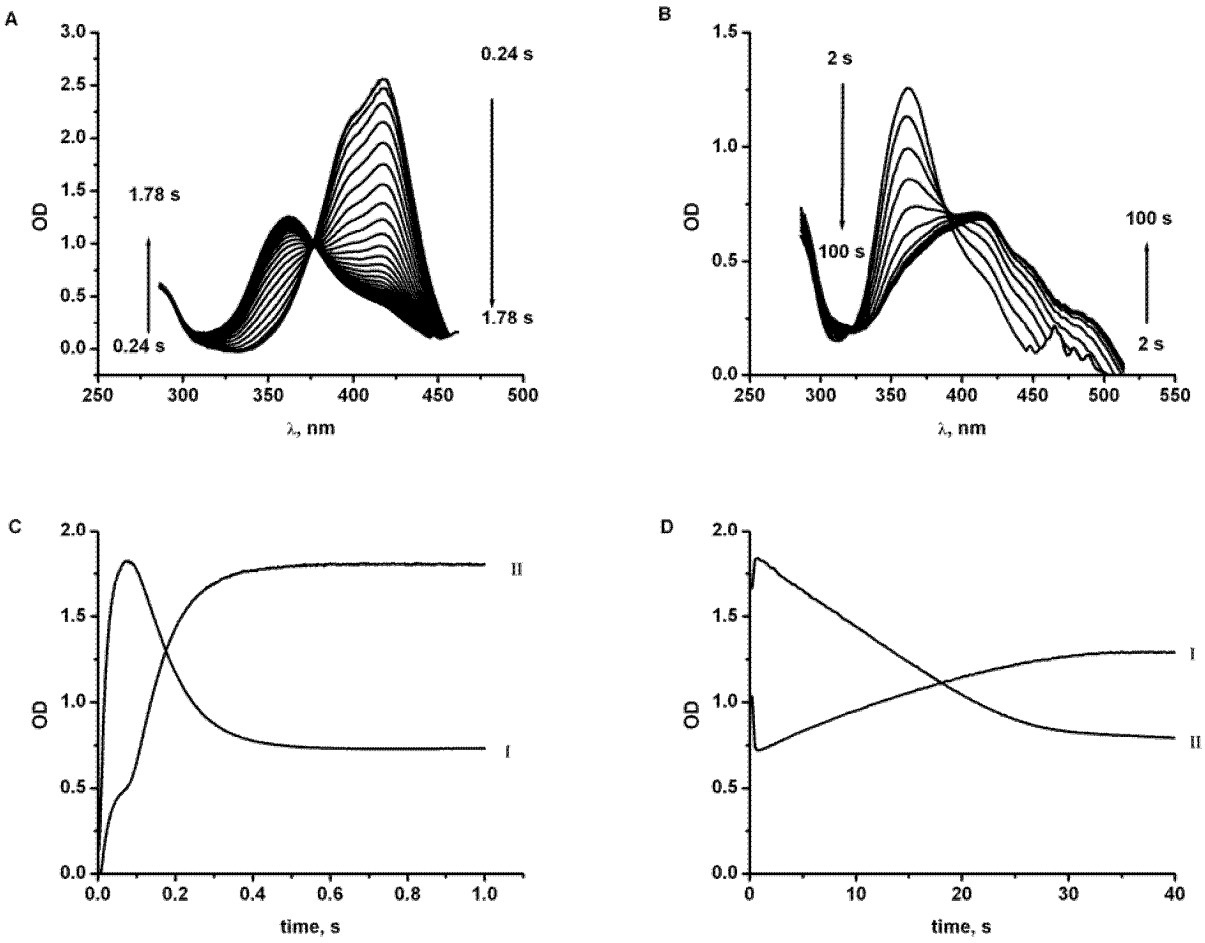

Figure 8. Reaction of 2,6-dimethylphenol with peroxynitrite and carbon dioxide. Panels A and B, time dependent spectra. Conditions: 1.2 mM 2,6-dimethylphenol, 0.5 mM peroxynitrite, 25 mM carbonate, pH jump from 7.2 to 10.5. Panels C and D, kinetic traces at 440 (curve I) and 360 nm (curve II) with 0.9 mM 2,6-dimethylphenol, 0.8 mM peroxynitrite, 25 mM carbonate, pH jump from 7.2 to 10.5.

The decay of the first intermediate with an absorption maximum at 420 nm is concomitant with a formation of another intermediate with an absorption maximum at 360 nm. The decay of the latter is zero-order and concomitant with the formation of absorption above 400 nm that is persistent for hours (see below). The kinetics depend on the ratio of peroxynitrite-to-phenol. Thus, when peroxynitrite and phenol are present in *ca.* equal concentrations, two consecutive intermediates are observed as discussed above. With phenol in at least a two-fold excess, only one

intermediate at 420 nm could be observed. It decays over several seconds and the decay is faster at higher peroxynitrite-to-phenol ratio. After the decay at 420 and 360 nm is complete, slow (hours) spectral changes are observed (Figure 9). Similar changes were observed with phenol due to the polymerization of a *para*-benzoquinone [1][4].

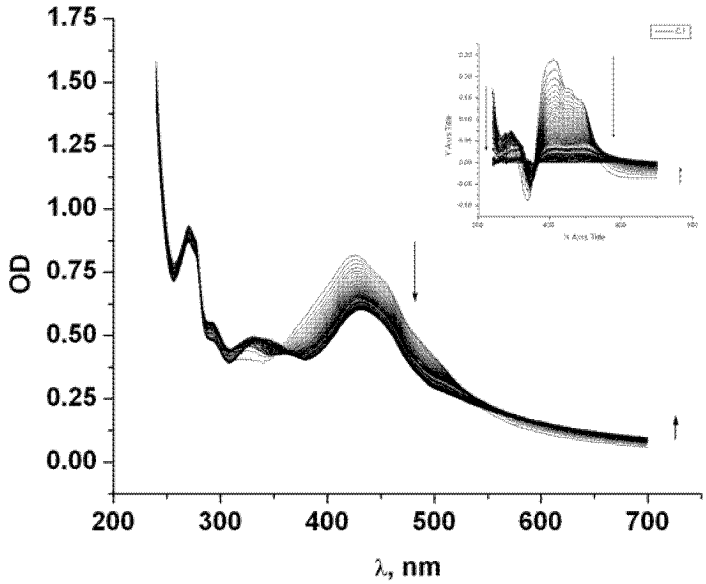

Figure 9. Spectral changes during 3 hours. Conditions as in Figure 8, panels A and B. Inset, differential spectral changes, the reference solution is that after 3 hours.

4.3 Discussion

4.3.1 Zero-order decay of I_{400}

When phenolate is the limiting reagent at alkaline pH, the yields of 2,2′-biphenol from I_{400} are poor (Table 2). Under these conditions, the decay of I_{400} is zero-order and independent of phenol concentrations. We propose that the decay is due to it fast (k_2 = (7.7 ± 0.5) × 10^7 $M^{-1}s^{-1}$ at pH 10.5) reaction of I_{400} with

[4] Chapter 3, Figure 2.

hydroquinone. Hydroquinone, as discussed previously [1], is a likely precursor of *para*-benzoquinone, but it is susceptible towards oxidation, especially at alkaline pH. Once formed, it is rapidly oxidized by peroxynitrite in the presence of carbon dioxide. When peroxynitrite has decayed, hydroquinone can be formed again as a by-product of the alkaline polymerisation of *para*-benzoquinone to humic acids (reaction 1) [2]. Thus, the zero-order decay of I_{400} could be explained as follows:

$$nBQ \xrightarrow{k_{dec}} HQ + polym_{n-1} \quad (1)$$

$$I_{400} + HQ \xrightarrow{k_1} BQ + PhOH \quad (2)$$

The polymerization of *para*-benzoquinone is a relatively slow process (hours) at pH 10.5 and *para*-benzoquinone concentration of *ca.* 10–20 μM, whereas reaction 2 is complete within less than a second.[5] Therefore, the concentration of hydroquinone would be stationary (equation 3) and the rate of the decay of I_{400} would be limited by the rate of the *para*-benzoquinone polymerization (equation 4).

$$\frac{\partial[HQ]}{\partial t} = k_{dec}[BQ]^n - k_1[HQ]\cdot[I_{400}] = 0 \quad (3)$$

$$\frac{\partial[I_{400}]}{\partial t} = -k_1[HQ]\cdot[I_{400}] = -k_d[BQ]^n \quad (4)$$

When the decay of I_{400} is zero-order, the decrease in the absorption at 400 nm is less than 0.05 absorption units which, given our estimate of the extinction coefficient, implies that the I_{400} concentration never reaches concentrations higher than 1 μM. Since the "initial" concentration of *para*-benzoquinone is about 20 μM[6],

[5] The second-order rate constant of the reaction 2 is *ca.* 10^8 $M^{-1}s^{-1}$, and the decrease of absorption at 400 nm is *ca.* 0.02 – 0.05, which, given our estimate of the extinction coefficient, implies that the concentration of I_{400} is in the range of *ca.* 0.3–1 μM. A pseudo-first order rate constant of reaction 2 is thus *ca.* 30–100 s^{-1}.

[6] See Figure 5, Chapter 3.

i.e. at least an order of a magnitude higher, it would not change significantly during the decay of I_{400}. Moreover, *para*-benzoquinone is formed again as a product of hydroquinone oxidation by I_{400} (Table 2). Thus, the zero-order decay of I_{400} would be observed (equation 5).

$$[I_{400}] = [I_{400}]_0 - k_{dec}[BQ]_0 t = [I_{400}]_0 - k't \quad (5)$$

4.3.2 pH-dependence of the decay of I_{400}

In the pH range from 7.5–10.5, provided that sufficient excess of phenol is present, I_{400} decays *via* its reaction with phenol (Figure 7D). I_{400} is an oxidant, and one would expect it to oxidize substrates more readily, when the latter are deprotonated. Therefore, the increase in the rate of the reaction of I_{400} with phenol in the pH range 7.5 to 10.5 (Figure 7A) could be explained by a faster reaction of I_{400} with phenolate than with phenol (pK_a = 9.9). Similarly, the rate constant of the reaction with hydroquinone increases *ca.* 200 times in this pH region, presumably due to deprotonation of hydroquinone (pK_a = 9.96).

Above pH 13 the decay of I_{400} accelerates even more dramatically (Figure 7B) and becomes independent of the phenol concentration (Figure 7D). It is likely, therefore, that at very alkaline pH I_{400} reacts directly with hydroxide or, possibly, hydroxide catalyzes an isomerization of I_{400}. The second-order rate constant of the reaction of I_{400} with hydroxide could be estimated at *ca.* 10^2 $M^{-1}s^{-1}$ and, given the rate constant with phenolate of *ca.* 3×10^2 $M^{-1}s^{-1}$ and typical phenol concentrations of several mM, this reaction prevails above pH 13. We suggested [1][7], based on pH- and concentration dependences of *para*-benzoquinone yields, that, apart from reacting with phenol to form 2,2′-biphenol, I_{400} may isomerize to hydroquinone and, therefore, be a *para*-benzoquinone precursor. One cannot exclude that this

[7] Chapter 3, p. 102–104.

isomerization is hydroxide-catalyzed and therefore more hydroquinone is formed at higher pH. Once formed, hydroquinone would react rapidly with I_{400}. That would explain why the formal reaction order in hydroxide at pH > 13 is higher than 1 (Figure 7C).

4.3.3 Yields of 2,2′-biphenol relative to I_{400}

As we reported previously [1][8] , biphenols are formed during the carbon dioxide catalyzed oxidation of phenol by peroxynitrite by two different mechanisms, which are distinguished by isomer ratio of 2,2′- to 4,4′-biphenols. One mechanism operates at high pH and phenol concentrations *via* the formation of I_{400} and its consecutive coupling with phenol. The second mechanism largely operates at neutral to slightly alkaline pH and moderate phenol concentrations and produces both 2,2′- and 4,4′-biphenols *via* the coupling of two phenoxyl radicals.

Yields of 2,2′-biphenol relative to I_{400} saturate at *ca.* 65% at alkaline pH and high phenol concentrations (Table 3). As we commented above, poor yields at lower phenol concentrations are explained by incomplete scavenging of I_{400} by phenol and its reaction with hydroquinone instead. As one can see from Table 4, calculated yields at lower pH become higher than 60%, but this has to do with the fact, that under neutral pH, 2,2′-biphenol is additionally formed by coupling of two phenoxyl radicals. It would therefore appear that the maximum yield of 2,2′-biphenol relative to I_{400} is *ca.* 65%.

That the yield of 2,2′-biphenol relative to I_{400} does not reach 100%, can be explained as follows. As described [1][9], there is an indication that 2,4′-biphenol might be formed along with 2,2′-biphenol *via* the I_{400}-pathway. Unfortunately, we could not demonstrate this definitely. If, however, 2,4′-biphenol is formed along

[8] Chapter 3, p. 96.
[9] Chapter 3, p. 80.

with 2,2′-biphenol, its yield might constitute another ~ 35% of the I_{400} concentration. Another plausible reason is that, even at high phenol concentrations, some *para*-benzoquinone is formed, and thus a reaction of I_{400} with hydroquinone cannot be completely excluded.

4.3.4 Properties of I_{400}

The identity of I_{400} is essential to asses the significance of our findings. We cannot characterize it by the usual methods, since I_{400} is formed in low concentrations (*ca.* 20 µM) and only exists for several seconds. We will therefore summarize the properties of I_{400} available at the moment. Given the absence of an ESR signal, I_{400} is diamagnetic and, most probably, a product of the two-electron oxidation of phenolate [1][10]. Its spectrum has a maximum at 400 nm with an extinction coefficient of $(6.1 \pm 0.1) \times 10^4\ M^{-1}cm^{-1}$ that remains unchanged between pH 5 and 11. Because UV-Vis spectra of phenols differ from those of the corresponding phenolates, and the pK_a values of most mono-substituted phenols lie in the pH range 7 to 11, we conclude that I_{400} is not a phenolate. It reacts rapidly with reducing agents, such as ascorbate, dithionite, and thiols, and hydroquinone. It is likely that I_{400} is a two-electron oxidant, since it reacts with $S_2O_4^{2-}$ rather than with $SO_2^{\bullet-}$, it oxidizes hydroquinone to *para*-benzoquinone and couples directly with phenol to form 2,2′-biphenol.

4.3.5 Substituted phenols

That phenolates, rather than phenols form I_{400}-like intermediates, and that phenolates with electron-withdrawing substituents do not form any, indicates that phenolate acts as a nucleophile during the formation of I_{400}. A similar tendency is observed in some electrophilic substitution reactions. For instance, electrophilic

[10] Chapter 3, p. 93, p. 95.

halogenation reactions are initiated by deprotonation of the phenolic hydroxyl group [3].

Para-substituted phenolates do not form intermediates with an absorption at *ca.* 400 nm and *diortho*-substituted phenolates do form such intermediates. This might indicate that the formation of I_{400}-like intermediates proceeds *via* the electrophilic attack on the *para*-position.

Diortho-substituted phenols form two consecutive intermediates with maxima at 420 and 360 nm (Figure 8). Interestingly, the decay of absorption at 360 nm is zero-order, but depends on the peroxynitrite/phenol ratio, as observed for phenol when the latter is a limiting reagent and *para*-benzoquinone is a principle oxidation product. The decay of the intermediate with an absorption maximum at 360 nm is concomitant with formation of absorption above 400 nm. The absorption above 400 nm, in turn, decays slowly during several hours. A similar decay was observed with phenol and was proved to be due to the alkaline polymerization of *para*-benzoquinone.[11] It is likely, therefore, that the intermediate with an absorption maximum at 360 nm, formed during the carbon dioxide catalyzed oxidation of 2,6-dimethylphenol by peroxynitrite, gives rise to a corresponding *para*-quinone. We commented in Chapter 3 that, apart from being a precursor of 2,2′-biphenol, under certain conditions, I_{400} could be a precursor of *para*-benzoquinone. With diortho-substituted phenols, formation of *para*-quinones as stable products is the only option, and this seems to be the case.

4.3.6 A provisional mechanism of I_{400} formation and its consecutive reactions

Previously, we commented on the mechanism of I_{400} formation and its consecutive reactions to give 2,2′-biphenol and *para*-benzoquinone[12]. Briefly, we

[11] Chapter 3, Figure 2.
[12] Chapter 3, p. 95–98.

concluded that I_{400} is, most probably, formed *via* the reaction of the peroxynitrite/carbon dioxide adduct with phenolate. When sufficient excess of phenol is present, it couples with phenol to give 2,2′-biphenol (and, possibly, 2,4′-biphenol). At high pH and/or low phenolate concentrations, it rearranges to hydroquinone, which is subsequently oxidized to *para*-benzoquinone.

Given that this intermediate is probably formed *via* the attack on a para-position of a phenolate ring (*cf.* above), reaction 6 may take place.

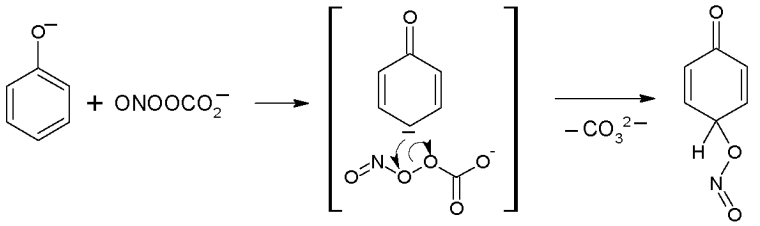

(6)

(I)

This *para*-nitrtito-substituted cyclohexadienone (I) could be a key intermediate in the formation of 2,2′-biphenol and *para*-benzoquinone. Indeed, the formation of 2,2′-biphenol can be rationalized in terms of a heterolytic coupling of phenolate with the *para*-cyclohexadienone intermediate and the concomitant formation of nitrite as a leaving group. According to the reaction 7, phenolate should couple with I_{400} faster than phenol, as observed.

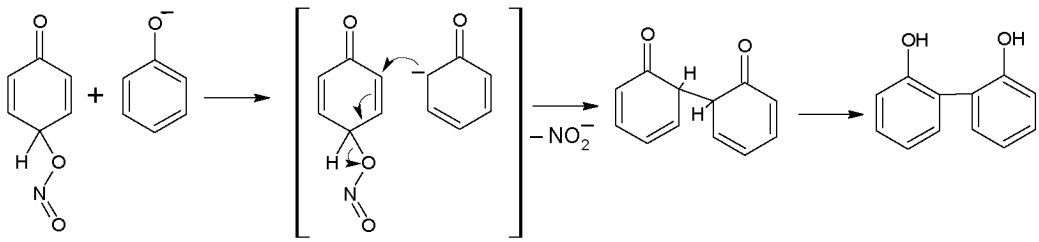

(7)

2,4′-Biphenol might be formed in the same way *via* the attack of a *para*-carbon atom of the phenolate. Thus, if 2,4′-biphenol is indeed formed along with 2,2′-biphenol *via* the I_{400}-pathway as discussed above, our reaction scheme would accommodate this result.

Formation of hydroquinone and its subsequent oxidation to *para*-benzoquinone is rather straightforward. Indeed, the nitrito-substituted cyclohexadienone intermediate may rearrange to phenyl nitrite (II), which is known to be hydrolytically unstable. It would thus give rise to hydroquinone and nitrite. This reaction might well be hydroxide-catalyzed and become more important at higher pH values. This would be in accord with our observation that above pH 13 I_{400} disappears due to its reaction with hydroxide, and not with phenol (Figure 7D), reaction 8.

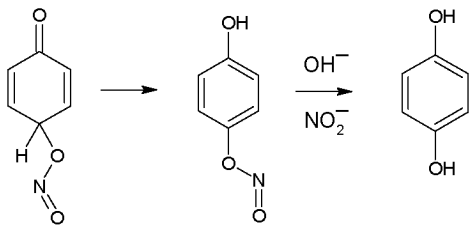

(II) (8)

Once formed, hydroquinone could be easily oxidized to *para*-benzoquinone by multiple ways – by peroxynitrite, I_{400}, and, at alkaline pH, by dioxygen.

The serious deficiency of this reaction scheme is that the UV-Vis spectrum of the *para*-nitrito-substituted cyclohexadienone intermediate (I) does not agree with the observed one. Indeed, UV spectra of *para*-cyclohexadienones show a band with strong intensity at 230–270nm and ε = 8,000–20,000 $M^{-1}cm^{-1}$ [3], whereas I_{400} absorbs at 400 nm with $\varepsilon \sim 60{,}000$ $M^{-1}cm^{-1}$. Therefore, if I_{400} were a *para*-cyclohexadienone, the observed absorption would be at unexpectedly long

wavelength and the extinction coefficient unexpectedly high. Evidence for the *para*-position is strong: one does not observe I_{400}-like intermediates with *para*-substituted phenols. One can experimentally not observe absorption changes at *ca.* 250 nm because phenol, present in excess, and all the oxidation products absorb significantly at these wavelengths. However, if a *para*-position is free, one may speculate that the initially formed intermediate (I) rearranges or exists in equilibrium with another species that absorb at higher wavelength due to, for example, a stronger conjugation or an appearance of a charge-transfer band. For instance, one can propose the formation of an ion pair intermediate IIb. A similar ion pair intermediate has been proposed in reactions of diacyl peroxide with phenols [3].

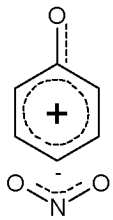

IIb

Another objection to the proposed reaction scheme might be that the formation the cyclohexadienone intermediate takes place exclusively at the *para*-position of a phenolate ring, although there is no reason for the substantial energy differences between transition states of attacks on the *ortho*- and *para*-position. However, the nitrosation of phenol by nitrous acid [4,5] and alkyl nitrites [6] is known to give rise to *ca.* 95% *para*-nitrosophenol and only little of the *ortho*-isomer. A similar isomer ratio would explain the selectivity observed here. Alternatively, *ortho*-cyclohexadienones are known for their tendency to rearrange to the more stable *para*-isomers [3], and one could propose that a similar rapid

rearrangement takes place with cyclohexadienone intermediates. By analogy to reactions of diacyl peroxides, one can postulate peroxocompound (III), formed *via* reaction 9, that reacts further to a cyclohexadienone. However, such a mechanism would require yet another non-characterized intermediate, and would seem excessively speculative without further evidence.

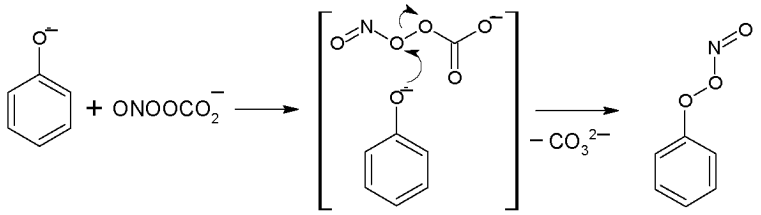

(9)

(III)

References

[1] Papina, A. A.; Koppenol, W. H. Two pathways of carbon dioxide catalyzed oxidative coupling of phenol by peroxynitrite. submitted to *Chem. Res. Toxicol.*; 2005.

[2] Erdtman H. Die Reaktion von Benzoquinone mit Alkali. *Zeitschrift fuer Pflnzenernaerung* 69:38-43; 1955.

[3] Waring, A. J. Cyclohexadienones. In Closs, G. L.; Fort, R. C.; Koch, K. F.; Meinwald, F.; Meinwald, Y. C.; von R Schleyer, P. eds. *Advances in Acyclic Chemistry.* New York: Academic Press; 2005:129-256.

[4] Challis B.C.; Higgins R.J. The Chemistry of Nitroso-compounds. PartVII. The First "Fast" Proton Transfer for an Aromatic Nitrosation. *J. Chem. Soc., Perkin Trans. 2:* 1597-1604; 1973.

[5] Williams D.L.H. *Nitrosation.* Cambridge: Cambridge University Press; 1988.

[6] Leis, J. R.; Rios A.; and Rodrigues-Sanchez L. Reactivity of phenolic nucleophiles towards nitroso compounds. Part 2. Reaction with alkyl nitrites (O-nitroso compounds). *J. Chem. Soc., Perkin Trans. 2* 2729-2733; 1998.

GENERAL DISCUSSION

Peroxynitrite is an inorganic toxin implicated in many diseases as a nitrating and oxidizing agent [1-3]. Its scavenging *in vivo* is an important and challenging task of modern toxicology. Calculations based upon published data for reactions between peroxynitrite and various compounds indicate that reaction with carbon dioxide is predominant in most biological fluids [4] and that any peroxynitrite scavenger should be present at near toxic levels in order to compete with carbon dioxide [5]. Therefore, the only feasible way to scavenge peroxynitrite *in vivo* is to scavenge the intermediates of its reaction with carbon dioxide.

Peroxynitrite reacts with carbon dioxide *via* a formation of a short-lived adduct $ONOOCO_2^-$ [6] which rapidly undergoes homolysis to trioxocarbonate(•1–) and nitrogen dioxide radicals [5,7,8]. It has been argued that this adduct is too short-lived to react with organic molecules [8,9] and thus cannot be scavenged. The only option to prevent the peroxynitrite-mediated oxidations *in vivo* would seem to trap trioxocarbonate(•1–) and nitrogen dioxide radicals.

Our study of carbon dioxide catalyzed oxidation of phenol by peroxynitrite reveals that the peroxynitrite/carbon dioxide adduct may exist long enough to react with organic molecules. Since it only reacts with electron-rich phenolates, the adduct is not a strong oxidant. It might, for that reason, be a more selective oxidant than the radical pair, which opens new and, possibly, more advantageous pathways to scavenge peroxynitrite *in vivo*.

Since reactions of the adduct have not been reported previously, it would seem useful to extend this study to other substrates. Reactions with thiols seem to be of particular interest due to their high *in vivo* concentrations. One might expect that thiolates would be more reactive than thiols, as observed for phenol. Given their pK_as of *ca.* 8, a significant fraction of thiols is deprotonated at physiological pH,

therefore, the reaction of the adduct with thiolates (if it takes place) might be physiologically relevant.

An important result of the present work is a discovery of a new non-radical pathway of 2,2′-biphenol formation during the reaction of phenol with peroxynitrite and carbon dioxide. Apart from a classical pathway of coupling of two phenoxyl radicals, at high pH and phenol concentration 2,2′-biphenol is formed *via* the heterolytic coupling of an intermediate with phenol, as followed by UV-Vis spectrophotometry. The identity of this intermediate remains uncertain, since we were unable to isolate and structurally characterize it. We could show, however, that (i) this intermediate is diamagnetic due to the absence of an ESR signal; (ii) its absorption spectrum with a maximum at 400 nm (ε_{400} = (6.1 ± 0.1) $\times 10^4$ $M^{-1}cm^{-1}$) does not change over a pH range of 5 to 11; (iii) formation of absorption above 350 nm is not observed for *para*-substituted phenols; (iv) the intermediate reacts rapidly ($k \sim 10^5$ $M^{-1}s^{-1}$ at pH 7) with reducing agents, it oxidizes hydroquinone to *para*-benzoquinone, and couples directly with phenol to give 2,2′-biphenol; (v) under certain conditions it may isomerize to hydroquinone and thus be a precursor of *para*-benzoquinone. The latter is formed in significant yields, but has not been previously found due to its instability in alkaline aqueous solutions. We provisionally assume that the structure of this intermediate is closely related to that of a *para*-nitrito-substituted cyclohexadienone. Structural characterization of the intermediate would be very desirable, but does not seem feasible in the present modification of the reaction due to low (*ca.* 20 μM) concentrations and relatively short (10–100s) lifetimes of the intermediate. Varying the solvent composition might be helpful since we observed, for instance, that in acetonitrile/water solutions the lifetime of the intermediate increases several times. Working with substituted phenols is another promising approach. For instance, electron rich phenols might form such intermediates in higher yields.

The reported novel non-radical pathway is in itself of fundamental interest since not many non-radical oxidative coupling reactions are known or proved to be radical-free. Furthermore, this pathway might well be relevant to the action of phenolic anti-oxidants. Indeed, some derivatives of hydroxycinnamic acids (e.g. p-coumaric, caffeic, felluric, and sinapinic acids) have been shown to strongly inhibit peroxynitrite-mediated aromatic nitration reactions [10,11], but the mechanism of the inhibition remains elusive. It has been reported that sinapinic acid reacts with peroxynitrite to produce exclusively the mono-lactone type dimer, the product of an oxidative coupling, and its formation has been rationalized in terms of a coupling of two aryloxyl radicals [10]. However, the appearance of intensely colored long-lived intermediates in this reaction [12] might indicate that a non-radical pathway operates, similar to the one we observed for phenolate. Although this pathway is not catalytic, we have shown that the intermediate reacts with biologically relevant reductants (thiols, ascorbate) *ca.* 10^4 times faster than with phenol. It is likely, therefore, that in the presence of such reductants, phenols could be recycled, and *in vivo*, where thiols and ascorbate are abundant, catalytic amounts of phenolic anti-oxidants would be sufficient to decompose peroxynitrite to innocuous nitrite and nitrate.

The novel non-radical pathway of biphenol formation might also be relevant to the mechanism of phenol nitrosation by peroxynitrite. Indeed, at alkaline pH in the presence of μM amounts of carbon dioxide, *para*-nitrosophenol is a major nitrogen-containing product [13,14], but no satisfactory mechanism of its formation is proposed (*cf.* Introduction). One cannot exclude that the intermediate we observe at high (mM) carbon dioxide concentrations might be related to the formation of *para*-nitrosophenol at lower (μM) concentrations of carbon dioxide.

References

[1] Beckman, J. S.; Carson, M.; Smith, C. D.; Koppenol, W. H. ALS, SOD and peroxynitrite. *Nature* **364**:584; 1993.

[2] Mulligan, M. S.; Hevel, J. M.; Marletta, M. A.; Ward, P. A. Tissue injury caused by deposition of immune complexes is L-arginine dependent. *Proc. Natl. Acad. Sci. USA* **88**:6338-6342; 1991.

[3] Moreno, J. J.; Pryor, W. A. Inactivation of a-1-proteinase inhibitor by peroxynitrite. *Chem. Res. Toxicol.* **5**:425-431; 1992.

[4] Lymar, S. V.; Hurst, J. K. Carbon dioxide: Physiological catalyst for peroxynitrite-mediated cellular damage or cellular protectant. *Chem. Res. Toxicol.* **9**:845-850; 1996.

[5] Squadrito, G. L.; Pryor, W. A. Oxidative chemistry of nitric oxide: The roles of superoxide, peroxynitrite, and carbon dioxide. *Free Radical Biol. Med.* **25**:392-403; 1998.

[6] Lymar, S. V.; Hurst, J. K. Rapid reaction between peroxonitrite ion and carbon dioxide: Implications for biological activity. *J. Am. Chem. Soc.* **117**:8867-8868; 1995.

[7] Lymar, S. V.; Hurst, J. K. Radical nature of peroxynitrite reactivity. *Chem. Res. Toxicol.* **11**:714-715; 1998.

[8] Merényi, G.; Lind, J. Thermodynamics of peroxynitrite and its CO_2-adduct. *Chem. Res. Toxicol.* **10**:1216-1220; 1997.

[9] Squadrito, G. L.; Pryor, W. A. Mapping the reaction of peroxynitrite with CO_2: Energetics, reactive species, and biological implications. *Chem. Res. Toxicol.* **15**:885-895; 2002.

[10] Niwa, T.; Doi, U.; Kato, Y.; Osawa, T. Inhibitory mechanism of sinapinic acid against peroxynitrite-mediated tyrosine nitration of protein in vivo. *FEBS Lett.* **459**:43-46; 1999.

[11] Kerry, N.; Rice-Evans, C. Peroxynitrite oxidises catechols to o-quinones. *FEBS Lett.* **437**:167-171; 1998.

[12] Akhter, S.; Green, J. R.; Root, P.; Thatcher, G. J.; Mutus, B. Peroxynitrite and NO^+ donors form colored adducts with sinapinic acid: potential applications. *Nitric Oxide: Biol. Chem.* **8**:214-221; 2005.

[13] Uppu, R. M.; Lemercier, J. N.; Squadrito, G. L.; Zhang, H. W.; Bolzan, R. M.; Pryor, W. A. Nitrosation by peroxynitrite: Use of phenol as a probe. *Arch. Biochem. Biophys.* **358**:1-16; 1998.

[14] Daiber, A.; Mehl, M.; Ullrich, V. New aspects in the reaction mechanism of phenol with peroxynitrite: The role of phenoxy radicals. *Nitric Oxide: Biol. Chem.* **2**:259-269; 1998.

Curriculum Vitae

Address	*Herbstweg 11* *8050 Zurich* *Switzerland*
Telephone	*044 313 26 33*
Mobile	*076 461 91 71*
E-mail	*papina@inorg.chem.ethz.ch* *alina.papina@hotmail.com*

PERSONAL DATA

Date of Birth	09.01.1977
Nationality	Russian
Swiss Permit	B
Family	Married with 1 child (2003)

EDUCATION

2000 – 2005	Ph.D., Inorganic chemistry, ETH Zurich, Zurich, Switzerland.
1994 – 1999	M.Sc., Chemistry, Novosibirsk State University, Novosibirsk, Russia.
1992 – 1994	Physico-Mathematical Boarding School at the Novosibirsk State University, Novosibirsk, Russia
1990 – 1992	Gymnasium № 123, Barnaul, Russia
1984 – 1990	Secondary School № 22, Barnaul, Russia

FURTHER TRAINING

2005	Seminar "Presenting – Publishing – Communicating" by the Center for Teaching and Learning of the ETH Zurich
2000 – 2001	Two semesters of German language course (Grundstufe 1, 2) by the Language Centre of the University and the ETH Zurich

LANGUAGES

Russian	Mother tongue
English	Fluent, written and spoken
German	Basic written, intermediate spoken
French	Basic

RESEARCH EXPERIENCE

2000 – 2005 Graduate Research, Bioinorganic and Solution Chemistry Group, Laboratory of Inorganic Chemistry, ETH Zurich (prof. Dr. W. H. Koppenol)

Main area of research: Kinetic and mechanistic studies of the carbon dioxide catalyzed reactions of peroxynitrite with phenols as model compounds of tyrosine.
Title of the Ph.D thesis: "The mechanism of carbon dioxide catalyzed oxidation of phenols by peroxynitrite"

1999 – 2000 Research Assistant, Laboratory of Photocatalysis on Semiconductors, Boreskov Institute of Catalysis, Novosibirsk, Russia (prof. Dr. E. N. Savinov)

Main area of research: Iron(III) hydroxides as catalysts for the gas-phase phenol oxidation and photooxidation by oxygen and hydrogen peroxide.

1997 – 1999 Undergraduate Research with the focus on Kinetics and Catalysis, Laboratory of Photocatalysis on Semiconductors, Boreskov Institute of Catalysis, Novosibirsk, Russia (prof. Dr. E. N. Savinov)

Title of the Diploma Thesis: "Catalytic and photocatalytic properties of nanocolloid Iron(III) hydroxide in reactions of hydrogen peroxide decomposition and dye oxidation"

TEACHING EXPERIENCE

2001 – 2003 Graduate teaching assistant, ETH Zurich

Laboratory instructor for the Department of Inorganic Chemistry

Responsibilities included introducing a subject of chemical kinetics and stopped-flow spectroscopy technique to advanced students

AREAS OF EXPERTISE

- Inorganic synthesis
- Heterogeneous catalysis, photocatalysis
- Kinetic analysis by stopped-flow spectroscopy and flash photolysis
- Analytical chemical techniques: UV-Vis, GC, HPLC, MS, EPR.

LIST OF PUBLICATIONS

1. Vanin, A. F.; Papina, A. A.; Serezhenkov, V. A.; Koppenol, W. H. The Mechanisms of S-nitrosothiol Decomposition Catalyzed by Iron. *Nitric Oxide* **10**:60-73, 2004.

2. Papina, A. A. and Koppenol, W. H. Two Pathways of Carbon Dioxide Catalyzed Oxidative Coupling of Phenol by Peroxynitrite. *Chem. Res. Toxicol*, in press.

3. Papina, A. A. and Koppenol, W. H. The Identity of a Long-lived Biphenol Precursor, Formed during Carbon Dioxide Catalyzed Oxidation of Phenolate by Peroxynitrite, in preparation.